



SCIENCE OF
TSUNAMI HAZARDS

The International Journal of The Tsunami Society

Volume 14 Number 2

1996

TWO GREAT TSUNAMIS / UJNR WORKSHOP

- TWO GREAT TSUNAMIS/UJNR WORKSHOP** 67
 George Curtis and James P. Lander
 University of Hawaii at Hilo, Hawaii, USA
- SOURCE MODEL OF THE 1946 ALEUTIAN TSUNAMI DERIVED FROM THE PREDOMINANT FREQUENCIES** 71
 Kuniaki Abe
 Nippon Dental University, Niigata City, Japan
- HUMAN FACTORS COMPOUNDING THE DESTRUCTIVENESS OF FUTURE TSUNAMIS** 79
 Daniel A. Walker
 University of Hawaii, Honolulu, Hawaii, USA
- ASTEROID TSUNAMI INUNDATION OF HAWAII** 85
 Charles L. Mader
 Mader Consulting Co., Honolulu, Hawaii, USA
- CAN A SUBMARINE LANDSLIDE BE CONSIDERED AS A TSUNAMI SOURCE?** 89
 Sin-Iti Iwasaki, Augustine Furumoto, Eiichi Honza
 National Research Institute, Tsukuba, Japan
- TSUNAMI RISK REDUCTION: THE OREGON STRATEGY** 101
 George R. Priest, D. A. Hull, B. F. Vogt, A. Karel, D. L. Olmstead
 Oregon Department of Geology and Mineral Industries, Portland, Oregon, USA
- USING M_w or M_t TO FORECAST TSUNAMI HEIGHTS** 107
 Augustine S. Furumoto
 Hawaii Civil Defense, Honolulu, Hawaii, USA
- NUMERICAL SIMULATION OF THE PROPAGATION OF THE 1993 SOUTH-WEST HOKKAIDO EARTHQUAKE TSUNAMI AROUND OKUSHIRI ISLAND** 119
 Shinji Sato
 Public Works Research Institute, Tsukuba, Japan
- DAMAGES OF COASTAL STRUCTURES IN AWAJI AND TOUBAN COASTS DUE TO 1995 HYOGOKEN NAMBU EARTHQUAKE** 135
 Shigenobu Tanaka and Shinji Sato
 Public Works Research Institute, Tsukuba, Japan

copyright © 1996
 THE TSUNAMI SOCIETY
 P. O. Box 25218,
 Honolulu, HI 96825, USA

OBJECTIVE: **The Tsunami Society** publishes this journal to increase and disseminate knowledge about tsunamis and their hazards.

DISCLAIMER: Although these articles have been technically reviewed by peers, **The Tsunami Society** is not responsible for the veracity of any statement, opinion or consequences.

EDITORIAL STAFF

Dr. Charles Mader, Editor

Mader Consulting Co.

1049 Kamehame Dr., Honolulu, HI. 96825-2860, USA

Dr. Augustine Furumoto, Publisher

EDITORIAL BOARD

Dr. Antonio Baptista, Oregon Graduate Institute of Science and Technology

Professor George Carrier, Harvard University

Mr. George Curtis, University of Hawaii - Hilo

Dr. Zygmunt Kowalik, University of Alaska

Dr. Shigehisa Nakamura, Kyoto University

Dr. Yuri Shokin, Novosibirsk

Mr. Thomas Sokolowski, Alaska Tsunami Warning Center

Dr. Costas Synolakis, University of California

Professor Stefano Tinti, University of Bologna

TSUNAMI SOCIETY OFFICERS

Mr. George Curtis, President

Professor Stefano Tinti, Vice President

Dr. Charles McCreery, Secretary

Dr. Augustine Furumoto, Treasurer

Submit manuscripts of articles, notes or letters to the Editor. If an article is accepted for publication the author(s) must submit a camera ready manuscript in the journal format. A voluntary \$50.00 page charge (\$35.00 for Tsunami Society Members) will include 50 reprints.

SUBSCRIPTION INFORMATION: Price per copy \$20.00 USA

ISSN 0736-5306

Published by **The Tsunami Society** in Honolulu, Hawaii, USA

TWO GREAT TSUNAMIS/UJNR WORKSHOP

University of Hawaii at Hilo, April 1-3, 1996

George Curtis and James P. Lander, Conveners

A conference was held in Hilo, Hawaii beginning on April 1, 1996 to commemorate the 50th anniversary of the disastrous earthquake and tsunami of the Aleutian Islands and the 100th anniversary of the disastrous earthquake and tsunami of Sanriku, Japan. These two events were important in shaping later organization and research on the tsunami problem; the 1946 event initiated research that led to the development of the Pacific Tsunami Warning System. The program included:

April 1 - A memorial service in the rebuilt area of Hilo that was devastated by the 1946 and 1960 tsunamis was held in conjunction with local officials and survivors. The afternoon opening ceremonies at the University featured invited speakers who described the effects of the two tsunamis and the role they played in shaping later developments in the field.

April 2 - Scientific sessions were held on the latest developments in the field, including instrumentation, warning and mitigation actions, source mechanisms, case studies, and models. An important theme was the application of the lessons learned from past tsunamis to public safety. A banquet was held in the evening at a restaurant overlooking Hilo Bay.

April 3 - A guided field trip was made to affected sites on Hawaii Island including visits to Hilo harbor, Laupahoehoe, the Civil Defense Office and the Hawaii Volcano Observatory (site of the earliest tsunami warnings), followed by an informal discussion/closing session and video tapes of numerical models, and barbeque dinner at the University that evening.

April 4 and 5 - Optional field trips that were held on the island of Oahu included the Pacific Tsunami Warning Center, the International Tsunami Information Center, the new Weather Service Forecast Office, and the Oceanography department at the University of Hawaii at Manoa.

The conference was sponsored by the Tsunami Society and the Natural Sciences Division of the University of Hawaii at Hilo and was organized by George Curtis of UH-Hilo/JIMAR and James Lander of the University of Colorado/CIRES. Although NSF support was not available, and therefore no formal proceedings are available, this was an official UJNR workshop by agreement between U.S. and Japan counterparts. Some 20 scientists from the U.S., 13 from Japan, two from Canada, and several non-scientists were registered.

Abstracts of the papers were provided to registrants with their programs. Participants were invited in advance to submit their papers to the Journal for review and publication in this special issue. Eight of them are included. Brief summaries of all papers not published in this issue follow.

For the first session, in *Semicentennial Reminiscences*, Doak Cox of the Univer-

sity of Hawaii described how 50 years ago he watched several cycles of the April 1 tsunami at Honolulu and later participated in the pioneering survey of its effects with Francis Shepard and Gordon MacDonald. He discussed field surveys of tsunamis in 1952, 1957, 1960, and 1964 and the application of the information obtained from those experiences, his services as tsunami-gaku-sha at the University and for IUGG, NAS, State Civil Defense, and his extensive historical publications.

Walt Dudley of UH-Hilo told of the Tsunami of April 1, 1946 in *That Morning in Hilo, Hawaii*. At 10 minutes to seven on the morning of April Fool's Day, a "tidal wave" struck Hilo without warning. The loss of life and property from that event was described, and it was pointed out that the deaths were not in vain, as the tragedy led to the development of the Pacific Tsunami Warning System.

In *The Tsunami of April 1, 1946: A Photographic Look at an Event That Changed the Course of Marine Geology*, Gerald Kuhn of the Foundation for Applied Research in Natural Science presented many of the remarkable photos (many in color) of the 1946 event taken by the aforementioned Fran Shepard. All his photos, drawings, and maps -many unpublished- have been collected and archived by Mr. Kuhn.

Mike Blackford, Director of the Pacific Tsunami Warning Center, outlined the scenario of the warning systems were the 1896 Sanriku and 1946 tsunamigenic earthquakes to occur today, to illustrate in detail how the regional and Pacific systems function.

For the next session, Y. Sekita of the Japan Meteorological Agency then described how the six regional warning systems function, including the usage of 150 new seismograph stations which are always online. The new stations include a broadband seismometer which enables calculation of the magnitude within 5 minutes of occurrence.

In a paper important to the theme of the conference, James Lander of CIRES/University of Colorado provided recent numerical information on the often anomalous records of the 1946 event, in the Alaska source area. For example, the wave at Scotch Cap lighthouse was 35 meters but no other area reported more than 6 meters. The aftershock area is now considered to be 180 by 140 km and oriented for directivity toward Hawaii.

The next session began with Kenji Satake of the Geological Survey of Japan providing new information on several tsunamigenic earthquakes in a paper with Jean Johnson of the University of Michigan. Tsunami waveform inversions were used to determine slips in the absence of adequate seismic data and are thus useful for prediction of future events.

George Priest, et al, of the Oregon Department of Geology described a pilot runup study of an area of the Oregon Coast using three scenarios based on a fault model of Whitmore and an inundation model by Mader. The results were compared with analysis of prehistoric tsunami deposits. Dr. Priest also presented a paper by Antonio Baptiste on a regional study of a possible Cascadia tsunami developed for a larger area but with somewhat less detail.

In the next session, Masami Okada of the Japan Meteorological Research Institute compared newer data with existing tables for calculation of arrival time as a

function of magnitude and source size (as well as distance). The updated methodology gives more accurate results in certain situations.

S. I. Iwasaki (National Research Institute for Earth Science and Disaster Prevention) delivered a message from Prof. Noboru Shuto, who was unable to attend, complementing the conference and emphasizing the need for awareness of tsunamis on these anniversaries and the need for more and better tsunami research.

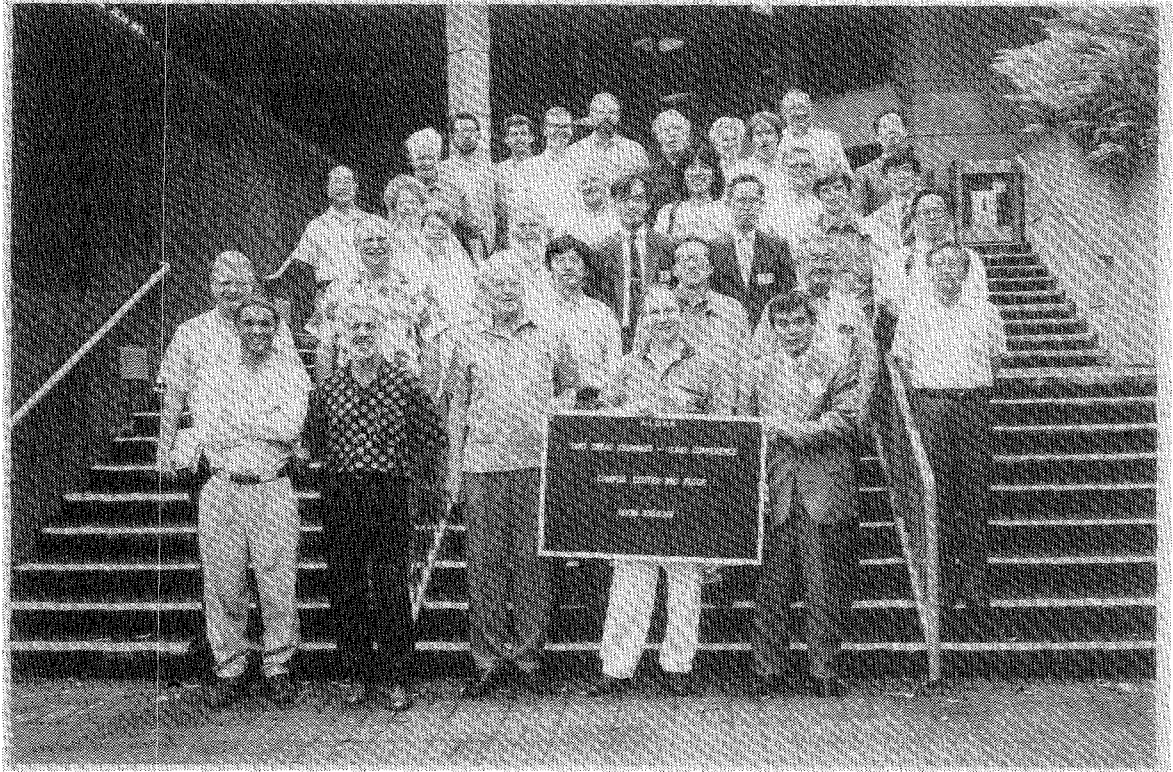
Gerard Fryer (and Charles Fletcher) pointed out that, except for Hilo, the shores of the Hawaiian Islands have been developed with little consideration for tsunami risk. They have identified two sites which appear to have deposits from ancient tsunamis and can thus contribute to the assessment of future risk. The deposits have been analyzed and will be carbon-14 dated.

Fred Raichlen of the California Institute of Technology presented a comparison of his results for breaking and non-breaking waves in hydraulic experiments with those obtained from numerical models. Agreement varied among several factors which he discussed.

S. I. Iwasaki (et al) and K. Hishiki of NEC authored a paper on the just-completed cable-connected gauge and seismic system deployed in the Sagami trench. They expect to detect events of magnitude 1.5 and waves with 1 mm resolution for regional prediction.

Kenji Satake (et al) presented his paper on the time and size of a historical Cascadia earthquake inferred from Japanese and American records around 1700 AD. The magnitude was estimated as 9 and the time as 2100 local.

Jim Lander then delivered a summary of the conference, as follows: "We are nearing the end of our workshop. Initially, there were problems with timing due to the change in fiscal years for the Japanese participants, and with budgets for U.S. funding agencies; also, we all have a problem with finding the time in our busy schedules to prepare papers and participate. Still, for those of us in the field of tsunami studies, being here in Hilo for the 50th anniversary of the important April 1, 1946 tsunami which struck an unsuspecting population was the place to be. I think the workshop has been a great success. I am impressed with the range of topics covered, with commemorative papers of the Sanriku and Aleutian tsunamis, reports from the JMA and Pacific Tsunami Warning Centers, from the Hawaii emergency preparedness, on source mechanism studies, on modeling of sources and wave forms, on deep ocean recording, on paleotsunami deposits and even the threat of tsunamis from meteorite impacts. Such a meeting would have been unthinkable fifty years ago when the research needs were for simple tsunami travel time charts and a visible recording seismograph for a warning system. The nascent international research on tidal waves begun in the early 1930's was interrupted by the war. The Aleutian tsunami with its disastrous effects in Hawaii revived the international research work in the IUGG and gave rise to the warning systems. This was our fifth UJNR symposium/workshop organized by the Task Committee on Storm Surges and Tsunamis of the UJNR Panel on Wind and Seismic Effects. The first was organized in Tsukuba, Japan in 1983, the second was held in Honolulu in 1990, the third in Osaka in 1993 and the fourth in Berkeley in 1995. Perhaps we can look forward to another workshop for the end/beginning of the millennium."



Two Great Tsunamis/UJNR Workshop participants on the steps of the Campus Center of the University of Hawaii at Hilo on April 2, 1996.

First Row: R. Siemers, C. Blay, G. Curtis, G. Priest, S. Tanaka

Second Row: L. Fuka, J. Lander, K. Satake, K. Fujima, G. Furumoto, K. Kajiura

Third Row: C. Lander, M. Blackford, S. Sato, M. Okada, H. Matsutomi

Fourth Row: K. Abe, N. Wiegen, F. Raichlen, T. Nakajima, D. Walker, G. Fryer, Y. Sekita

Back Row: S. Wiegen, S. I. Iwasaki, C. McCreery, ??, W. Roper, O. Magoon, E. J. Mader, G. Kuhn, C. Mader, Y. Sekita

Source Model of the 1946 Aleutian Tsunami Derived from the Predominant Frequencies

Kuniaki Abe

Niigata Junior College, Nippon Dental University
Hamauracho 1-8, Niigata City, 951 , Japan

Abstract

Amplitude spectra were obtained for tide gage records of the 1946 Aleutian tsunami, observed in coasts of North America, Hawaii and Japan, and the azimuth dependence were noticed in the predominant frequencies. The predominant frequencies were 0.00134 and 0.00016 Hz for Honolulu and Sitka, respectively. These stations are located in the directions normal to the long axis of the assumed source and parallel to the short axis, respectively. Based on the model spectra explaining the directivity we derived the source size to be consistent with the observed predominant frequencies assuming the average sea depth of 2000 m for the source area. At the same time the dislocation was inversely estimated to be 4.7m from assumptions of a cylindrical propagation of the initial rise and pure dip slip in a very shallow depth. The model fault has a length of 330 km, width of 45 km, dislocation of 4.7 m , upper depth of 5 km as a pure thrust of azimuth angle of 250 ° . The small aspect ratio contributed to a large energy radiation in the direction normal to the fault strike. This model was applied to tsunami records observed at Hachinohe in Japan and Crescent City in USA. The observed spectra were compared with the model spectra after correcting the shelf responses. In the former case the predominant frequency almost agreed with the predicted one. In the latter case the predominant frequency does not agree to one at the predicted relative azimuth, 211°, but that at 260°. This difference was caused by a refracting wave path on the continental slope of the source.

Introduction

A theoretical model of tsunami spectra by Yamashita and Sato(1980) clarified the directivity of predominant frequencies of tsunami spectra and the dependence on fault parameters in a constant sea depth. Abe(1993) applied it to the observed spectra for the 1990 Mariana tsunami and 1992 Nicaragua tsunami, and showed that the observed spectra can be approximated by superpositions of the source spectra and shelf responses. At that time he used average sea depths for the sloping sea bottoms in the sources. These results suggest that a spectral analysis is effective in deriving fault parameters from the observed tsunami spectra. Recently Abe and Okada(1995) used it to obtain a model of the 1993 Noto earthquake tsunami.

The 1946 Aleutian tsunami is known as one of big tsunamis but the earthquake did not excite strong seismic waves($M_s=7.4$) proportional to the tsunami. It is called a tsunami earthquake by Kanamori(1972). The seismic mechanism is not well studied because of a lack of widely distributed seismological data. Johnson and Satake(1995) noticed the importance of tsunami wave to estimate asperity of the seismic source at Aleutian -Alaska subducting region.

The earthquake started at an epicenter of 163.5W and 52.75N on 12h 28m, 1 April 1946. The tsunami excited by the earthquake propagated to the west coasts of North and South America, Hawaii and the Pacific coast of Japan and was observed at many tide stations(e.g.Green,1946). The records at these stations show that the tsunami began as pushing waves in all the stations. This fact suggests that the earthquake accompanied an elevation of sea bottom at the south side of the source region and the tsunami was generated by the elevation. Moreover, from the travel times the source is estimated to be on the sloping region of the continental shelf facing the Aleutian trench. A thrust fault is a possible mechanism, which is an elastic rebound of the upper plate at the subduction zone of the Pacific plate.

Method

The theoretical spectra by fault formation is applied to the 1946 Aleutian tsunami in a constant sea

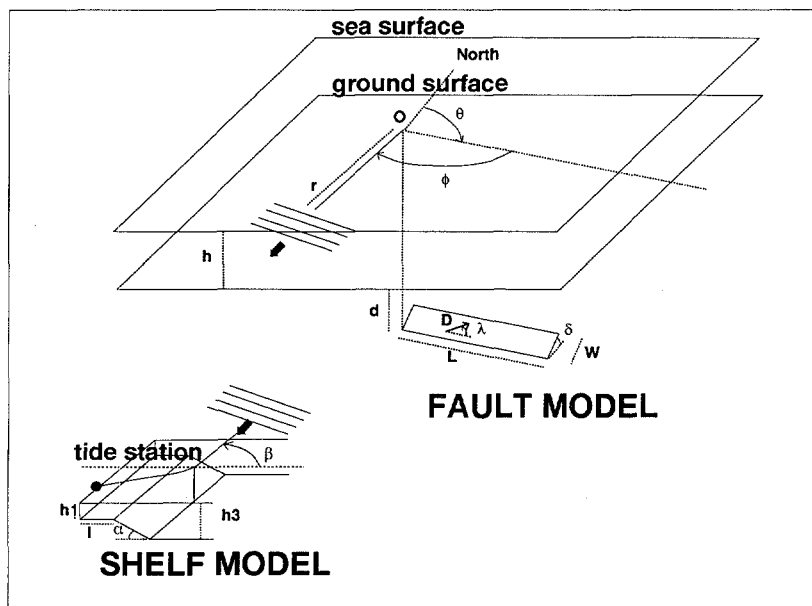


Figure 1. Definitions of parameters in models

depth h of 2000 m, which is an average depth of the continental slope. Since a typical thrust fault is assumed on the continental slope, the dip angle δ of 15° , slip angle λ of 90° and azimuth angle θ of 250° are selected for the fault parameters(Figure 1). The dip angle is approximately a sloping angle of the subducting plate and the azimuth angle is in the direction parallel to the trench axis. In the background of this work there is an idea that predominant frequencies of tsunami depend on the source size and the azimuth angle relative to fault strike. The origin of coordinate O(54° N, 163° W) is assumed to be at the north-east margin of the source, which is estimated from the travel time, and the x axis is taken to be positive to the south west direction along the strike. The relative azimuth angle ϕ is defined as an angle measured in the clockwise direction to a observation point of distance r , as shown in Figure 2. Tide stations recording the tsunami are plotted in the same figure. From this figure we understand that Honolulu is approximately located in the direction of 270° and Sitka is located of 180° .

A spectral analyses are carried out on tsunamis observed at Yakutat, Sitka, Clayquot, Crescent City,

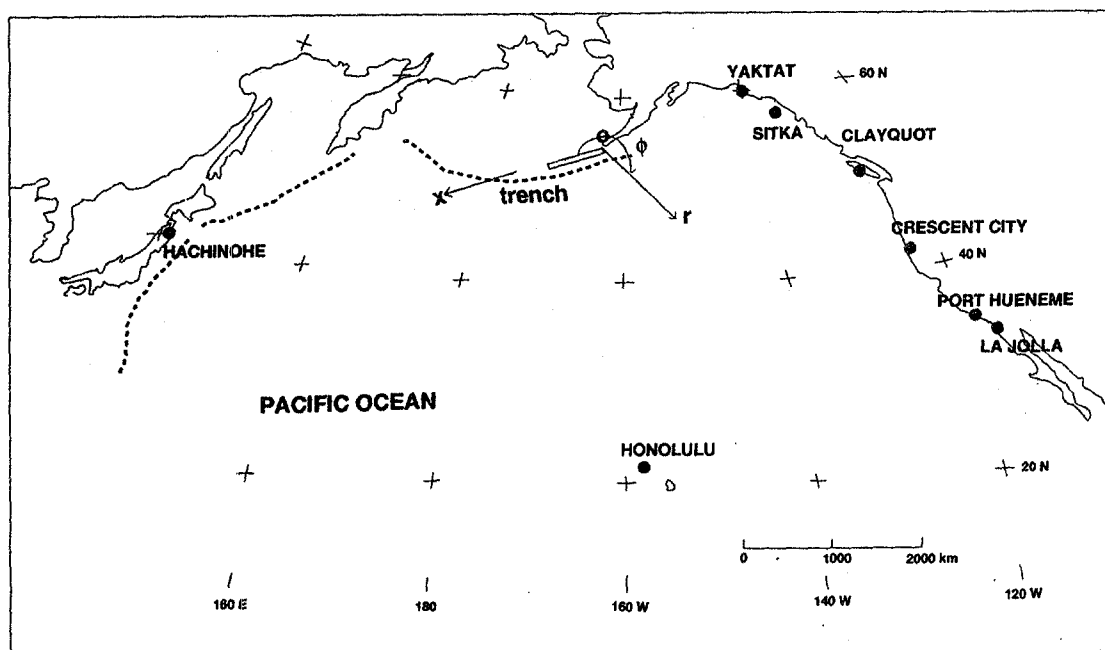


Figure 2. Locations of origin O and tide stations(solid circles)

Port Hueneme, La Jolla(Green,1946) and one at Hachinohe prepared by Hachinohe meteorological station . From the arrival times, time histories of the sea level are sampled at the interval of 1 minute for 6 hours and the displacement spectrum is obtained using Goertzel method after correcting the ordinary tide. But the total sampling time is 2 hours in Honolulu from the lack of data. Predominant frequencies are read for the two special stations, Honolulu and Sitka. These values are used to determine the length and width of the model in comparison with the calculated ones in the assumption of the parameters. Dislocation is backwardly estimated from the decay curve of the initial level of the tsunami with the dependence inversely proportional to square root of the propagation distance. The derived model is checked with other tsunami records.

Results

The amplitude spectra obtained for the stations are shown in Figure 3. The variation depending on the relative azimuth angle ϕ is clearly observed. At the normal direction to the fault strike, as shown in the case of Honolulu $\phi = 279^\circ$, a predominant frequency of 0.00134 Hz (period of 12.4 minutes) is observed with a large amplitude of 0.22 ms. On the other hand at the parallel direction, as shown in the case of Sitka $\phi = 178^\circ$, a predominant frequency of 0.00016 Hz (104 minutes) is observed with a small amplitude of 0.023 ms. It is observed that the predominant frequencies vary from the largest value at Honolulu to the smallest one at Sitka with decrease of the relative azimuth angle. This variation shows the directivity of tsunami radiation being expected from the model spectra. The theoretical model predicts that the predominant frequencies depend on the width and length. In the normal direction the predominant frequency corresponds to tsunami wavelength at the source, which is determined by the fault width and in the parallel direction it corresponds to one determined by the length. After some trials the best fit model is derived with length L of 330 km and width W of 45 km. In the calculation an upper margin of the fault is assumed shallow in depth of 5 km ($d = 16.6$ km). To explain the dislocation the initial levels are plotted on a log-log graph for the distance r of the abscissa and the level was backwardly followed. Two meters is an estimated value at epicentral distances of 20-50 km, which is the source region, as shown in Figure 4. In the two-dimensional

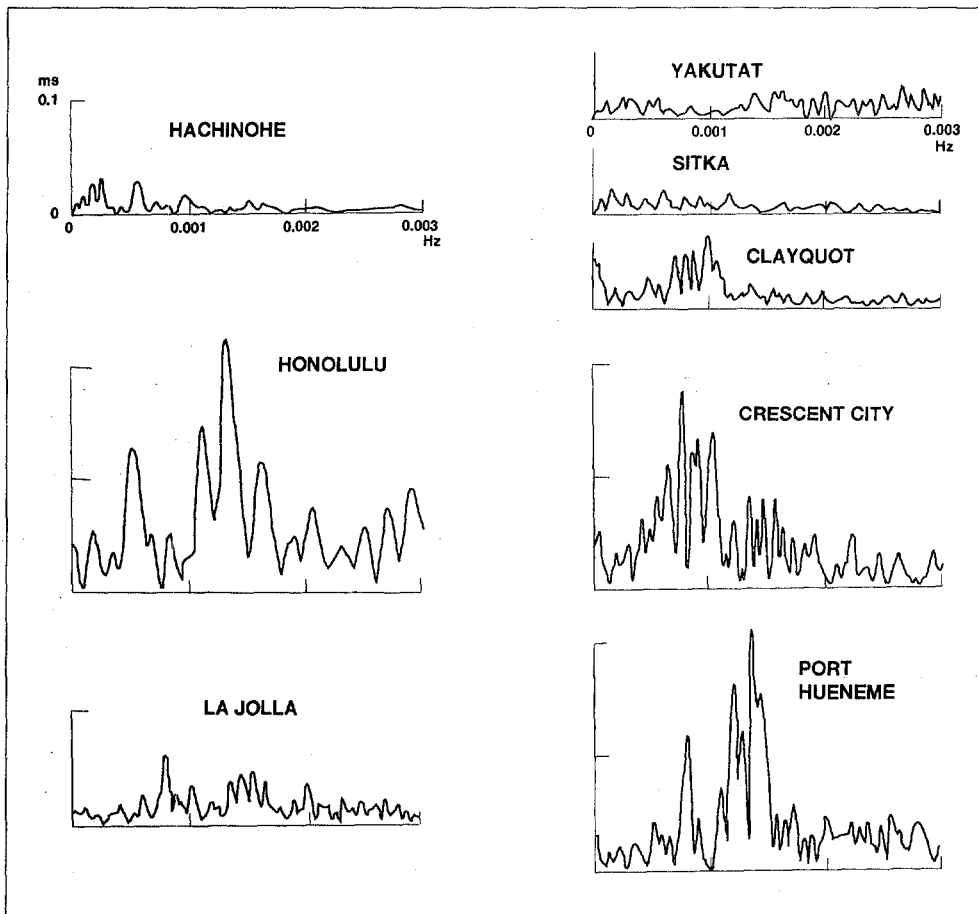


Figure 3. Tsunami amplitude spectra observed

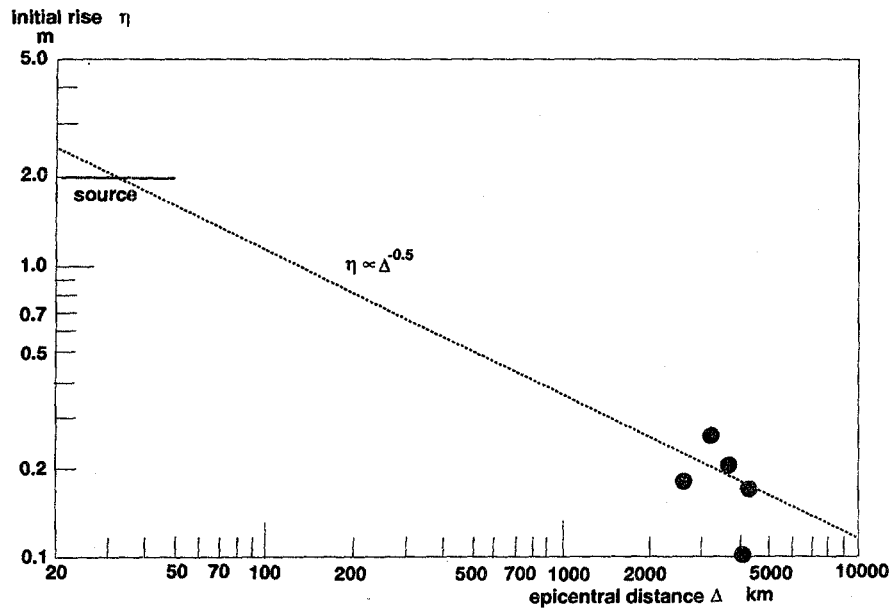


Figure 4. Initial rises observed (solid circles) and the decay curve (dotted line)

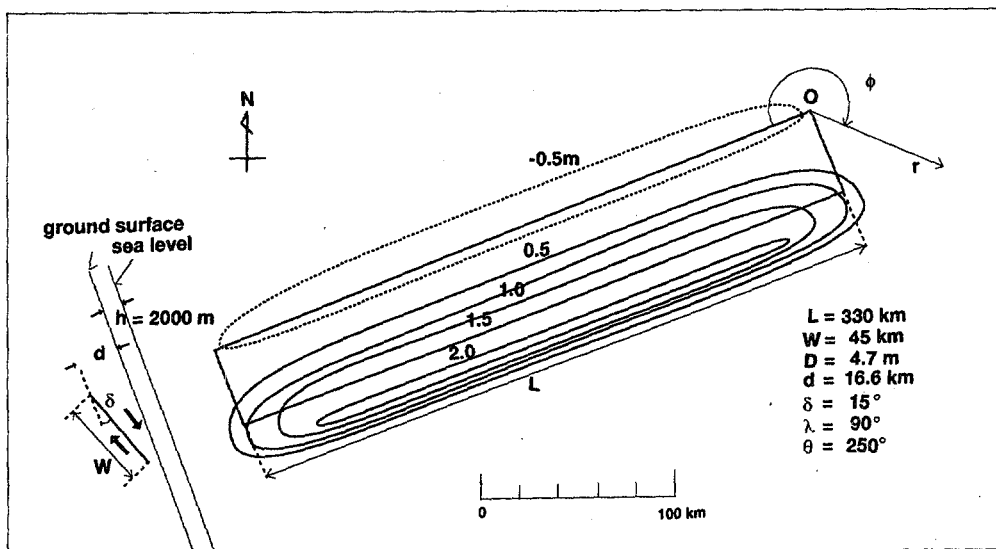


Figure 5. Vertical displacement on the fault model

propagation amplification of 2 by total reflections at tide stations is canceled by decaying due to a geometrical spreading at the source into half. We assumed such a cancellation in the wave decay. Johnson and Satake (1995) estimated the seismic moment of 30×10^{20} Nm for this earthquake. The dislocation D of 4.7 m is consistent to their results. The vertical displacement field caused by the fault is shown in Figure 5 (Mansinha and Smylie, 1971). The maximum elevation of 2 m which is consistent with the height inversely obtained. As a characteristic property of thrust faults a small

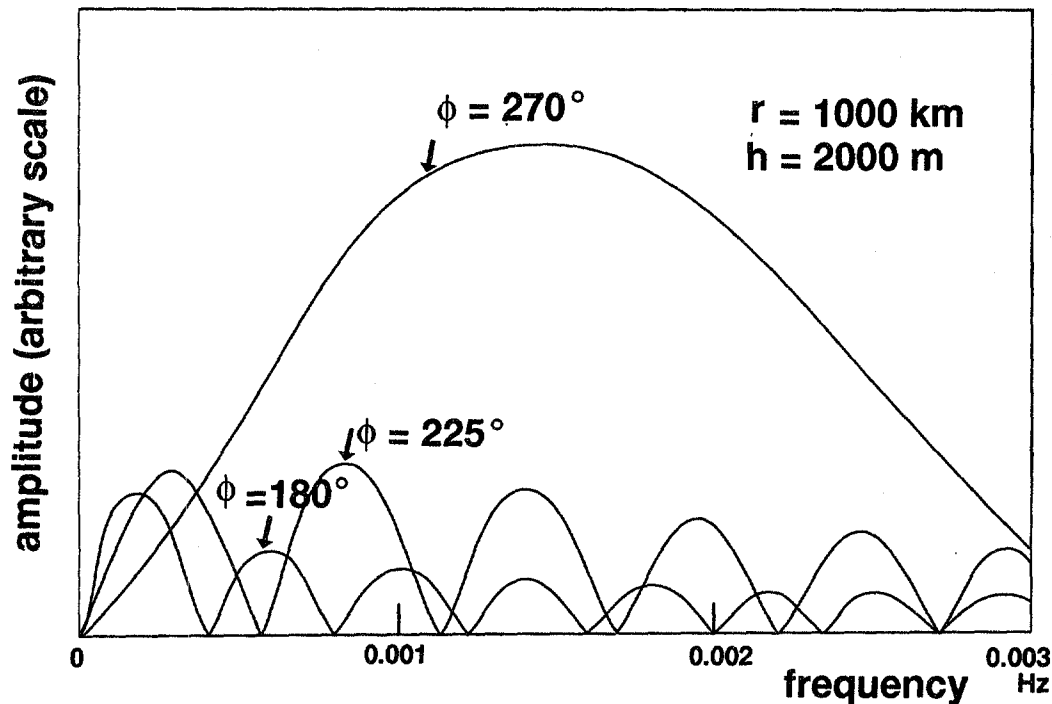


Figure 6. Tsunami spectra expected from the model

subsiding area with small amplitude is accompanied by a large elevation area with large amplitude. The location is shown in Figure 2. Tsunami spectra, expected from the fault model, is shown in Figure 6. It is estimated at a distance r of 1000km. This result shows that tsunami radiated in the direction normal to the strike propagates with a large amplitude of the predominant frequency and the predominant frequency rapidly decreases with decrease of the relative azimuth angle.

Discussion

The model spectra were compared with spectra derived from tide gage records at Crescent City and Hachinohe. The effect of shelf response to the observed tsunami was taken into consideration. Details of shelf response corrections were discussed by Abe(1993). In his shelf model one dimensional model is used as shown in Figure 1. For Crescent City tide station, the shelf parameters are depth h_1 100 m, width l 25 km, ocean depth h_3 2000 m, slope connecting shelf and ocean $\tan \alpha$ 0.048, incident angle β of 20° to the direction normal to the coast line. For Hachinohe, the parameters are width l 40 km, slope $\tan \alpha$ 0.0253, incident angle β of 30° . Other parameters for Hachinohe were the same as those for Crescent City. The results are shown in Figure 7. In Hachinohe the smallest predominant frequency fits well. In Crescent City the observed spectrum does not fit the one expected at a relative azimuth angle of 211° , which is a calculated relative azimuth, but one of 260° . In the sea of constant depth, waves do not refract and the ray path is straight but in the real sea, having the trench, ray path is not straight. Especially there is a possibility that the sloping source region bring a modification of radiation pattern due to refraction. This is one of possible explanations.

We assumed the sea depths of 2000m at the source and at the shelf. But an average sea depth of the Pacific ocean is 4300m. It is considered that this difference dose not affect the spectra.

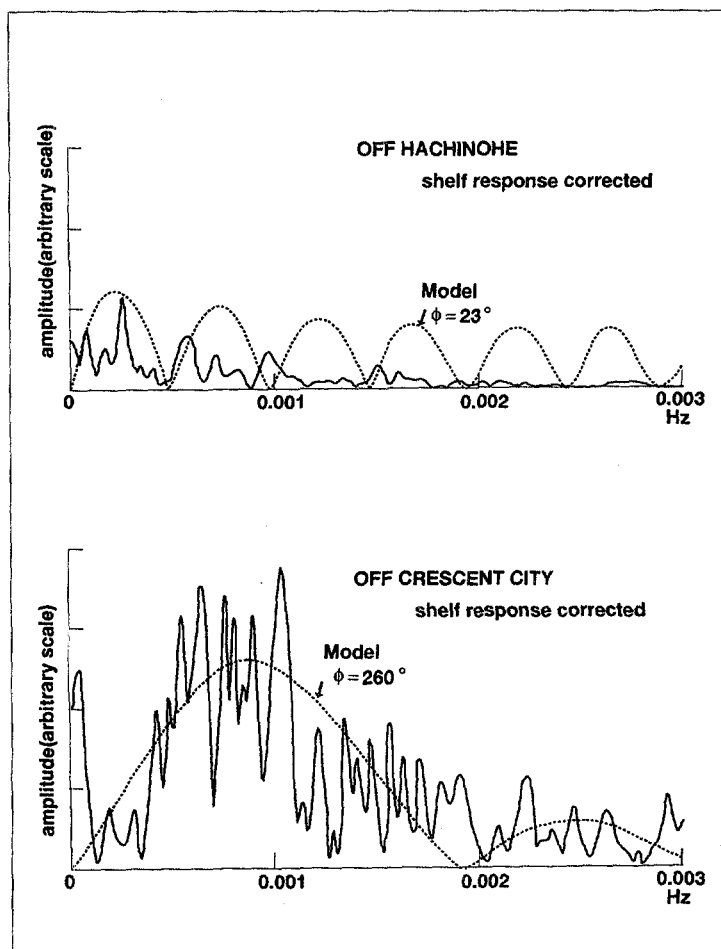


Figure 7. Comparisons of observed spectra and model spectra

At Port Hueneme the predominant frequency of 0.00134 Hz, which is the same as Honolulu, was observed. The tide station is located in the azimuth direction $\phi=215^\circ$. It is a relation similar to the case of Crescent City. There was a peak at the frequency corresponding to predominant frequency of Crescent City. The predominant frequency at Port Hueneme is explained by the refraction and trapping of high frequency by the Santa Cruz island in front of the station.

Conclusions

Amplitude spectra were obtained for the tsunami records observed at North America, Honolulu and Japan during the Aleutian tsunami on 1 April 1946. Azimuth angle dependence was observed at the predominant frequencies. To explain the azimuth dependence a fault model was derived. The results shows that the length of 330 km, width of 45 km are consistent with the observed predominant frequencies. The small aspect ratio is considered to cause an energy concentration in the normal direction. Small differences of the relative azimuth angles between predicted one and observed one for the predominant frequencies were observed and attributed to refraction on the sloping sea bottom at the source.

Acknowledgement

The author thanks the staff of Hachinohe meteorological station for providing the tide gage data.

References

- Abe,Ku., 1993, Tsunami spectra as a synthesis of source spectrum and shelf response, Proceed. IUGG/IOC International Tsunami Sympo.,151-163.
- Abe,Ku. and M.Okada,1995,Source model of Noto-Hanto-Oki earthquake tsunami of 7 February 1993, PAGEOPH,144,621-631.
- Green,G.K.,1946,Seismic sea wave of April 1, 1946, as recorded on tide gages, Trans. American Geophysical Union,27,No.6,490-500.
- Johnson,J.M. and K.Satake,1995,Asperity distribution of Alaska-Aleutian earthquakes as inferred from tsunami waveforms,Abst. Seismol. Soc.Japan,No.2(in Japanese).
- Kanamori,H.,1972,Mechanism of tsunami earthquakes,Phys.Earth Planet. Interiors,6,346-359.
- Mansinha,L. and D.E.Smylie,1971,Displacement fields of inclined faults, Bull.Seismol.Soc.Am.,61,1433-1440.
- Yamashita,T. and R.Sato,1980,Generation of tsunami by a fault model,J. Phys.Earth,22,45-440.

HUMAN FACTORS COMPOUNDING THE DESTRUCTIVENESS OF FUTURE TSUNAMIS

Daniel A. Walker
School of Ocean and Earth Science and Technology
Hawaii Institute of Geophysics and Planetology
University of Hawaii, Honolulu, HI USA

ABSTRACT

On the occasion of the 100th and 50th anniversaries of the great tsunamis of 1896 and 1946, it is appropriate to reflect upon the human aspects of these and other more recent tsunamis. Many of the fatalities and injuries associated with past tsunamis can be attributed to such deficiencies as: a lack of awareness of tsunami hazards, human error, inadequate support of mitigation efforts, and poor communications between scientists, government agencies, and the general public. Without an objective analysis of the current status of such deficiencies and, if necessary, the implementation of effective methods for their reduction or elimination, unnecessary tragedies of the past may be repeated. Historical tsunami incidents in Hawaii are analyzed and compared to those associated with more recent incidents to determine whether corrective measures are needed. The most serious deficiencies are found in the following areas: a lack of knowledge of tsunami hazards at nearly every level of our society, an ineffective warning system for locally generated tsunamis primarily affecting the Kona, Kau, and Puna coasts of the Big Island, and the probability of unacceptably high levels of false warnings for Pacific-wide tsunamis. Suggested methods are offered for the reduction or elimination of these dangerous deficiencies.

INTRODUCTION

As individuals studying large water waves generated by displacements of the ocean floor, we do so both out of a sense of scientific curiosity and a sense of responsibility to save lives through improvements in tsunami warnings systems. However, if we continue to ignore those human factors which have in the past contributed to the destructiveness of tsunamis, the incorporation of our successes into the improvement of warning systems may come too late; and, even if warning systems are improved in a timely manner, they could still be ineffective in saving lives. In the following sections of this report, we discuss examples of those factors drawn in part from Hawaii's history and offer recommendations for their elimination or reduction in future tsunamis.

HUMAN FACTORS

Lack of Education

Fifty years ago at Laupahoehoe School a few miles north of Hilo, the children were about to start the school day when the ocean began to behave in an unusual way. The water receded exposing the ocean floor, and the children began to explore this unexpected new environment. The teachers were also puzzled by this phenomenon. None of the teachers or students comprehended the terrible implications of what they saw. For a few moments all had a chance to save their lives, but those moments soon passed and many died (Dudley and Lee, 1988). Of all the knowledge they had gained in their years as students, if their teachers had only spent a few minutes telling them about tsunamis or if their parents had instilled in them the traditional Hawaiian knowledge of tsunamis, many of those children would be our ages today and they might even be joining us in this commemoration for those less fortunate.

On 1 April 1946, the story of Laupahoehoe was repeated to some extent on all of the major islands in Hawaii.

How many of the fatalities on that day were due to the tsunami and how many were due to ignorance?

More than 48 years later, Oahu Civil Defense officials estimated that from 200 to 400 surfers were in the ocean along Oahu's North Shore on 4 October 1994 at the expected arrival time of a possible tsunami from the large 8.2 Ms earthquake off the coast of northern Japan (personal communication, David Kinolau, Civil Defense Coordinator for District 5 of the City and County of Honolulu). Certainly all were aware of the tsunami warning. Were they ignoring the warning because the surf was unusually good that day? Were they actually waiting to ride the tsunami? Were they in the ocean as a result of school being canceled because of the tsunami warning? Many older adults dismissed the surfers and other beach goers as stupid or crazy. Yet it is difficult to imagine that so many would be in the ocean if they really understood the destructive power of tsunamis. In fact, I believe that those individuals did not really know what they were dealing with. They did not have sufficient knowledge to make an intelligent decision.

Statewide the number of individuals in the ocean or in inundation zones could have amounted to several hundred. Instead of a non-event on 4 October 1994, the earthquake on that date could just as easily have been a powerful tsunami from Kamchatka or the Aleutian Islands. Many on the northern shores who were enjoying the beach and surf could have died; and the total number of deaths, and the physical damage could have far exceeded the totals for 1 April 1946. Fortunately, that did not happen on that day. But how many more days do we have before it does? Also, what were the factors which contributed to the disregard of the warning by so many of Hawaii's children

and young adults?

One explanation is that it has been 30 years since the Hawaiian Islands have experienced a significant Pacific-wide tsunami, while 13 such tsunamis struck Hawaii from 1900 through 1965 (Walker, 1994). This has produced a generation of students, teachers, political leaders, government administrators, and civil servants who have no first-hand knowledge of tsunamis. Very few individuals are aware of the frequency and severity of tsunamis which struck Hawaii from 1900 through 1965. As a result most segments of our society are either complacent or ignorant in terms of the inevitable tsunami hazards in Hawaii's future.

Another explanation is related to the issue of false warnings and the fact that the previous warning of 1986 was viewed as false by the general public. They are not aware of the fact that about 3 of 4 warnings will be associated with tsunamis that have runups of less than a meter (Walker, 1996). Perhaps their thinking is that if a tsunami warning is issued and there is no tsunami, then the warning system obviously doesn't work very well. Also they may believe that there are few if any significant tsunamis in Hawaii, and that warnings are for the most part a nuisance that can be ignored.

Finally, some of the individuals in the ocean and in inundation zones may have had extensive experience in those environments in times of large surf. They had a feeling that large tsunamis may be no more dangerous than large surfing waves.

Poor Communications

The lack of education is a result of poor communications. Generally, scientists have focused primarily on understanding tsunamigenesis, not realizing that it may be years before their findings will be successfully incorporated into existing warning systems. In the interim many unnecessary deaths, injuries, and property losses may occur because some of those same tsunami researchers, who are best qualified to do so, did not devote more time in their community to increasing awareness of tsunami hazards and effective mitigation efforts among the general public, as well as government, business, and educational leaders.

Sluggish Bureaucracies

Even in the best of times, issues requiring actions on the part of government agencies often require years or decades to accomplish. Indeed, proactive initiatives or rapid responses to immediate needs are exceptions to standard government procedures. Improvements and educational initiatives urgently needed to reduce future tsunami losses may be tragically delayed by this undesirable characteristic of government agencies.

Limited Resources

The phrase "There is no money to do that!" is increasingly prevalent at all levels of government. This phrase could also be translated to mean: "There is money, but after more important projects are taken care of, there will be nothing left for any tsunami efforts. Maybe next year!" Government agencies have increasingly limited resources and many urgent priorities. If we are unsuccessful in justifying the costs of needed educational initiatives, hazard mitigation efforts, and improvements in the reliability of warning systems to appropriate Federal or State agencies in a timely manner, the consequences could be unnecessary losses of lives and a severe disruption of the State's economy.

Self-Preservation, Resistance to Change, and Avoidance of Reality

If the primary objective of tsunami research is to save lives, a selfless examination of the most efficient method for achieving this objective is required. Securing required funding for any new initiatives will take limited resources from other individuals, programs, or areas of investigation.

Tsunami researchers, themselves, may be required to reorder their priorities. Some resistance is likely; and, even if extremely convincing arguments are made, individual or agency selfishness could prevent required initiatives from occurring in a timely manner. Also, key individuals from whom support is needed may find it more convenient to ignore the inevitability of numerous future tsunami incidents (i.e., false warnings, large Pacific-wide tsunamis, and locally generated tsunamis on the Big Island).

RECOMMENDATIONS

Because no discernible tsunami was observed by the general public during the last tsunami warning, the disregard evident in that warning may be increased during the next warning unless interim efforts are undertaken to increase education and awareness of tsunami hazards. Because of the growth and development of the State during the quiet period of the past 30 years, the property destruction associated with the next powerful tsunami will be far greater than in 1946. Without improvements in the public awareness of tsunami hazards and their awareness of the limitations of the warning system, unnecessary fatalities and injuries in Hawaii could easily exceed those of 1946.

Tsunamis should be viewed primarily in terms of their tragic human consequences rather than in terms of their scientific interest. The best way that we can commemorate 1 April 1946 and 15 June 1896 is to do what we can to minimize future losses of life and injuries. In my opinion, the most efficient and rapid methods for doing this in Hawaii are provided in the recommendations which follow.

– The general public needs to know that:

- (a) 13 Pacific-wide tsunamis with runups of 1 meter or more struck the Hawaiian Islands from 1900 through 1965;
- (b) 8 of the 13 had runups of 10 feet or more above sea level, 5 of the 13 were 20 feet or more, 4 of the 13 were 30 feet or more, and 2 of the 13 were 50 feet or more (in Hawaii values in feet are preferable to values in meters);
- (c) large tsunamis are inevitable and the quiet of the past 30 years will not continue indefinitely; and,
- (d) existing data suggests that runups associated with 3 of 4 warnings will be less than 1 meter (Walker, 1996), and of the 1 in 4 warning for runups greater than 1 meter, more than half may have values in excess of 10 feet.

The general public also needs to understand the meaning of runups, inundation, and evacuation zones. They need to know what to do in case of a tsunami and the possible signs of a tsunami. Finally, the general public needs to know that tsunamis are not like surfing waves. In coastal areas they may have periods of 15 minutes compared to the 15 seconds of more familiar surfing waves. Therefore, they are “thicker”, more powerful, and have time to flood low-lying areas. As initial tsunami waves recede from low-lying areas, they can interact with later incoming tsunami waves to produce unusual walls of water. In coastal areas later waves in a tsunami can be larger than earlier waves, and dangerous conditions can persist for several hours. The debris laden outflow from low-lying areas can produce powerful and unusual currents.

Appropriate government agencies need a clear and comprehensive understanding of the limitations of the warning system. They need to know that “false” warnings have been and will continue to be the most likely type of tsunami incident in the minds of the general public. They

need to know that an adequate warning system for locally generated tsunamis does not exist and that significant locally generated tsunamis on the Big Island (Cox and Morgan, 1977) may be more frequent than they now believe. Scientists can advise those agencies on how false warnings might be reduced and how an effective warning system for the Big Island could be installed.

- Appropriate government agencies have to face the inevitability of large tsunamis. They cannot wishfully think that the quiet of the past will continue indefinitely. Those agencies have only the choice of either reducing unnecessary fatalities by taking actions before the next large tsunami or waiting until after that tsunami with greater losses of life.
- Scientists have to persist in their efforts to improve education and awareness of tsunami hazards and the reliability of warning systems. Timidity on these issues are not in the public interest, and, unless we speak out, scientists may be used as scapegoats in future tsunami incidents (i.e., false warnings, small Pacific-wide tsunamis, locally generated tsunamis with no warnings, or large Pacific-wide tsunamis).
- Scientists and appropriate government agencies cannot continue to avoid providing the increasingly cynical public with the knowledge that they need to make informed decisions respectful of tsunami warnings - especially the most vulnerable segment of the public in this ocean state, namely our children and young adults.

FINAL REMARKS

Increased awareness of tsunami hazards and improved communications among the public, scientists, and government agencies are the first and most important steps towards reducing the disastrous effects of future tsunamis. Hopefully, this could be accomplished before the next large tsunami strikes Hawaii; but time may be running out.

ACKNOWLEDGMENT

School of Ocean and Earth Science and Technology contribution 4082, and Hawaii Institute of Geophysics and Planetology contribution 885.

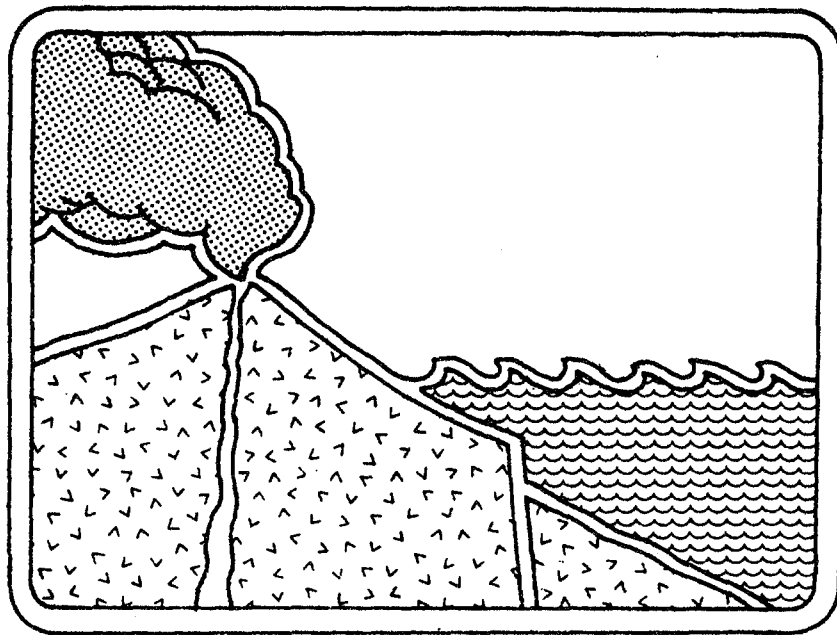
REFERENCES

- Cox, D.C. and J. Morgan, 1977, *Local Tsunamis and Possible Local Tsunamis in Hawai'i*, HIG-77-14, Hawai'i Inst. of Geophysics, 118 pp.
- Dudley, W. and M. Lee, 1988, *Tsunami!*, Univ. of Hawai'i Press, Honolulu, Hawai'i, 132 pp.
- Walker, D. A., 1994, *Tsunami Facts*, School of Ocean and Earth Science and Technology Report 94-03, Univ. of Hawai'i, 93 pp.
- Walker, D. A., 1996, *Future Tsunamis in Hawai'i*, TMI Publication No. 6, Honolulu, Hawaii, 14pp.

The *Science of Tsunami Hazards* is on line at the following URL:

<http://www.ccalmr.ogi.edu/STH>

Comments and suggestions for this web site should be sent to Dr. Antonio Baptista at : baptista@ccalmr.ogi.edu.



ASTEROID TSUNAMI INUNDATION OF HAWAII

Charles L. Mader
Mader Consulting Co.
Honolulu, HI 96825-2860, U.S.A.

ABSTRACT

A study of the tsunami wave inundation to be expected from asteroid impact into the oceans of the world has been in progress for several years. The recent Shoemaker-Levy-9 asteroid impact with Jupiter is typical of the type of event being investigated. A tsunami wave in deep water of 100 meter height and 2000 second period is chosen as representative of the wave expected from a Jupiter type asteroid. Possible Jupiter asteroid parameters (that would result in such a tsunami wave) are 5 km diameter, 5 gm/cc, traveling at 20 km/sec with a range of at least a factor of two for size and density and a velocity range of 10 to 30 km/sec. Such an asteroid impacting with the Pacific Ocean is expected to create a cavity to the ocean floor approximately 150 km wide. The location of the impact can be anywhere from half way between Hawaii and Asia or America for a high density asteroid to near the Hawaiian island chain for a smaller, lower density asteroid.

The modeling was performed using the *SWAN* code which solves the nonlinear long wave equations. The tsunami propagation and inundation was modeled using a 30 second grid of the topography of the Hawaiian islands.

The asteroid tsunami wave results in inundation of much of the Hawaiian islands to between 150 and 300 meters. Video animations of the asteroid tsunami inundation of the Hawaiian islands and the U.S.A. East and West coasts are available.

ASTEROID TSUNAMIS

Tsunami waves generated by earthquakes have typically had a maximum deep ocean amplitude of 10 meters and periods of 500 to 2000 seconds. Tsunami waves with amplitudes of approximately 100 meters are referred to as mega-tsunamis and may be generated by landslides such as the 105 Ka Lanai event described in reference 2 or by asteroid impact with the ocean described in reference 3. The landslide tsunamis have shorter periods and thus the tsunami wave amplitude is not maintained as the wave travels from the source. Large asteroid generated tsunami waves have long periods and waves with large amplitudes that can propagate across an ocean basin.

The recent Shoemaker-Levy-9 asteroid impact with Jupiter is typical of the type of event being investigated. To generate a 100 meter high, 2000 second period tsunami that can traverse an ocean basin, an approximately 150 km wide cavity in the ocean to the ocean floor is required. Possible Jupiter asteroid parameters which could generate such a cavity are diameters of 5 km, densities of 5 gm/cc, and velocities of 20 km/sec. The proposed Jupiter asteroid characteristics vary at least by a factor of two in diameter and density with velocities between 10 and 30 km/sec. The location of the asteroid impact needs to be in the deep ocean (at least 3000 meters deep) and a large, high density asteroid can be located almost anywhere in the ocean basin; while a smaller, lower density asteroid would need to be located nearer the region of interest.

A tsunami wave with a 100 meter height and period of 2000 seconds generated west of the Hawaiian island chain and its interaction with the islands was modeled as described below. Similar modeling has been done for all the ocean basins. Detailed inundation studies have been performed for all the United States coastal regions.

MODELING THE ASTEROID TSUNAMI INUNDATION

The asteroid tsunami was modeled using a 30 second grid of the Hawaiian islands topography. The modeling was performed using the *SWAN* non-linear shallow water code which includes Coriolis and frictional effects. The *SWAN* code is described in reference 1. The calculations were performed on 50 Mhz 486 personal computers with 16 megabytes of memory. The 30 second grid of the Hawaiian island chain was 840 x 600 cells and the time step was 1.5 seconds. The results were essentially independent of the friction coefficient since friction becomes less important at the large inundation levels characteristic of mega-tsunamis.

The interaction of a 100 meter high, 2000 second tsunami wave with the Hawaiian island chain is shown in Figure 1 as contour plots with contour intervals of 50 meters.

The island of Oahu initial topography and the area inundated by the 100 meter high, 2000 second tsunami wave is shown in Figure 2 as picture plots with contour intervals of 50 meters. The island is inundated to 150 meters and in some regions as high as 300 meters.

Similar results were obtained for the other Hawaiian islands with inundations between 100 and 300 meters.

Acknowledgments

The author acknowledges the encouragement and contributions Dr. Jack Hills and Dr. Johndale Solem of the Los Alamos National Laboratory.

1. Charles L. Mader *Numerical Modeling of Water Waves*, University of California Press, Berkeley, California (1988).
2. Carl Johnson and Charles L. Mader, "Modeling the 105 Ka Lanai Tsunami", *Science of Tsunami Hazards*; Vol 11, pages 33-38 (1994).
3. Anthony T. Jones and Charles L. Mader, "Modeling of Tsunami Propagation Directed at Wave Erosion on Southeastern Australian Coast 104,000 Years Ago," *Science of Tsunami Hazards*, Vol 13, pages 45-52 (1995).

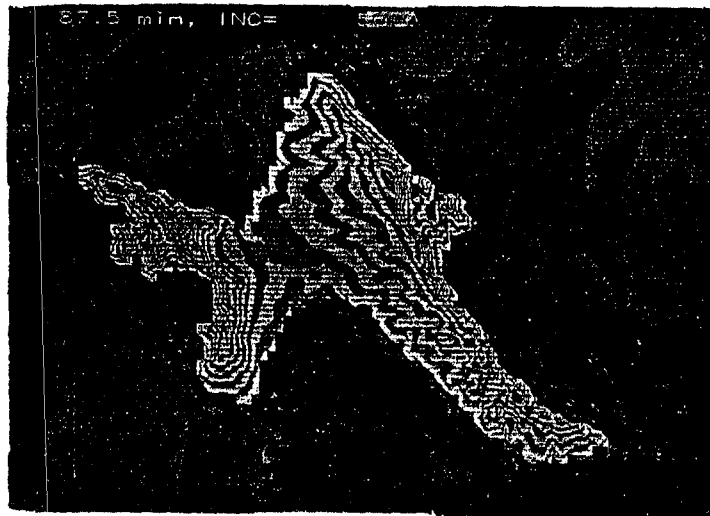


Figure 2. Picture plots showing the initial topography of the island of Oahu and surrounding ocean floor in the first graph and showing the island at maximum inundation in the second graph. The land and water contour intervals are 50 meters. Most of the island is inundated to 150 meters and local inundation to over 300 meters occurs particularly on the leeward side of the island.

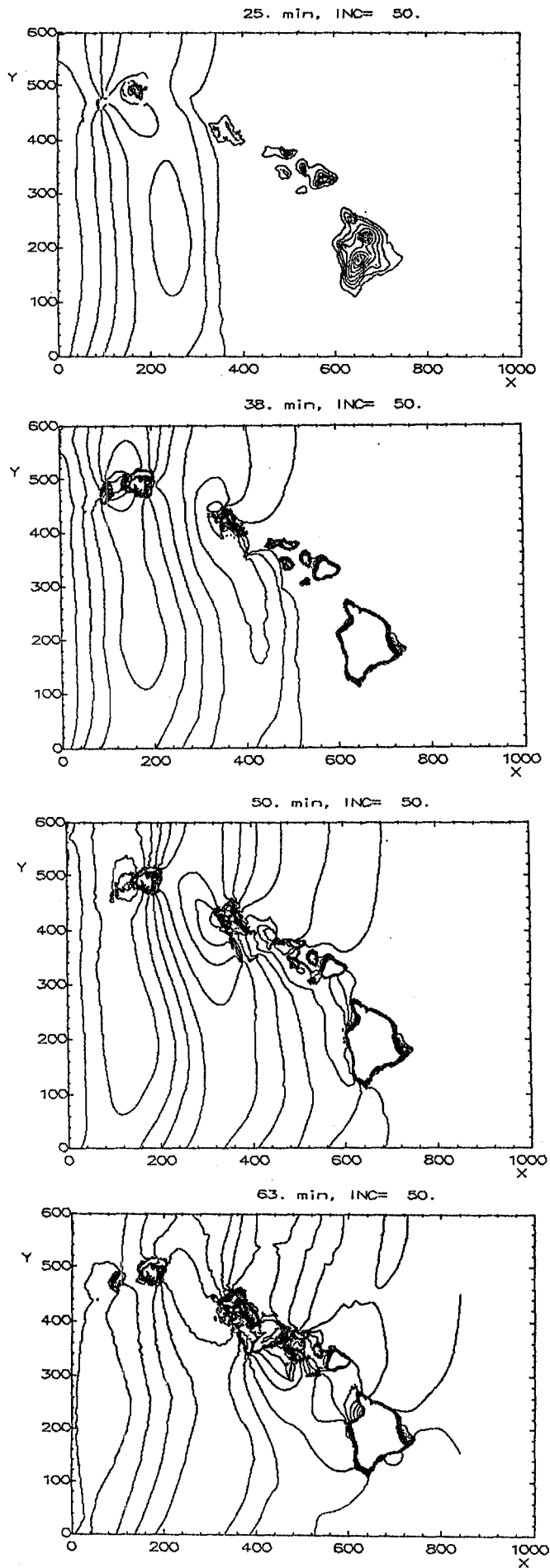


Figure 1. A 100 meter high, 2000 second tsunami wave interacting with the Hawaiian island chain. The contour interval is 50 meters for the ocean. The land contours are 500 meters on the first plot. The X and Y coordinates are 30 seconds each.

**CAN A SUBMARINE LANDSLIDE BE CONSIDERED
AS A TSUNAMI SOURCE?**

Sin-Iti Iwasaki
National Research Institute for Earth Science and Disaster Prevention
3-1 Tennodai, Tsukuba, Ibaraki 305 JAPAN

Augustine S. Furumoto
Tsunami Adviser, Office of the Vice-Director for Civil Defense
State of Hawaii
Honolulu, Hawaii, U. S. A.

Eiichi Honza
Geological Survey of Japan
Higashi, Tsukuba, Ibaraki 305 JAPAN

ABSTRACT

We found evidence for a submarine landslide off the coast of Tohoku district of Japan. To investigate the tsunami due to the submarine landslide, we used a hybrid method for the calculation: an analytical method for the generation stage and numerical calculation with Boussinesq approximation for the propagation stage.

The submarine landslide was modeled by a sliding slab with an area 30 km x 20 km and thickness of 100 m. The sliding velocity was assumed to vary from 5 m/s to 30 m/s. The double amplitude distributions and wave forms of the tsunami at the 200 m water depth contour were compared with the results of numerical simulations of the Meiji Sanriku Tsunami in 1896 (Aida, 1977). The double amplitude distribution for a sliding velocity of 30 m/s showed almost the same characteristic as the Meiji Sanriku Tsunami, but wave forms were quite different.

INTRODUCTION

Geological structure throughout the Tohoku and Kuril forearc areas have been mapped by several investigators (Honza et al., 1978 by seismic reflection and sampling; Scientific Members of the Operation, 1979, by multi-channel seismic reflection; Scientific Party, 1980, by DSDP drillings). Using these data, Honza et al. (1996) re-estimated hypocenters of twenty shallow earthquakes from 1951 to 1989 and concluded that the hypocenters of the earthquakes in the Tohoku forearc area should be shifted seaward or to deeper parts under the forearc area.

On the other hand the Tohoku forearc area is well known as a high tsunamigenic zone, with disastrous tsunamis generated by earthquakes in 1896, 1933, 1952 and 1968. It is widely recognized that the deeper the focus, the smaller the tsunami. Then, what are causes of these tsunamis if the foci are deep? Submarine landslide is a possibility. Landslide by itself can generate a tsunami or it can enhance a tsunami generated by tectonic dislocation during an earthquake.

Historical records (e.g. Moore, 1978) can be cited where submarine landslides have generated tsunamis. But, generation mechanism was different for each landslide. Most studies about landslide tsunamis dealt with energy transfer from landslides to tsunamis (Wiegel, 1964; Striem and Miloh, 1976; Murty, 1979). Quantitative studies are very few. One of the few is that by Jiang and Leblond (1992), but they considered turbidity currents or muddy flows instead of landslides. Furthermore, we do not have measurements appropriate for quantitative discussions about tsunamis due to landslides. We have no method to prorate that portion of the tsunami generated by tectonic movement and that portion generated by landslide.

In this paper, through a combination of analytical method and numerical simulations we investigated the possibility whether a landslide can generate a tsunami or not.

A MODEL OF A SUBMARINE LANDSLIDE

Figure 1 shows the cruise tracks of surveys carried out in the Tohoku and Kuril forearc areas. The vertical cross section of the multi-channel seismic reflection profiling along line LM2 is shown in Figure 2. Traces of landslides are found in the middle of LM2. Dotted lines correspond to boundaries among landslides occurring at different times. We inferred that the traces revealed five separate landslide events.

For our landslide model, from the result of multi-channel seismic reflection profiling, we assigned 100 m to the vertical height. For the width in east-west direction we assigned 20 km as shown in Figure 2. The length in the north-south direction we assumed 30 km. We further assumed that this landslide model moves along a slope in the eastern (offshore) direction with a constant velocity.

A HYBRID METHOD FOR CALCULATION

Procedure.

In the generation mechanism for a tsunami due to tectonic movement and to landslide,

the distinguishing point is the source movement. For generation solely by tectonic movement, the generating source jerks upward only. For a landslide, the generating mass moves along a slope. For generation by tectonic movement, the process can be considered to be instantaneous and we can separate the generation stage from the propagation stage. But, for a landslide, we cannot.

Figure 3 shows the flow chart of the calculation. We first calculate the initial wave form of a tsunami due to a landslide by the analytical method. Then this initial wave form is transferred to numerical simulation program as the initial condition. We again calculate the wave form at the next time step produced by the continuing landslide. The results of the second step are added to the numerical simulations results of the former step. This routine is continued to the end of the movement of the landslide.

Analytical Solution: The Initial Wave Form.

Although the model landslide is three dimensional, we approximate it with a two dimensional model. Three dimensional initial wave forms can be represented by super-position of two dimensional wave solutions.

The submarine landslide is modeled by a rectangular slab. The slab moves horizontally on the ocean floor in an ocean of constant depth with constant velocity. The schematic view is shown in Figure 4. Here, d denotes the water depth, $2b$, ζ_0 , and V_h denote the length, thickness and velocity of the slab, respectively.

By means of time dependent Green's function (Kajiura, 1963), the initial sea surface deformation after a small duration Δt after generation is:

$$\eta_A = \frac{V_h}{\pi} \cdot \Delta t \cdot \left[\tanh^{-1} \left(\frac{\sin \left(\frac{\zeta_0}{2d} \pi \right)}{\cosh \left(\frac{x-d}{2d} \pi \right)} \right) - \tanh^{-1} \left(\frac{\sin \left(\frac{\zeta_0}{2d} \pi \right)}{\cosh \left(\frac{x+d}{2d} \pi \right)} \right) \right] \quad (1)$$

Figure 5 shows the initial forms of the tsunami caused by submarine landslide (a) for shallow water depth case, and (b) for intermediate water depth case. Tsunami generation regions are restricted to the fore and rear side of the slide. Each wave form decays fast with distance. To calculate the initial wave forms for a sloping bottom, we assumed the water depth at the generation section as locally invariant and calculated the wave forms according to equation (1), and then for the next step we increased the water depth and held it invariant for the calculations.

Although landslides occur on slopes, horizontal slab motion is justified for a model because submarine slopes on the average are in the range of 3° to 4° and because both the fore and rear waves decay rapidly with distance.

Numerical Simulation

Basic equations are:

$$\frac{\delta \eta}{\delta t} + \frac{\delta M}{\delta x} + \frac{\delta N}{\delta y} = 0 \quad (2)$$

$$\frac{\delta M}{\delta t} + gd \frac{\delta \eta}{\delta x} = \frac{\delta}{\delta x} \left[\frac{d^3}{3} F_1 \right] \quad (3)$$

$$\frac{\delta N}{\delta t} + gd \frac{\delta \eta}{\delta y} = \frac{\delta}{\delta y} \left[\frac{d^3}{3} F_1 \right] \quad (4)$$

$$F_1 = \frac{\delta^2 u}{\delta t \delta x} + \frac{\delta^2 u}{\delta t \delta y}$$

η : water level,
 M, N : discharge fluxes in x, y directions,
 $M = (d + \eta)u, N = (d + \eta)v$
 d : still water depth
 u, v : velocities in the x, y directions, and
 g : gravity constant.

The above equations are based on the linear Boussinesq approximation. As can be seen in Figure 5, the waves are not long waves. However for the intermediate water depth case, the waves generated at the fore and rear side of the slide superpose on each other and approach the shape of a long wave. So, we adopted a linear model that included dispersion effects. Whether the wave was a long wave or not was considered a posteriori.

The 300 km by 400 km region used for the simulation has been delineated in the map of Figure 1. The origin of the coordinate system was placed at the southwest corner of the region on the undisturbed free surface of the ocean. The vertical axis z is upwards; the x coordinate is positive eastward and the y coordinate is positive northward. Line LM2 which includes the landslide section is located along the coordinate $y = 200$ km. The grid size is 500 m for both the x and y directions. The time step is 1 second. We stopped the simulation at the 200 m water depth contour. Points where water depth is less than 200 m were assumed to have 200 m water depth.

RESULTS

Figure 6 shows perspective views of the tsunami after 1, 3, 7 and 15 minutes from the onset of the landslide. The landslide with sliding velocity of 20 m/s moved in the offshore direction. At the on-shore side, the first wave is a large depression followed by a small flooding, while on the offshore side the first wave is flooding followed by a depression. In Figure 6 at $t = 3$ min lapse time, a second depression can be seen. This is the result of continuous generation of tsunami due to the landslide. The wave height distributions exhibit strong dependence on the direction of the movement of the landslide. Complicated distribution of wave heights and small dispersion effect appear at $t = 15$ min. These characteristics are

quite different from those of tsunamis by tectonic movement. Both on the on-shore and off shore sides, the maximum wave height appear near the $y = 200$ km line which runs through the long axis of the landslide region.

Figure 7 shows the maximum double amplitude distributions at the 200 m water depth contour along the coast at 10 km intervals. In regards to the station numbers on the horizontal axis of the figure, Station 1 corresponds to $y = 400$ km at 200 m depth of Figure 1, and Station 21 corresponds to $y = 200$ km at 200 m depth.

The sliding velocity was varied from 5 km/s to 30 km/s. The velocity dependence of the maximum double amplitude is almost linear. Figure 8 shows the examples of numerical simulations of the Meiji Sanriku Tsunami of 1896 generated by tectonic movement type source carried out by Aida (1977). The maximum double amplitude distribution for the MJ-2 model (upper diagram, broken line profile) agrees with that of landslide tsunami for the case of sliding velocity of 30 m/s.

Figure 9 shows the water level time histories of the tsunami at several points along the 200 m depth contour. Every profile shows long wave characteristics with slight dispersion effect. the ratios of the first depression to second crest become large according to the increase of the distance from the center line of the source. This is another difference in property compared with that of a tectonic movement tsunami.

CONCLUSIONS AND DISCUSSIONS

We employed a hybrid method for the calculation of submarine landslide tsunami using a rather simple model. This method can deal quantitatively with tsunami generated by submarine landslides. The parameters necessary for the calculation are landslide dimensions (length, width, thickness), sliding velocity and direction and location of landslide.

The maximum double amplitude distribution of waves show almost the same profile as that of waves by tectonic movement tsunamis. But, we can distinguish a tsunami by landslide from a tsunami by tectonic movement from the profile of the generated wave itself.

For future reference we mention the following factors:

1. The most ambiguous part in selecting parameters of submarine landslides is the fixing of the velocity of landslides. This must be selected through the dynamics of landslides.
2. In the analytical model, we assumed the water depth was locally constant. For more accurate calculations, a generation model on a sloping bottom without long wave approximation is necessary.

ACKNOWLEDGEMENTS

The simulation program used was originally developed at Tohoku University under the TIME (Tsunami Inundation Model Exchange) project and modified by the senior author. The detailed water depth data near the Tohoku Coast was compiled by M. Okada of the Meteorological Research Institute. The authors express sincere thanks.

REFERENCES

- Aida, I., 1977, Relation between tsunami inundation heights and water surface profiles on a 200 m depth contour. *Zisin*, 30, 11-23 (in Japanese).
- Honza, E., 1978. Geological map of the Japan Trench, 1/1 million. *Marine Geol. Map Ser.* 11, Geol. Surv. Japan.
- Honza, E., A. S. Furumoto and S. I. Iwasaki, 1996. Tectonic setting and earthquakes in the Japan and Southwest Kuril Trench areas. *Sci. Tsunami Haz.*, 14, 1, 49-62.
- Jiang, L., and P. H. LeBlond, 1992. The coupling of a submarine slide and the surface waves which it generates. *Jour. Geophys. Res.*, 97, C8, 12, 731-744.
- Kajiura, K., 1963. The leading wave of a tsunami. *Bull. Earthq. Res. Inst.*, 41, 535-571.
- Moore, D. G., 1978. Submarine slides, rockslides and avalanches, 1. in *Natural Phenomena*, edited by B. Voight, Elsevier Sci. Pub. Co., 563-604.
- Murty, T. S., 1979. Submarine slide-generated water waves in Kitimat Inlet, British Columbia. *Jour. Geophys. Res.*, 84, C12, 7,777-7,779.
- Scientific Member of the Operation, 1979. Multi-channel seismic reflection data across the Japan Trench. *IPOD-Japan Basic Data Ser. 3*, Ocean Res. Inst, Univ. Tokyo, Tokyo, Japan.
- Scientific Party of Legs 56 and 57, 1980. *Initial Report of Deep Sea Drilling Project, 56, 57*. U. S. Govt. Print. Off., Washington, D. C.
- Striem, H. L., and T. Miloh, 1976. Tsunamis induced by submarine slumping off the coast of Israel. *Inter. Hydrog. Rev.*, 53 (2), 41-55.
- Wiegel, R. L., 1964. *Oceanographical Engineering*, 532 pp., Prentice Hall, Eaglewood Cliffs, N. J.

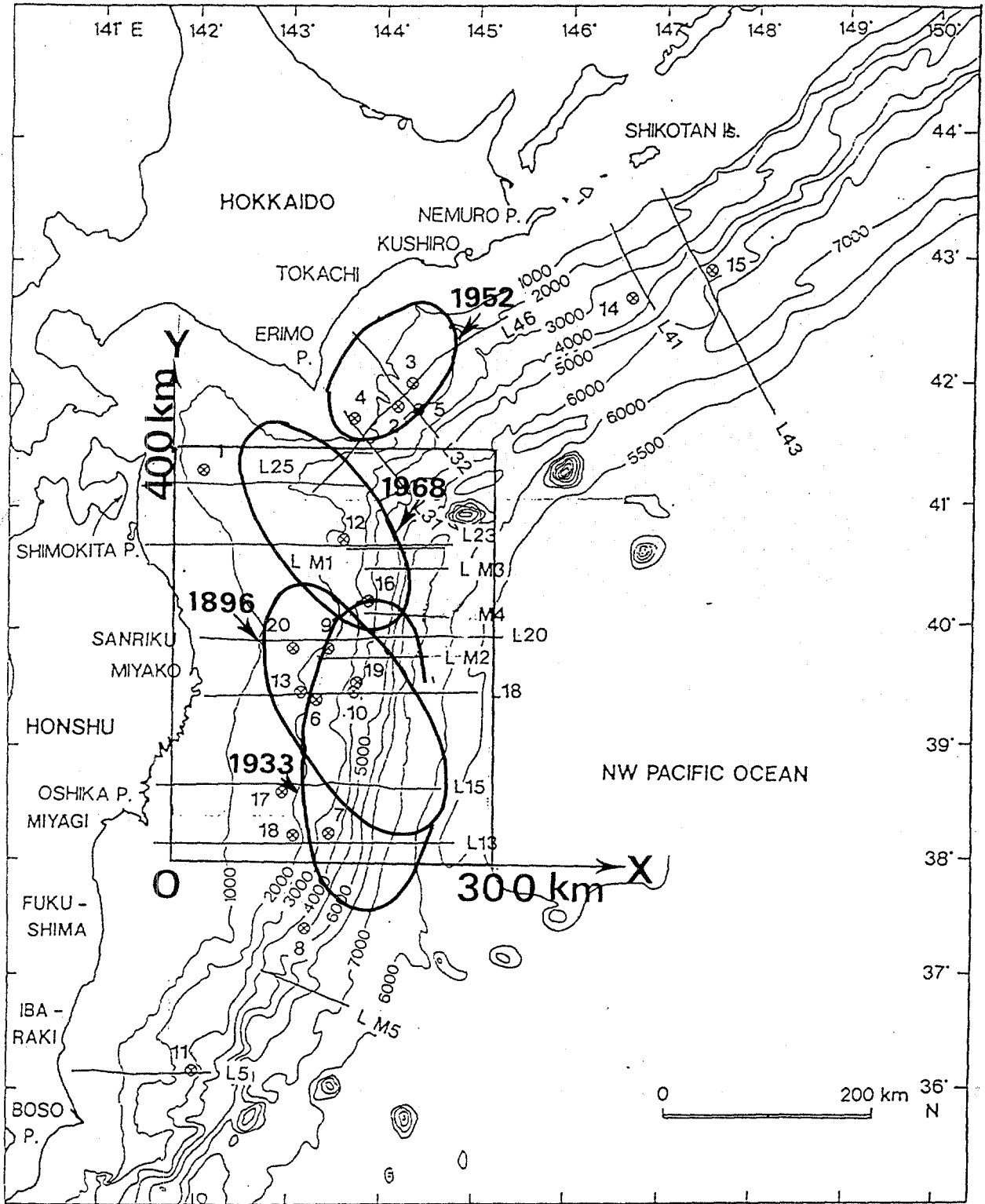


Figure 1. Track lines of single and multi-channel seismic reflection profiling. Line numbers with M mean multi-channel seismic reflection profiles. Small circles with x's show the epicenters of shallow and large earthquakes ($D < 20$ km and $M_s > 6.5$) (adapted from Honza et al., 1996). Areas encircled by bold lines are the source regions of tsunamis in 1896, 1933, 1952 and 1968. The region of numerical simulation and the coordinate system are also shown.

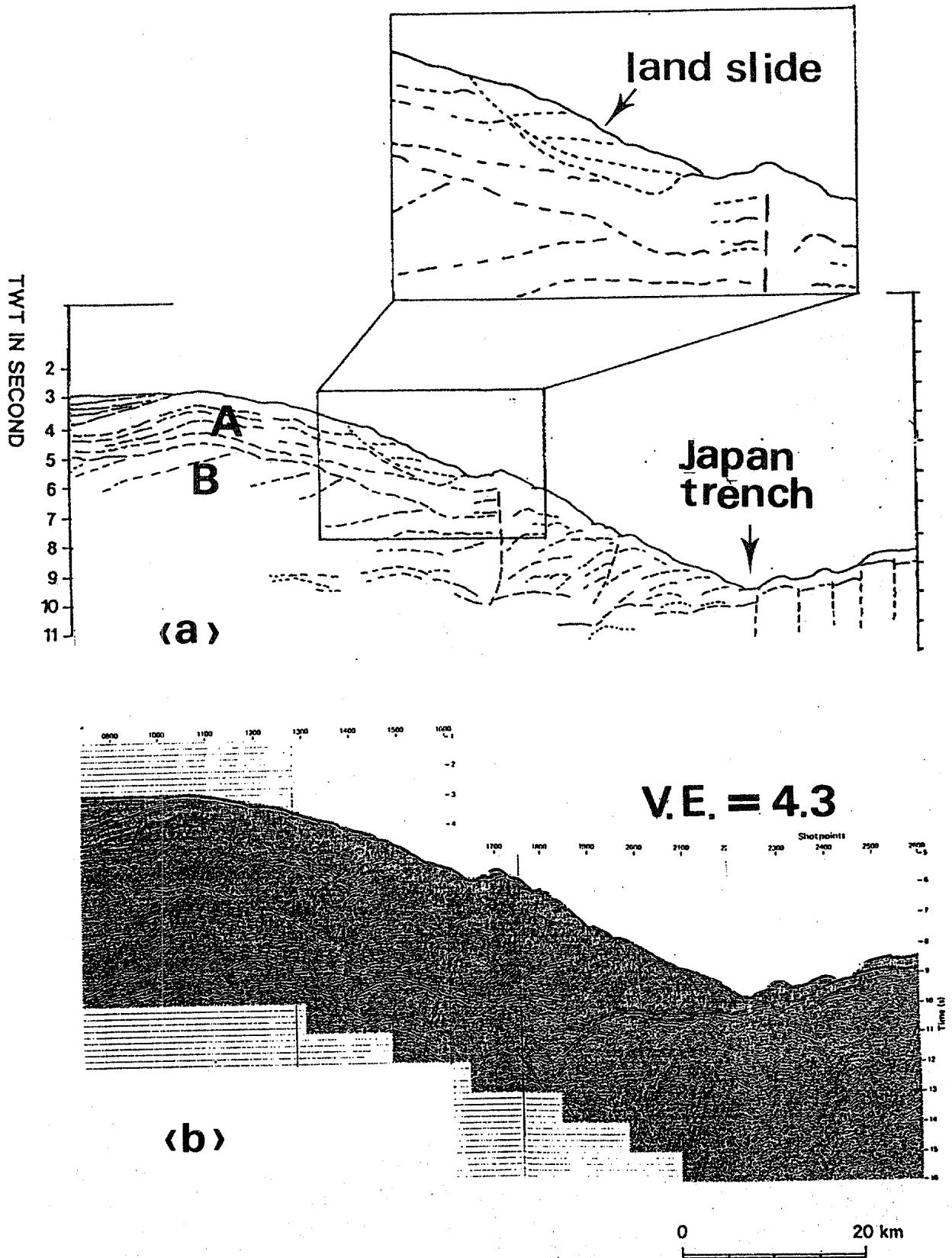


Figure 2. (a) Multi-channel seismic reflection profile with (b) original profile along the line M2. The Neogene sediments (Unit A) cover the Upper Cretaceous sediments (Unit B). Landslide traces are shown in the middle of the line M2. V. E. = vertical exaggeration.

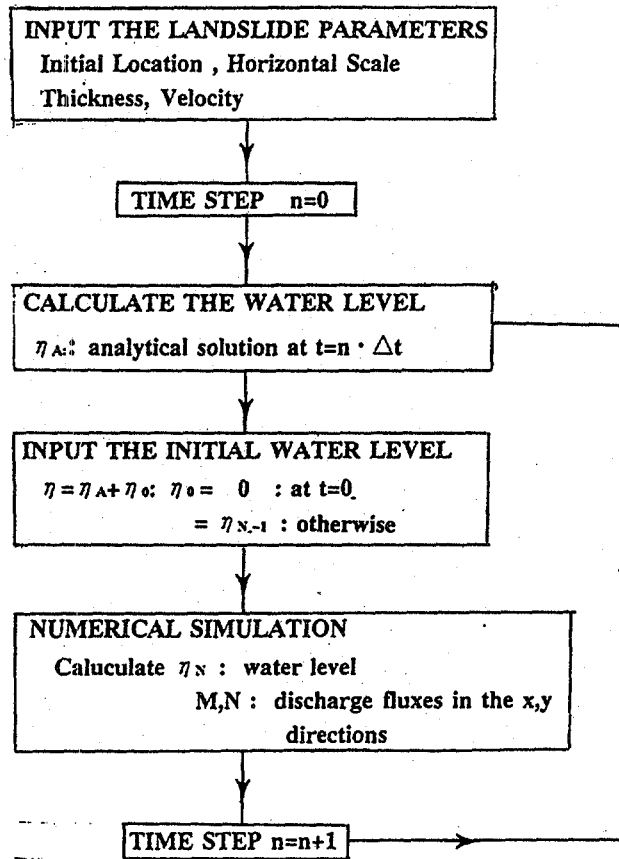


Figure 3. Flow chart of a hybrid model for the calculations of tsunamis generated by submarine landslides.

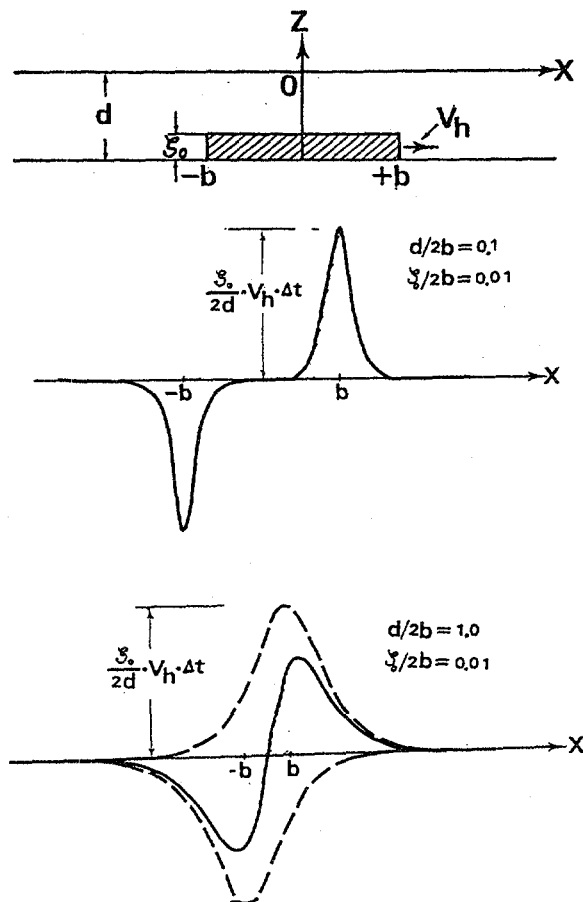


Figure 4. Schematic view of two dimensional landslide model in an ocean of constant depth. See text for symbol definitions.

Figure 5. Two dimensional initial wave profiles due to landslides for (a) shallow water depth ($d/2b = 0.1$) case and (b) intermediate water depth ($d/2b = 1.0$) case. Δt is time step. Generating sections are restricted to fore and rear side of slide. Waves decay rapidly with distance.

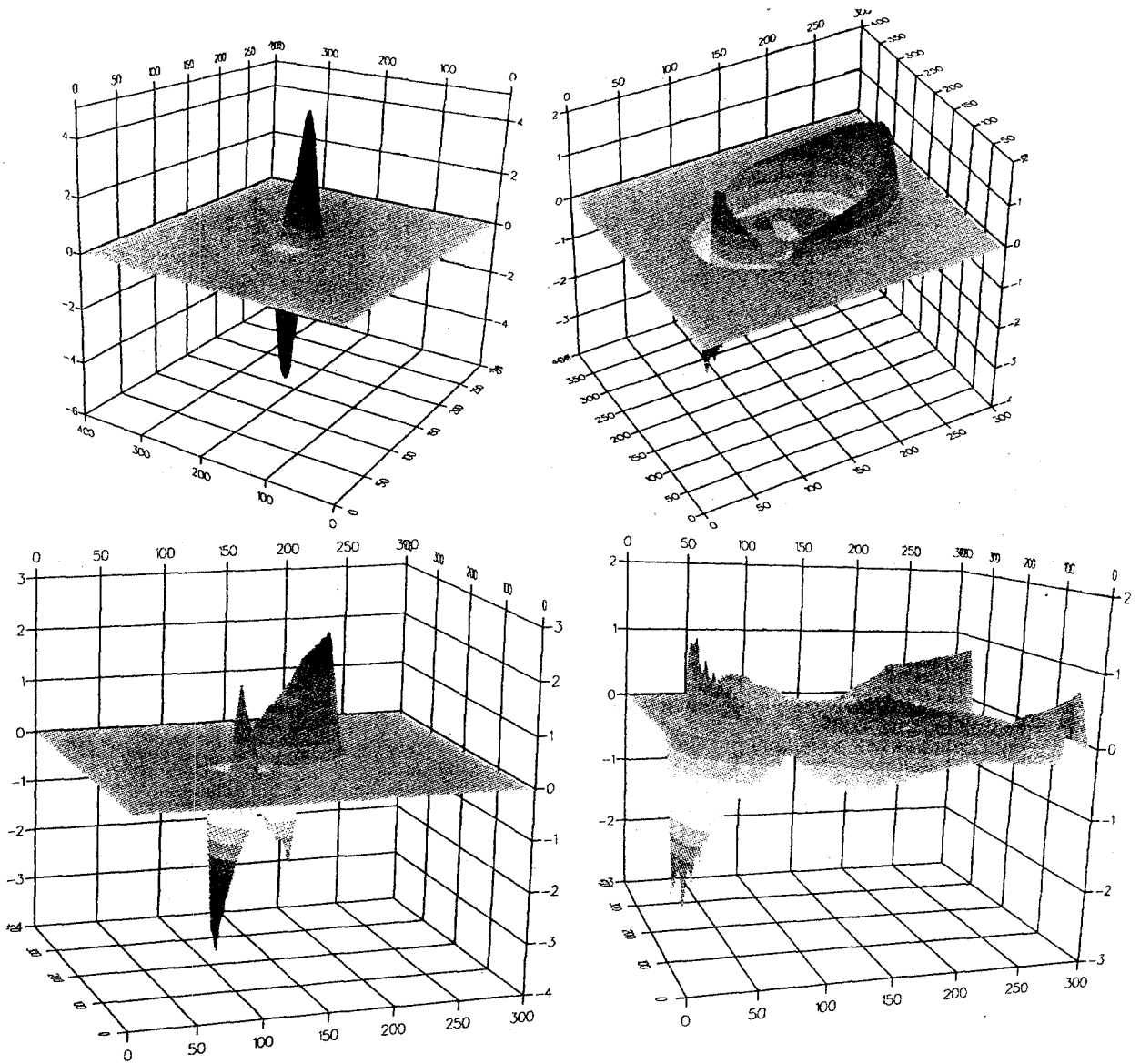


Figure 6. Perspective views of tsunamis due to landslide after 1 (upper left), 3 (lower left), 7 (upper right) and 15 (lower right) minutes from the onset of movement. The vertical axes are scaled in meters whereas the horizontal axes are scaled in kilometers.

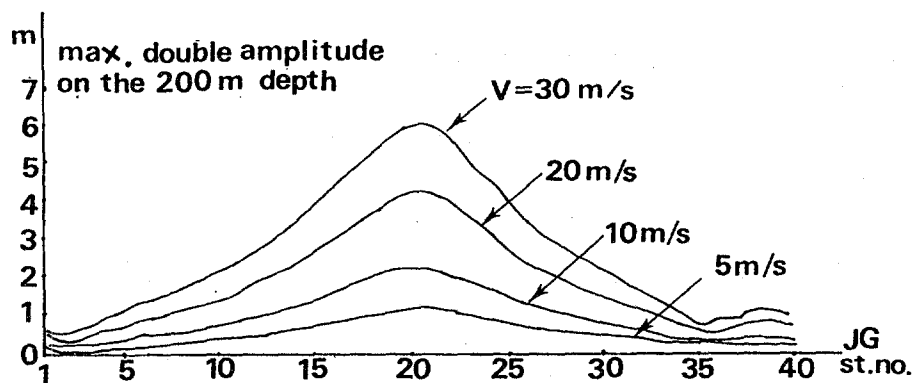


Figure 7. The maximum double amplitude distributions on the 200 m water depth contour. Velocities of landslides were varied from 5 m/s to 30 m/s. Station No. 1 corresponds to the northwest corner of the numerical simulation region. The rest of the stations were taken at 10 km intervals in the y-direction.

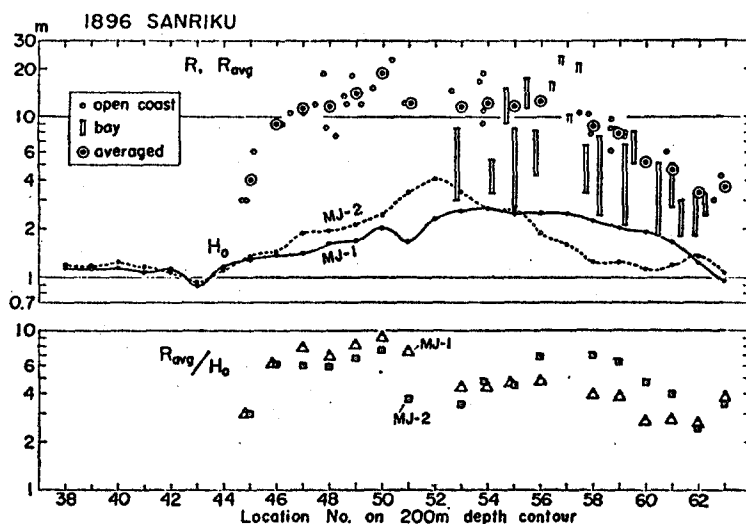


Figure 8. Numerical simulation results for the Meiji Sanriku Tsunami of 1896. The upper figure shows the maximum double amplitude distribution at the 200 m water depth contour (adapted from Aida, 1977).

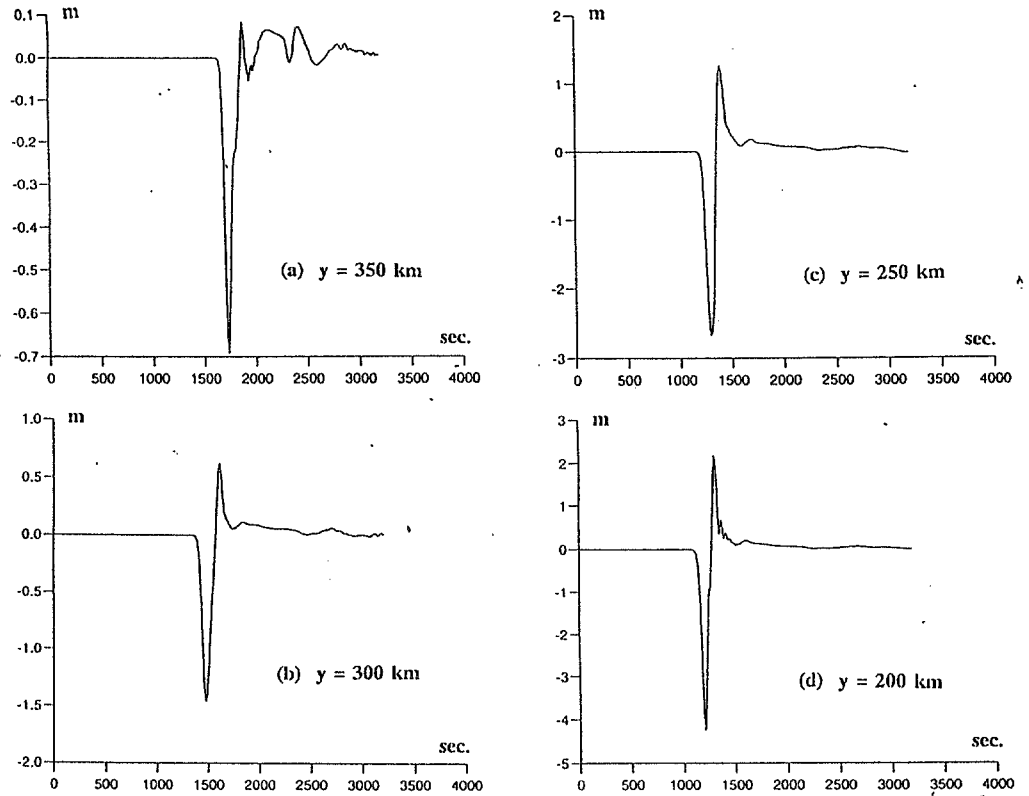
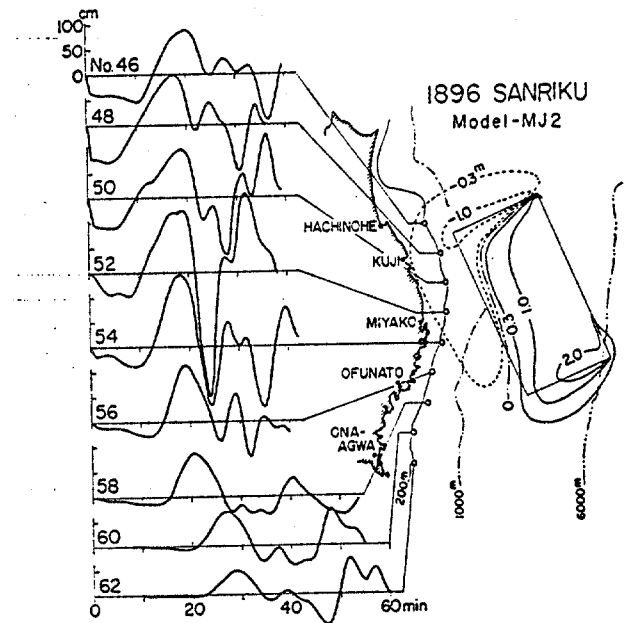


Figure 9. Water level time histories at Station 6, 11, 16 and 21.

Figure 10. Water level time histories on the 200 m water depth contour off the Tohoku district simulated by Aida (1977) for the 1896 tsunami. The tsunami generation model MJ-2 is also shown.



TSUNAMI RISK REDUCTION: THE OREGON STRATEGY

George R. Priest, Donald A. Hull, Beverly F. Vogt, Angeline Karel and Dennis L. Olmstead
Oregon Department of Geology and Mineral Industries
Suite 965, 800 NE Oregon St. #28
Portland, Oregon 97232

ABSTRACT

The Oregon coast is vulnerable to tsunami inundation from both distant and local sources. Locally generated tsunamis from M_w 8-9 earthquakes on the Cascadia subduction zone have a 10-20 percent chance of occurrence in the next 50 years, and distant tsunamis, while smaller, occur more often. Both pose a significant risk to low lying areas such as Seaside and other towns along the Oregon coast that have large permanent and transient populations. The Oregon Department of Geology and Mineral Industries (DOGAMI) is seeking to mitigate these hazards by an integrated strategy of legislative initiatives, education, warning systems, and hazard mapping. Most recently, the Oregon Legislature passed Senate Bill 379 limiting construction of essential facilities in tsunami inundation zones. DOGAMI is pursuing innovative earthquake and tsunami hazard mapping projects on the coast, both to implement this bill and to respond to local government needs.

The Oregon Department of Geology and Mineral Industries (DOGAMI) has lead responsibility for mitigation of earthquake and tsunami hazards in the State of Oregon. The risk of inundation from distant tsunamis was recognized as a result of flooding from the 1964 Alaskan tsunamis. These waves reached to elevations of 3-5 m along the open coast in Oregon, caused four deaths and \$734,000 of damage (Schatz and others, 1964; Lander and Lockridge, 1989). While worrisome, the threat from distant tsunamis did not cause any large-scale mitigation programs to be implemented at the state level. This lack of action was in large part because the international tsunami warning system based out of Hawaii and Alaska offered adequate warnings.

Heaton and Kanamori's (1984) paper alerted the Pacific Northwest of the United States and Canada that the Cascadia subduction zone was probably capable of M_w 8-9 earthquakes, and later work of Atwater (1987), Adams (1990), Darienzo and Peterson (1990) confirmed this hypothesis with geologic evidence. Later geological work demonstrated that the last Cascadia earthquake in Oregon was probably about 300 years ago, giving a 10-20 percent chance that another could occur in the next 50 years (Peterson and others, 1991; Darienzo and Peterson, 1995). This newly recognized threat from great earthquakes and tsunamis prompted DOGAMI to begin an accelerated mitigation program in 1987. The program initially focused mainly on earthquake risk to Oregon's largest population center, Portland, but has, in the last five years expanded to include tsunami hazards. Starting with a modest educational effort, principally oral presentations to decision makers, the program rapidly expanded and has led to extensive inundation mapping and passage of legislation aimed at tsunami risk reduction.

The current Oregon strategy is aimed at four parallel approaches:

1. Public education
2. Inundation mapping
3. Legislation limiting construction of essential facilities in inundation zones
4. Warning systems

PUBLIC EDUCATION

One of the most cost effective educational tools is installation of permanent and semi-permanent warning signs. A group of interested state and local workers cooperated to design logos for all tsunami warning and evacuation signs, so the public will immediately recognize the hazard when they see the logos (Figure 1). It is hoped that other Pacific Rim governments utilize the same graphic design, so visitors will see the same logo wherever they travel. The graphics and specifications for the signs are available at the following address:

Orville Gaylor
Traffic Section, Oregon Department of Transportation
132 Transportation Bldg.
Salem, Oregon 97310
Phone: 503-986-3603
e-mail: orville.d.gaylor@state.or.us

A second type of sign is the educational marker. These large, imposing signs have been installed in areas where physical evidence of past Cascadia subduction zone tsunamis has been discovered. They are permanent installations that have instructions for tsunami response, illustrations of the subduction zone fault, and locations where in the local area the tsunami deposits have been found.

Other steps in the education effort include publication of an article in a popular tourism magazine, articles in technical journals, coordination with educational organizations, and state legislation. In 1995 the Oregon Legislature passed Senate Bill 378 (SB 378) which requires schools in potential inundation zones to teach students in grades kindergarten through eight about tsunamis and evacuation. SB 378 requires three evacuation drills a year in these schools. Local emergency managers will guide the schools in evacuation planning. Coordination between DOGAMI, Oregon Emergency Management, the Oregon Department of Education, and the Oregon Museum of Science and Industry, has resulted in an outreach plan that will utilize educational service districts, Federal Emergency Management Agency "Tremor Troops," and the Internet to teach about tsunami hazards and mitigation measures.



Figure 1. Official tsunami warning and evacuation signs for the State of Oregon. The evacuation sign has a separate arrow that goes beneath to show the safest evacuation direction. The color of the signs is blue, not black, as shown in this illustration.

Other educational efforts include visits to media contacts, preparation of a video, and publication of a general interest brochure. As evacuation routes are defined in coastal communities, we plan to work with telephone companies to include evacuation information in telephone books.

INUNDATION MAPPING

Inundation maps at the local and regional reconnaissance level were completed and published by the Department in 1995. Local detailed maps at both the 1:12,000 and 1:4,800 scale were completed as a pilot study in the Siletz Bay area (Priest and others, 1995; Baptista and others, 1995; Peterson and others, 1995). Companion earthquake hazard maps illustrating zones of potential liquefaction, slope instability, and amplification of shaking were also produced for Siletz Bay (Wang and Priest, 1995). Additional detailed inundation mapping projects have been funded for the Yaquina Bay and Seaside-Gearhart areas. The entire coast was mapped at the reconnaissance scale of 1:24,000,¹ utilizing a partnership between DOGAMI and the Oregon Graduate Institute of Science & Technology (Priest, 1995). The latter maps were produced to implement Oregon Senate Bill 379, which limits construction of certain essential and special occupancy buildings in the tsunami inundation zone.

TSUNAMI HAZARD MITIGATION BY SENATE BILL 379

Senate Bill 379 (SB 379) was passed by the Oregon Legislature in 1995. It requires DOGAMI to map the zone of expected tsunami inundation as basis for limiting new construction of essential and special occupancy facilities. Examples of essential facilities prohibited from construction in the inundation zone include schools, hospitals, fire stations, police stations and emergency response facilities. The bill also requires developers of larger buildings to consider alternative mitigation strategies prior to construction, if the building must be built in the inundation zone. The new law provides a review process for granting exceptions to the prohibition in situations that require an essential facility to be located in the inundation zone. DOGAMI is responsible for reviewing requests for exceptions and providing review and consultation for mitigation plans. SB 379 is expected to result in improved public safety as new buildings are constructed in coastal towns, many of which are experiencing rapid population growth.

FEDERAL LEGISLATION

The United States Congress is considering legislation to develop a national system of insurance for natural hazards, including earthquakes, hurricanes, volcanic eruptions and tsunamis. This 1995 legislation (Senate 1043 and House of Representatives 1856) includes tsunami mitigation measures that could lead to improved preparation in Oregon and other states on the Pacific coast.

WARNING SYSTEM

The existing international tsunami warning system is not designed to be effective in the short interval between a Cascadia subduction zone earthquake and arrival of the first tsunami

¹ These maps (DOGAMI Open-File Reports O-95-9 through O-95-66) are available from the Nature of the Northwest Information Center, (phone: 503-872-2750 or e-mail: naturenw@state.or.us).

wave. The State of Oregon is working with a coalition of Federal and state government agencies to improve tsunami warning for local Cascadia earthquakes. Federal agencies cooperating in this effort are the National Oceanic and Atmospheric Administration, U.S. Geological Survey and Federal Emergency Management Agency. Cooperating states are Alaska, California, Hawaii, Oregon and Washington.

Some coastal towns are developing their own warning systems to mitigate the threat from Cascadia tsunamis. The leading example is the City of Cannon Beach on the northern Oregon coast, where a system of solar-powered loud speakers has been installed. The monthly testing of this system provides an important tool for continuing public education. When testing occurs, the loudspeakers broadcast the sound of a cow "mooing" rather than an actual siren, so there can be no mistaking a test for the actual warning. The system is activated by a local fire department operator, so it is not entirely automated but depends on human judgment. So far the system has only been activated once, when slight shaking was felt from a 1993 crustal earthquake. The low seismicity of most of the Oregon coast generally leads to few such false alarms.

OTHER MITIGATION EFFORTS

DOGAMI conducted a preliminary inventory of critical and essential facilities vulnerable to earthquake or tsunami hazards on the Oregon coast (Charland and Priest, 1995). This work alerted local authorities about potential vulnerability of their critical buildings to the combined hazards of shaking and tsunami inundation. The work laid the groundwork for later passage of Senate Bill 379.

There is a current effort in Oregon to formulate guidelines for preparation of site specific seismic hazard reports. The guidelines, if adopted by professional licensing boards for geologists and engineers, will contain requirements for tsunami hazard assessment at coastal sites.

MEASURING AND MAINTAINING EFFECTIVENESS

Without the reminder of frequent earthquakes and tsunamis, the State of Oregon must work continuously to keep awareness at a high level. DOGAMI measures the effectiveness of mitigation efforts, particularly public education, by polling. These polls have shown a steady increase of public awareness of the tsunami hazard over the last few years, but a large proportion of the population is still unaware, so there is room for much improvement.

REFERENCES CITED

- Atwater, B.F., 1987, Evidence for great Holocene earthquakes along the outer coast of Washington State: *Science*, v. 236, p.942-944.
- Adams, J., 1990, Paleoseismicity of the Cascadia subduction zone turbidites off the Oregon-Washington margin: *Tectonics*, v. 9, p. 569-583

- Baptista, A.M., Qi, Ming, and Myers, E.P., III, 1995, Siletz Bay: A pilot investigation of coastal inundation by Cascadia subduction zone tsunamis, *in* Priest, G.R., ed., Explanation of mapping methods and use of the tsunami hazard map of the Siletz Bay area, Lincoln County, Oregon: Oregon Department of Geology and Mineral Industries Open-File Report O-95-5, p. 21-44
- Charland, J.W., and Priest, G.R., 1995, Inventory of critical and essential facilities vulnerable to earthquake or tsunami hazards on the Oregon coast: Oregon Department of Geology and Mineral Industries, Open-File Report O-95-2, 52 p.
- Dariento, M.E., and Peterson, C.D., 1990, Episodic tectonic subsidence of late Holocene salt marshes, northern Oregon central Cascadia margin: *Tectonics*, v. 9, no. 1, p. 1-22.
- Dariento, M.E., and Peterson, C.D., 1995, Magnitude and frequency of subduction-zone earthquakes along the northern Oregon coast in the past 3,000 years: *Oregon Geology*, v. 57, no. 1, p. 3-12.
- Heaton, T.H., and Kanamori, H., 1984, Seismic potential associated with subduction in the northwestern United States: *Bulletin of the Seismological Society of America*, v. 74, no. 3, p. 933-941.
- Lander, J.F., and Lockridge, P.A., 1989, United States tsunamis (including United States possessions) 1690-1988: National Oceanic and Atmospheric Administration Publication 41-2, 265 p.
- Peterson, C.D., Dariento, M.E., and Clough, C., 1991, Recurrence intervals of coseismic subsidence events in northern Oregon bays of the Cascadian margin: Final technical progress report to Oregon Department of Geology and Mineral Industries, 14 p.
- Peterson, C.D., Dariento, M.E., Doyle, D., and Barnett, E., 1995, Evidence for coseismic subsidence and tsunami inundation during the past 3,000 years at Siletz Bay, Oregon, *in* Priest, G.R., ed., Explanation of mapping methods and use of the tsunami hazard map of the Siletz Bay area, Lincoln County, Oregon: Oregon Department of Geology and Mineral Industries Open-File Report O-95-5, p. 45-69
- Priest, G.R., 1995, Explanation of mapping methods and use of the tsunami hazard maps of the Oregon coast: Oregon Department of Geology and Mineral Industries, Open-File Report O-95-67, 95 p.
- Priest, G.R., Baptista, A.M. Qi, M., Peterson, C.D., and Dariento, M.E., 1995, Simplified explanation of the tsunami hazard map of the Siletz Bay area, Lincoln County, Oregon, *in* Priest, G.R., ed., Explanation of mapping methods and use of the tsunami hazard map of the Siletz Bay area, Lincoln County, Oregon: Oregon Department of Geology and Mineral Industries Open-File Report O-95-5, p. 1-20.
- Schatz, C.E., Curl, H.C., Jr., and Burt, W.V., 1964, Tsunamis on the Oregon coast: Oregon Department of Geology and Mineral Industries, *Ore Bin*, v. 26, no. 12, p. 231-232.
- Wang, Y., and Priest, G.R., 1995, Relative earthquake hazard maps of the Siletz Bay area, coastal Lincoln County, Oregon: Oregon Department of Geology and Mineral Industries GMS-93, 3 1:12,000 scale maps and text.

USING M_w OR M_t TO FORECAST TSUNAMI HEIGHTS

Augustine S. Furumoto
Tsunami Adviser
Office of the Vice Director for Civil Defense
State of Hawaii
Honolulu, Hawaii, U. S. A.

ABSTRACT

Methods to forecast tsunami heights in real time using moment magnitude by seismic data M_w or moment magnitude by tsunami data M_t are proposed. But before these methods could be used, a forecaster must ascertain whether a tsunami earthquake has occurred or not. If a tsunami earthquake has occurred, then the forecaster must determine M_t . Tsunami earthquakes are prone to occur very close to a subduction trench on the continental side of the trench.

To obtain M_t , the forecaster should use the arrival times of the tsunami at tide stations one to two hours travel time from the epicenter. Using tsunami travel time charts for the tide stations, the tsunami generating area is outlined. From the length of the long axis of the generating area, the moment magnitude by tsunami data M_t is derived.

From M_w (for earthquakes that are not tsunami earthquakes) or from M_t the tsunami height in the open ocean in the far field can be calculated by the method proposed by Ward (1982) and the expected run-up height at selected sites can be forecast by inversion of the formula for calculating M_t as originally proposed by Katsuyuki Abe (1981).

As juggling figures and using calculators to apply the formulas in real time under the stress of a tsunami alert exposes the forecaster to dangerous mistakes, numerical tables were developed to avoid calculations during an alert.

These methods were tested, after the fact, for the Kurile tsunami of October 4, 1994. The methods gave accurate forecasts for tsunami height in the deep ocean off the Washington-Oregon coast and for wave heights in Honolulu Harbor and Hilo Harbor in Hawaii.

INTRODUCTION

First, a few concepts to be used in this paper will be clarified.

A *tsunamigenic earthquake* is an earthquake that has generated a tsunami.

Seismic moment M_0 has been defined as,

$$M_0 = \mu s A, \quad (1)$$

where μ is the modulus of rigidity of the rocks in which an earthquake fault is embedded, s is the average slip that has occurred during an earthquake and A is the area of the fault face. As M_0 is a very large number, a more convenient index called *seismic moment magnitude* M_w is more frequently used (Bolt, 1988):

$$M_w = (2/3) \log M_0 - 10.7, \quad (2)$$

where M_0 is in dyne-cm. When M_0 is expressed in newton-meters, the defining equation (2) becomes,

$$M_w = (2/3) \log M_0 - 6.033. \quad (3)$$

We distinguish between M_w and M_t , which is *moment magnitude determined by tsunami data*. Generally M_w and M_t for tsunamigenic earthquakes agree numerically, as M_t was defined so as to agree with M_w numerically. But there have been a few instances where M_w and M_t did not agree. A notable case was the Aleutian earthquake of April 1, 1946. Kanamori's (1972) analysis using elastic wave data yielded $M_w = 7.8$, and the analysis by Brune and Engen (1969) also using elastic wave data resulted in $M_w = 8$. Meanwhile Abe (1981 b) using tsunami data found $M_t = 9.3$. Tsunamigenic earthquakes with M_t values larger than M_w values are called *tsunami earthquakes* (Kanamori, 1972).

In forecasting tsunamic heights in the distant field, whether wave height in the deep ocean or tsunami run-up at a distant coast, the value that should be used is M_t . As in 90% of tsunamigenic earthquakes, M_w and M_t agree numerically, M_w will do; but forecasters in real time must be certain that the values agree. In case of disagreement of values, M_t is to be used.

Once the value of M_t is in hand, forecasters can use the method of Ward (1982) for estimating the tsunami wave height in the deep ocean or that of Abe (1981 a) to estimate tsunami run-ups at distant shores.

In this paper we explain the technique of determining M_t in real time and then illustrate the applications of Ward's and Abe's methods.

DETERMINING MOMENT MAGNITUDE M_t BY TSUNAMI DATA

Tide gauge data from scores of tide stations throughout the Pacific Basin are being routinely telemetered to the Pacific Tsunami Warning Center (PTWC). Digitized tide records are compressed and sent to PTWC every hour from tide stations considered to be critical for tsunami monitoring, and every three hours from stations with lower priority. During a tsunami watch following the occurrence of a potentially tsunamigenic earthquake, PTWC issues bulletins listing the source parameters of epicentral latitude and longitude, origin time and surface wave magnitude. Then the bulletin lists the expected time of arrival of tsunami at various tide stations and population centers. About an hour after the origin time of the earthquake, Laboratoire Geophysique in Papeete, Tahiti, will inform the PTWC the value of seismic moment M_0

determined from its array of ultra-long period seismometers. From this value of M_0 , the first estimates of tsunami heights can be made.

However the tsunami forecaster must be certain whether he is dealing with a tsunami earthquake or not. Tsunami earthquakes occur close to subduction trenches and on the continental side of the trench (Tanioka and Satake 1996). If the earthquake did occur close to the trench, the forecaster must use tsunami data to establish the size of the tsunami generating source and in turn the M_t .

As the tsunami arrives at various tide stations away from the tsunami source area and as the data are telemetered to PTWC, the arrival times and maximum wave heights as recorded by the tide gauges are listed on the tsunami bulletin. When such a bulletin has been received by emergency management agencies of states, provinces and equivalent political entities in the far field, the forecaster of each agency can use the arrival times listed in the bulletin to determine the tsunami source area and then the moment magnitude M_t , by the technique described in the next few paragraphs.

The origin time of the earthquake is subtracted from the arrival times at tide stations to obtain the tsunami travel times. Using Tsunami Travel Time Charts published by the National Ocean Survey of the National Oceanic and Atmospheric Administration (NOAA) in 1972, arcs are drawn on a map of the Pacific Ocean to outline the tsunami generating source. An example of the tsunami travel time chart usable for the tide station in Adak is shown in Figure 1. For Japanese tide stations, M. Okada of the Meteorological Research Institute of the Japan Meteorological Agency has produced tsunami travel time charts with contour intervals in minutes (Figure 2).

The source area for the Kurile tsunami of October 4, 1994, outlined by retracing tsunami travel times, is shown in Figure 3. The northern margin of the source area is indeterminate because of lack of data from stations to the north. However a unilateral slip was assumed to establish the northern boundary.

From the tsunami source area, the length L of the major axis is measured in kilometers. Ward (1982) has shown that empirically L is related to M_0 , the seismic moment, by

$$L = M_0^{.33284} / (5.684 \times 10^4), \quad (4)$$

where M_0 is in newton-m. If we approximate the exponent of M_0 by .333, the equation simplifies to

$$\log M_0 = 14.264 + 3 \log L. \quad (5)$$

Substitute $\log M_0$ into equation 3 to obtain M_w , or in this case M_t . In the example of Figure 3, the length L is 220 km, so that

$$\begin{aligned} M_0 &= 2 \times 10^{21} \text{ N-m, and} \\ M_t &= 8.2. \end{aligned} \quad (6)$$

These were the parameters of the earthquake.

During a tsunami watch or alert, to lessen the chances of error arising from stress, instead of juggling with formulas and calculators, it is better to use Table 1 to obtain M_t if the value of L has been determined.

TABLE 1
RELATIONS AMONG M_w , M_t , M_o AND L

Moment Magnitude M_w or M_t	Seismic Moment M_o $\times 10^{20}$ N-m	Rupture Length L km
8	11.2	183
8.1	15.8	205
8.2	22.4	230
8.3	31.6	258
8.4	44.6	290
8.5	63.0	325
8.6	89.0	365
8.7	126	409
8.8	178	459
8.9	251	515
9.0	354	578
9.1	501	648
9.2	707	728
9.3	999	816
9.4	1410	916
9.5	1993	1028
9.6	2815	1153
9.7	3977	1294
9.8	5617	1452
9.9	7935	1629
10.0	11200	1827

FORECASTING TSUNAMI HEIGHT IN DEEP OCEAN

Ward (1982) plotted available data on tsunami heights in the deep ocean as a function of moment magnitude and distance from the tsunami source. The tsunami source is assumed to be an elongated ellipse and the distance is measured in the direction perpendicular to the strike of the vertical dip slip fault. He plotted the data on a graph and then drew lines through the graph corresponding to distances of 1000, 3000, 5000 and 7000 km. The figure is not shown here because I have not yet applied for permission from the author to use the figure.

However using the figure from Ward (1982), Table 2 was derived to forecast tsunami height in the deep ocean for given moment magnitude and distance from the source.

TABLE 2
OPEN OCEAN TSUNAMI HEIGHT (in meters)
BY DISTANCE AND MOMENT MAGNITUDE
(Using Ward, 1982)

Mw	1000 km	3000 km	5000 km	7000 km
7.5	0.05	0.01		
8.0	0.3	0.1	0.06	0.02
8.5	1.3	0.5	0.3	0.2
9.0	4.5	1.9	1.2	0.9
9.5	10	6.0	4.3	3.0

FORECASTING TSUNAMI WAVE HEIGHTS AT DISTANT COASTS

Abe (1981 a) has worked out the correlation between moment magnitude M_t and tsunami run-up for several selected places. The selected places were Honolulu and Hilo in Hawaii, the California coast, the Aleutian islands and the coasts of Japan. The correlation took into account the location of tsunami sources, as the direction of arrival of a tsunami greatly affects the height of the tsunami at any given bay or harbor.

In Abe's correlation, the height H of the run-up in meters is related to M_t by the equation:

$$M_t = \log H + B; \quad B = C + \Delta C, \quad (7)$$

where C was set at 9.1 and ΔC is the correction factor for a tsunami from a selected source to a particular distant coast.

In Table 3, for the column on Hilo, Abe(1981 a) had the value of 0.0 for the source region of Aleutians, but as this seems to have been an error, a recalculation using historic data yielded value of -0.7, which was inserted into the table. The inserted value is compatible with run-ups for the events of 1938, 1946, 1957 and 1986.

Table 3. VALUES OF ΔC

Source Region	Honolulu	Hilo	California	Japan	Aleutians
Peru, Chile	0.2	-0.6	0.2	0.0	0.2
Aleutians	0.5	-0.7	0.2	0.3	
Kamchatka, Kuriles, Japan	0.2	-0.3	0.2	0.0	0.0

Table 4 for Honolulu and Table 5 for Hilo were compiled using equation (7) with the appropriate correction factors.

TABLE 4.
EXPECTED TSUNAMI RUN-UPS (in meters) FOR HONOLULU
FOR SELECTED SOURCES AND MOMENT MAGNITUDE

Mt or Mw	Peru, Chile	Aleutians	Kamchatka, Kurile, Japan
7.6	0.02	0.01	0.03
7.8	0.03	0.02	0.05
8.0	0.05	0.03	0.08
8.2	0.07	0.04	0.13
8.4	0.13	0.06	0.20
8.6	0.2	0.1	0.32
8.8	0.32	0.16	0.50
9.0	0.5	0.25	0.8
9.2	0.8	0.4	1.3
9.4	1.3	0.6	2.0
9.6	2.0	1.0	3.2
9.8	3.2	1.6	5.0
10	5.0	2.5	8

TABLE 5.
 EXPECTED TSUNAMI RUN-UPS (in meters) FOR HILO
 FOR SELECTED SOURCES AND MOMENT MAGNITUDE

Mt or Mw	Peru, Chile	Aleutians	Kamchatka, Kuriles, Japan
7.6	0.12	0.15	0.08
7.8	0.2	0.3	0.13
8.0	0.3	0.4	0.2
8.2	0.5	0.6	0.3
8.4	0.8	1	0.5
8.6	1.3	1.6	0.8
8.8	2.0	2.5	1.3
9.0	3.2	4.0	2.0
9.2	5	6.3	3.2
9.4	8	10	5
9.6	13	16	8
9.8	20	25	13
10	32	40	16

TESTING THE METHODS

The methods were tested in hind sight using the case of Kurile tsunami of October 4, 1994. The Laboratoire Geophysique of Papeete reported Mw to be 8.2. Retracing tsunami travel times gave source length of 220 km, which corresponds to Mt = 8.2. As Mw = Mt, this was not a tsunami earthquake.

At the time of the tsunami, a sea bottom pressure gauge installed by the Pacific Marine Environment Laboratory of NOAA was operating at 45.5° N, 130° W, west of the Oregon-Washington coast. When the recorder of the pressure gauge was retrieved, it contained a clear record of the October 4, 1994 tsunami (Figure 4). The recorded maximum tsunami height was 6 cm. As the distance from the source to the gauge was 6200 km and as Mw = Mt = 8.2, interpolation with Table 2 gave an expected tsunami height of 6 cm. This agreement is satisfactory.

For wave heights at distant coastlines, Honolulu Harbor and Hilo Harbor in Hawaii were

selected because of availability of data. Visual observation in Honolulu Harbor gave a double amplitude wave height of about 1 foot (Sigrist 1994), for an amplitude of about 15 cm. The tide gauge at Hilo recorded a 30 cm amplitude as maximum. Both values agree with Tables 4 and 5. The agreement is very satisfactory.

Figure 4 includes tide gauge records of the tsunami for Port Orford and Newport, both in Oregon. Application of the formula for the California coast did not give agreeable results. The constant listed under California were obviously calculated from data along the open coastline of California. For ports, harbors and inlets, the constants for Abe's formula must be calculated separately using historical data. This was done for the case of Hilo Harbor.

CONCLUSIONS

With the methods described in this paper, forecasting tsunami wave heights in real time in the open ocean and wave heights at selected distant coasts is now possible. Without doubt, forecast methods using numerical simulation and calculation would be more reliable and more accurate, but these simulation methods have not been adapted to be useful in real time situations. Even if numerical simulation methods become fully operational, the Mw, Mt methods proposed here can be a "first cut" attempt in real time forecasting.

Application of these methods requires the rapid distribution of tide gauge data by PTWC in real time. Perhaps arrangements can be made so that tide gauge data are automatically listed in computer network bulletin boards so that the various regional emergency management agencies can freely tap the data bank in real time.

Forecasting should be the responsibility of various regional and local emergency management agencies. PTWC can hardly be expected to issue forecasts to all places, especially when each harbor and port has its own response system, as evidenced by tide gauge records of Port Orford and Newport.

But we do hope that PTWC will develop the capability to discern whether a detected tsunamigenic earthquake is a tsunami earthquake or not.

When sea bottom gages in the deep ocean starts operating routinely, the data from these gauges will be a great boon for outlining the tsunami source. In addition, data from these gauges will tell us the shape of the tsunami wave train, a bit of information very useful in forecasting what would be the response of a vital harbor to the approaching tsunami.

ACKNOWLEDGEMENTS

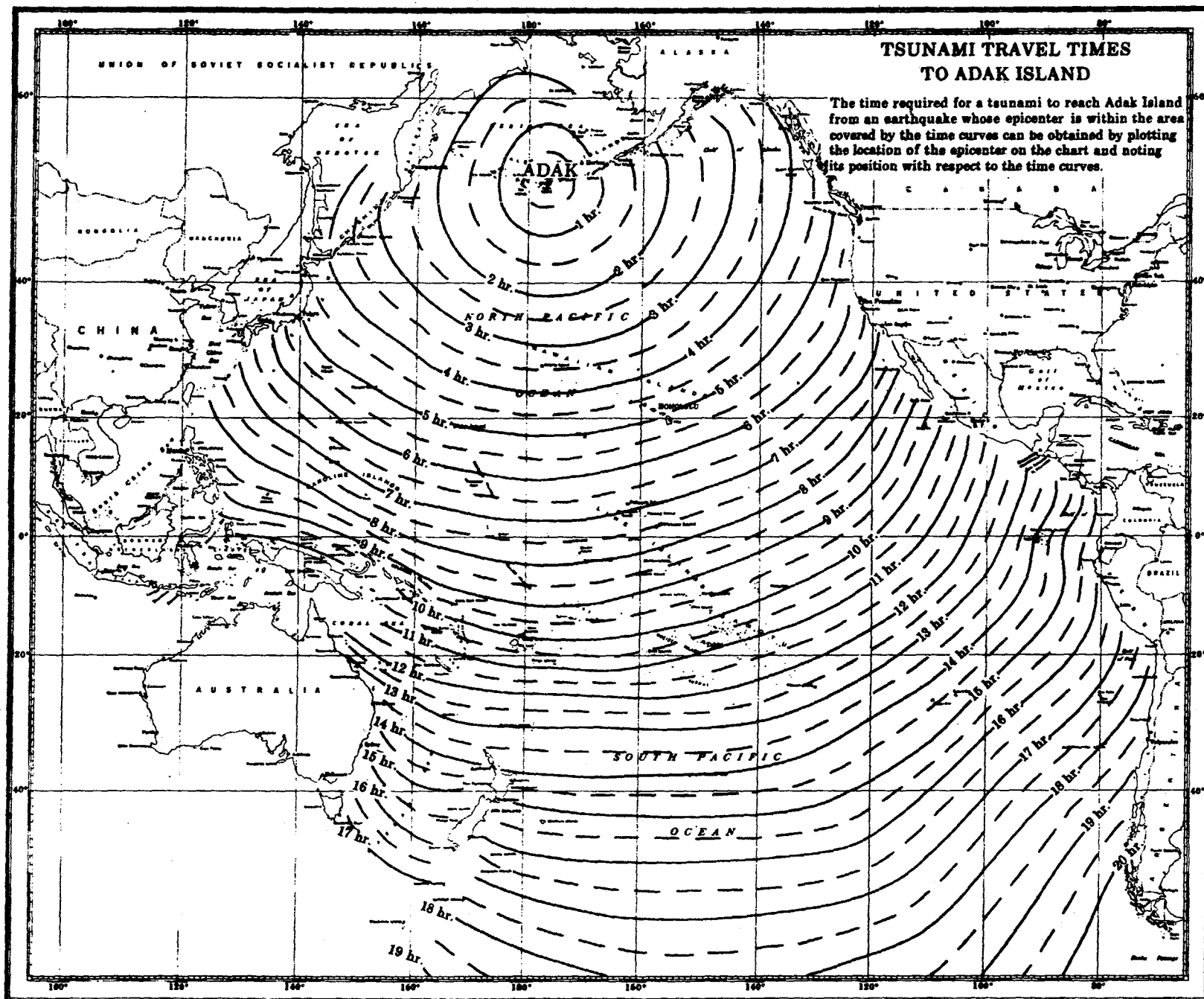
I thank M. Okada of the Meteorological Research Institute at Tsukuba, Japan, for inviting me often to his institute for cooperative research. This paper is one of the products of the visits.

I also thank Dr. Eddie Bernard of PMEL-NOAA for the use of Figure 4, and especially for the tsunami mitigation workshops he has arranged which provided much inspiration for this paper.

REFERENCES

1. Katsuyuki, 1981 a. "A new scale of tsunami magnitude, Mt." in *Tsunamis: their Science and Engineering*. ed. K. Iida and T. Iwasaki. Terra Sci Pub. Tokyo. pp 91-101.
2. Abe, K., 1981 b. "Magnitudes of large shallow earthquakes from 1904 to 1980." *Phys. Earth Planet. Int.*, vol. 27, 72-92.
3. Bernard, Eddie, 1996. Workshop Number 4 on Tsunami Mitigation Initiative, February 12-14, 1996.
4. Brune, J., and G. Engen, 1969. "Excitation of mantle love waves and definition of mantle wave magnitude." *Bull. Seism. Soc. Am.*, vol 59, 923-933.
5. Kanamori, H., 1972. "Mechanism of tsunami earthquakes." *Phys. Earth Planet. Int.*, vol. 6, 346-359.
6. National Ocean Survey, 1971. *Tsunami Travel Time Charts, for Use in the Tsunami Warning System*. National Oceanic and Atmospheric Administration, Rockville, MD.
7. Sigrist, Dennis, 1994. Private communication.
8. Tanioka, Y., and K. Satake, 1996. "Fault parameters of the 1896 Sanriku Tsunami Earthquake as estimated from tsunami numerical modeling." Paper presented at Two Great Tsunamis: U. S. Japan Anniversary Symposium, April 1996.
9. Ward, S. N. 1982. "On tsunami nucleation, II. An instantaneous modulated source." *Phys. Earth Planet. Int.*, vol. 27, 272-285.

Figure 1. Tsunami Travel Times to Adak Island. (from National Ocean Survey, 1971)



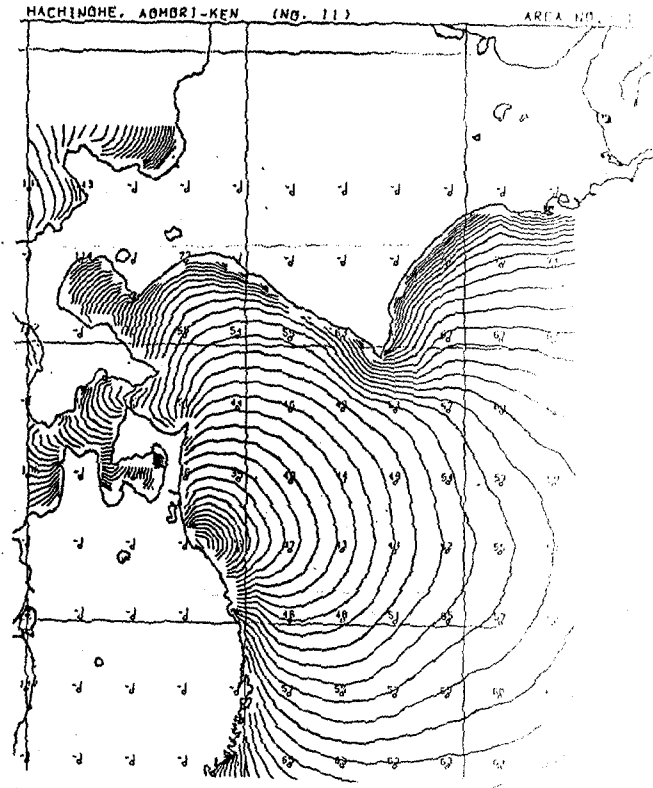


Figure 2. Tsunami Travel Times to Hachinohe, Japan. (Courtesy of M. Okada)

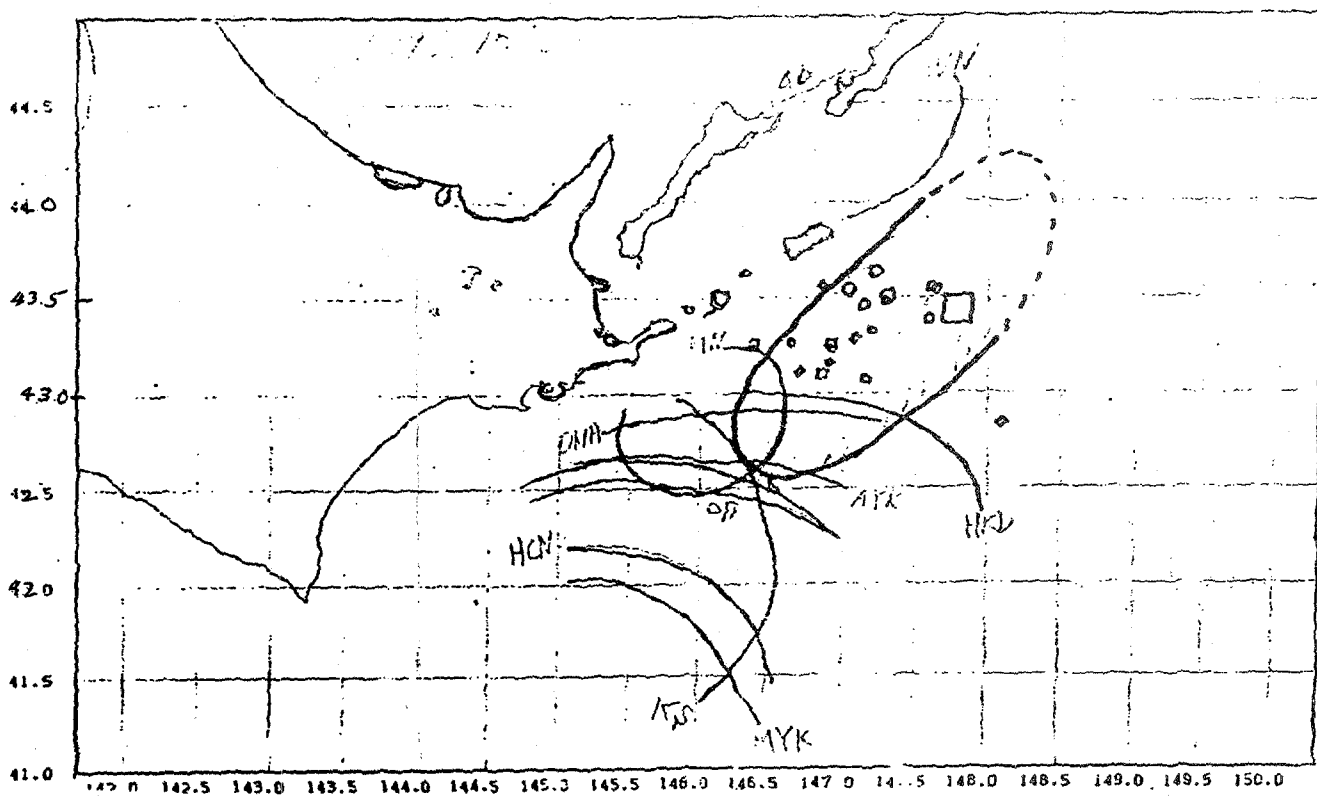
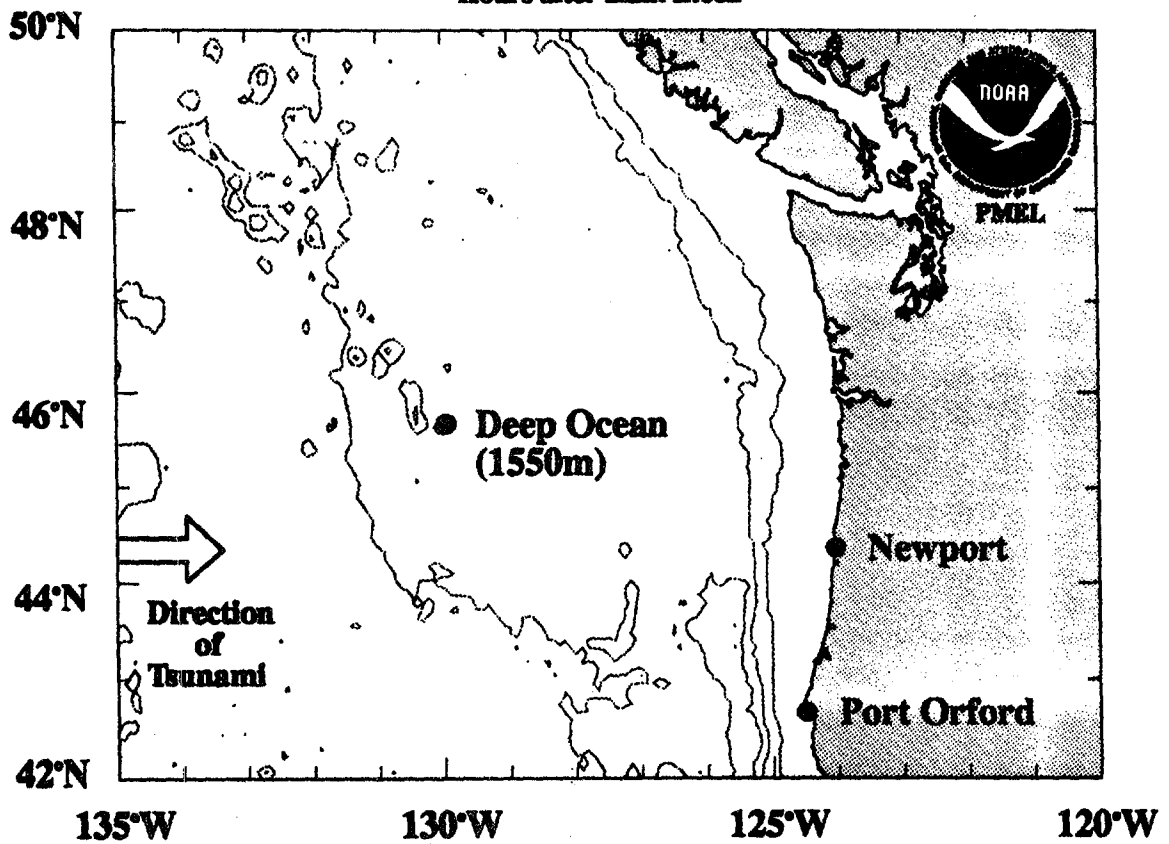
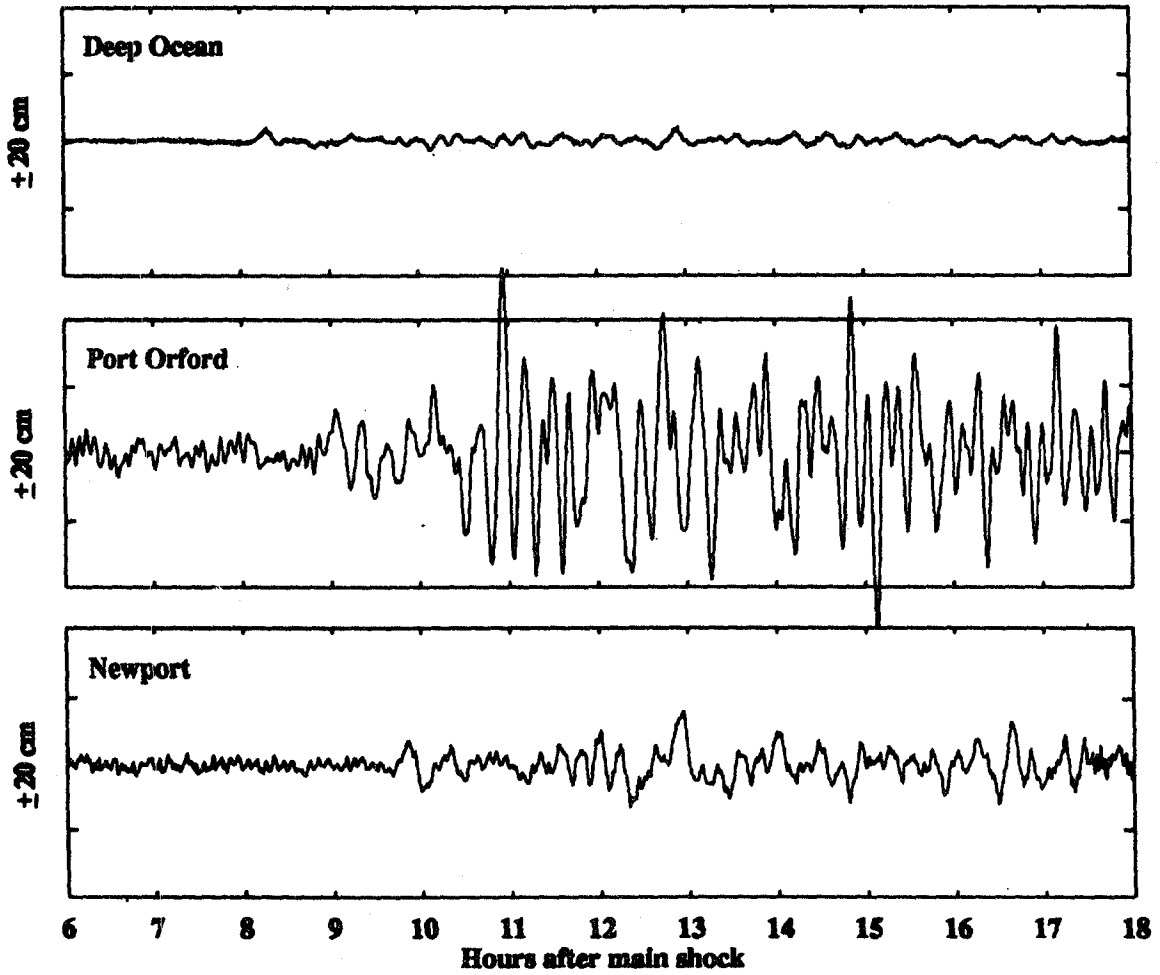


Figure 3. Tsunami Source of the Event of October 4, 1994. (Courtesy of M. Okada)

Figure 4. Recordings of the Tsunami of October 4, 1994. (Bernard 1996)



NUMERICAL SIMULATION OF THE PROPAGATION OF THE 1993 SOUTHWEST HOKKAIDO EARTHQUAKE TSUNAMI AROUND OKUSHIRI ISLAND¹

Shinji SATO

Dr. Eng., Coastal Eng. Div., Public Works Research Institute

1 Asahi, Tsukuba, 305 JAPAN

ABSTRACT

This paper reports a numerical simulation of tsunami propagation for the 1993 Southwest Hokkaido earthquake tsunami. The model is based on the Boussinesq equation which includes the effects of frequency dispersion. Energy dissipation due to breaking at tsunami wave front is modeled. The validity of the model was tested with the existing laboratory data of dispersive wave trains breaking on a slope. The model was then applied to the simulation of the 1993 Southwest Hokkaido earthquake tsunami around the southern part of Okushiri Island. The comparison with the physical model demonstrates that it is the dispersion of wave front which caused focusing the wave energy to the narrow region on the lee side of the island, consequently increase in the tsunami height.

I. INTRODUCTION

A large earthquake shook northern Japan at 22:17 on July 12, 1993, Japan Standard Time, and generated huge tsunamis which caused devastating damage mainly on Okushiri Island. This earthquake was named the 1993 Southwest Hokkaido earthquake; the epicenter was close to Okushiri Island. The sea bottom displacements that generated the tsunamis are located in the region west of Okushiri Island. The first tsunami attacked the island from the west as early as 5 minutes after the origin time. At the Cape Aonae, located at the southernmost edge of the island (see Fig. 1), a part of the district was flushed over by the first tsunami. The complex bottom topography near the Cape Aonae, such as the Okushiri Spur, was considered to be responsible for the peculiar transformation of the tsunami. The complex behaviour of the tsunami, such as dispersion and breaking of the tsunami front, may affect the distribution of inundation heights of the tsunami. Although eye-witnesses of the tsunami were scarce since the earthquake occurred at night, the field survey reported that the inundation heights were anomalously large at Hamatsumae, located about 2 km northeast to the Cape Aonae (Fig. 2; Hokkaido Tsunami Survey Group, 1993). As shown in Fig. 2, the town of Hamatsumae is located on the lee side of the tsunami source, hence more than 20m runup height there is difficult to be explained.

The propagation of the tsunami was numerically simulated by many researchers (e.g., Takahashi et al., 1994; Yamashita et al., 1994; Kato and Tsuji, 1994). However, the anomalously large inundation height at Hamatsumae cannot be explained adequately by the models based on nonlinear non-dispersive long-wave equation (shallow-water equation). In the present study, a numerical simulation was performed by a model based on the Boussinesq equation. The model simulated the propagation of tsunami including the effect of the dispersion and the breaking of the tsunami front. The validity of the model was confirmed with the existing laboratory data and inundation heights surveyed on Okushiri island.

II. NUMERICAL MODEL

2.1 Basic Equations

Numerical computations were carried out by using the nonlinear dispersive wave model proposed by Sato and Kabiling (1994), which includes turbulence effects due to wave breaking. The turbulence effects are modeled by the "eddy-viscosity" model. The basic equations are expressed as follows:

the conservation of mass,

$$\frac{\partial \eta}{\partial t} + \frac{\partial Q_x}{\partial x} + \frac{\partial Q_y}{\partial y} = 0, \quad (1)$$

the conservation of linear momentum in the x direction,

$$\begin{aligned} \frac{\partial Q_x}{\partial t} + \frac{\partial}{\partial x} \left(\frac{Q_x^2}{d} \right) + \frac{\partial}{\partial y} \left(\frac{Q_x Q_y}{d} \right) + g d \frac{\partial \eta}{\partial x} \\ = \frac{1}{3} h^2 \left(\frac{\partial^3 Q_x}{\partial x^2 \partial t} + \frac{\partial^3 Q_y}{\partial x \partial y \partial t} \right) - \frac{g n^2}{d^{7/3}} Q_x \sqrt{Q_x^2 + Q_y^2} + \nu_e \left(\frac{\partial^2 Q_x}{\partial x^2} + \frac{\partial^2 Q_x}{\partial y^2} \right), \end{aligned} \quad (2)$$

the conservation of linear momentum in the y direction,

$$\begin{aligned} \frac{\partial Q_y}{\partial t} + \frac{\partial}{\partial x} \left(\frac{Q_x Q_y}{d} \right) + \frac{\partial}{\partial y} \left(\frac{Q_y^2}{d} \right) + g d \frac{\partial \eta}{\partial y} \\ = \frac{1}{3} h^2 \left(\frac{\partial^3 Q_x}{\partial x \partial y \partial t} + \frac{\partial^3 Q_y}{\partial y^2 \partial t} \right) - \frac{g n^2}{d^{7/3}} Q_y \sqrt{Q_x^2 + Q_y^2} + \nu_e \left(\frac{\partial^2 Q_y}{\partial x^2} + \frac{\partial^2 Q_y}{\partial y^2} \right), \end{aligned} \quad (3)$$

where η is the surface elevation, Q_x and Q_y are the flow rates in x and y directions respectively, h is the water depth, d ($=h + \eta$) is the total depth, n ($=0.026\text{m}^{-1/3}\text{s}$) is the Manning roughness parameter, g is the gravity acceleration and ν_e is the eddy viscosity. 121

The dispersion terms were transformed by using Eq. (1) as

$$\frac{1}{3}h^2\left(\frac{\partial^3 Q_x}{\partial x^2 \partial t} + \frac{\partial^3 Q_y}{\partial x \partial y \partial t}\right) = -\frac{1}{3}h^2 \frac{\partial^3 \eta}{\partial x \partial t^2}, \quad (4)$$

$$\frac{1}{3}h^2\left(\frac{\partial^3 Q_x}{\partial x \partial y \partial t} + \frac{\partial^3 Q_y}{\partial y^2 \partial t}\right) = -\frac{1}{3}h^2 \frac{\partial^3 \eta}{\partial y \partial t^2}, \quad (5)$$

which were discretized by central differences. An efficient ADI (Alternating Directional Implicit) scheme proposed by Maa (1990) was used in numerical integration. The ADI scheme, compared with explicit leap frog scheme which introduces upwind finite difference in the discretization of the advection term, has the advantage of achieving efficient and stable computation without losing accuracy. The variables η , Q_x and Q_y were arranged in a horizontally staggered two-dimensional mesh, and the spatial derivatives in Eqs. (1) - (3) were replaced by central differences. The variables η and Q_x at the next time step were implicitly solved from Eqs. (1) and (2). The variables η and Q_y were then solved from Eqs. (1) and (3). The details of the algorithm were described in Maa (1990) although dispersion term was not included in his formulation. The land boundaries were set along the line where the still-water depth was zero, at which waves were assumed to be fully reflective. The surface elevation of the incident wave was specified at the incident boundary.

2.2 Momentum Mixing Due To Wave Breaking

During the 1983 Central Japan Sea earthquake tsunami, dispersion and breaking of the wave fronts offshore were observed (Shuto, 1985). In laboratory experiments of the 1993 Southwest Hokkaido earthquake tsunami, Noguchi et al. (1995) reported that shoaled tsunami experienced breaking in shallow sea. In order to compute tsunami transformation including wave breaking, appropriate estimation of the breaking point and the associated eddy viscosity ν_e must be estimated.

Sato and Kabiling (1994) proposed a numerical model of monochromatic wave transformation in surf zone based on the Boussinesq equations. The wave breaking criterion was set empirically such that waves start breaking when the ratio of the water particle velocity u_s at the crest surface to the wave celerity C exceeded a critical value (0.4 ~ 0.6). The use of the ratio u_s/C as the breaking criterion is reasonable since it was based on the physical process of wave breaking and was successfully applied to the breaking of compound wave trains by Watanabe et al. (1984). Sato and Kabiling (1994) computed the eddy viscosity in surf zone in terms of energy dissipation coefficient introduced by Watanabe and Dibajnia (1988). The same approach is used in the present study with following modifications.

The critical value of u_s/C for the incipient wave breaking was determined to be 0.4 on the basis of the comparison with the laboratory measurements explained later. The water particle velocity u_s at the surface was estimated from the Boussinesq theory in which vertical profile of the horizontal component of water particle velocity was assumed to be parabolic. The wave celerity C was determined by

$$C = \sqrt{g(h + \eta)}, \quad (6)$$

which is considered to be a good approximation in shallow water.

The eddy viscosity model by Sato and Kabiling (1994) was formulated for periodic waves. In their model, the spatial distribution of eddy viscosity in surf zone was estimated on the basis of the computed wave field. Although this approach was verified for a wide range of laboratory data, it cannot be directly applied to tsunami since the transformation of tsunami is transient. In order to simulate the momentum mixing due to tsunami breaking in a simple manner, the eddy viscosity was assumed to be constant in the present study in

an area shallower than the instantaneous breaking point determined from u_s/C criterion. Since the breaking phenomenon in shallow water is characterized by the water depth at the breaking point, the velocity scale of the breaking-induced turbulence is estimated by the wave celerity at the breaking point. The dimensional argument leads to the following formulation of the eddy viscosity:

$$\nu_e = \alpha \sqrt{gh_{b\max}} \cdot h_{b\max} \quad (7)$$

where $h_{b\max}$ is the largest depth of incipient wave breaking and α is a non-dimensional coefficient to be calibrated by comparison with existing data of breaking tsunami transformation. The value of ν_e was determined by Eq. (7) in the area shallower than $h_{b\max}$ and set at the molecular viscosity of water elsewhere.

The numerical model presented in this study is first verified with the existing laboratory data for a uniform slope in order to demonstrate its capability of modeling frequency dispersion effects. Then, the model is applied to tsunami simulation around Okushiri Island. The simulated tsunami is compared with the 1/1100 scale laboratory model results as well as the field runup measurements. Goto (1984) reported that, on the basis of numerical simulation of tsunami based on the Boussinesq equation, dispersion terms should be included in the area shallower than 30m and the grid size should be smaller than 10m in prototype scales. In the present simulation, therefore, the dispersion terms should be included in the area shallower than 3cm and the grid size should be smaller than 1cm. In the present computations, the dispersion terms were actually included in the area shallower than 15cm. The smallest grid of 2cm was used in all the computations, which was the smallest grid size limited by available computer resources.

III. COMPARISON WITH 1D (UNIFORM SLOPE) PHYSICAL MODEL

Tsuruya et al. (1984) performed a series of experiments, in a 163m long and 1m wide wave flume, to investigate the transformation of dispersive wave trains breaking on a gently sloping bottom. Results of the present numerical model were compared with the measurements for a long wave with period of 40s on a 1/200 slope. The leading wave started from a rise in water level. The computations were carried out in a narrow domain, 100m long and 10cm wide. The shore boundary was set at the still water shoreline where normal flux was assumed to be zero. The incident boundary was set at the depth of 50cm. The experimental data indicate that the water-surface profile at the incident boundary was well approximated by a sinusoidal wave. A sinusoidal wave was therefore used as the input to the numerical model. Although the incident wave was sinusoidal, the shoaled wave on the slope was observed to start to disperse and break. Water surface elevations in shallow water simulated by the numerical model were compared with those measured at various stations shown in Fig. 3. The comparison was carried out mainly for the condition of incident wave steepness $H_o/L_o = 1.92 \times 10^{-4}$, where H_o is the equivalent deep-water wave height and L_o the deep-water wavelength.

Figure 4 shows water surface elevations measured and simulated at station C. Tsuruya et al. (1984) reported that waves at station C were dispersed but not broken. The computational time step Δt was varied from $\Delta t = 0.02s$ to $\Delta t = 0.005s$. The time t in the computations was the time elapsed from the initiation of sinusoidal wave input at the incident boundary, which did not correspond to the time in experiments since the reference time was not specified in Tsuruya et al. (1984). In the experiment, the wave front was dispersed into two waves at this station with the height of the first wave being about 1.8cm. In the computations, dispersion into two waves was simulated with time steps $\Delta t = 0.01s$ and $\Delta t = 0.005s$. The wave heights of the dispersed wave tended to increase with the decrease in time step, although they were underestimated even with $\Delta t = 0.005s$. Since the significant difference is not noticed in the results of $\Delta t = 0.01s$ and $\Delta t = 0.005s$, the time step of $\Delta t = 0.01s$ was used in the following computations.

Figures 5 (a) and (b) show measured and computed surface elevations at Station C for various wave steepness. The dispersion of the wave front was more pronounced and the height of each wave was larger as

the incident wave steepness increased. The broken line in Fig. 5 (b) shows surface elevation computed by the non-dispersive shallow-water theory. It is evident in Fig. 5 that the measured wave fronts are modeled well with the Boussinesq model although it tends to underestimate the height of each wave in the dispersed wave trains. The computation with shallow-water theory failed to simulate the multiple wave formation at the front.

According to Tsuruya et al. (1984), wave breaking for $H_o/L_o = 1.92 \times 10^{-4}$ occurred between station C and B. Wave heights in dispersed wave train were gradually decreased as they approached shoreline. The value of α in Eq. (7) was determined by the comparison of measured and simulated wave profiles. Wave profiles at station S were compared in Fig. 6 for $\alpha = 0.3$ and $\alpha = 3$. In the experiment, no dispersed waves were observed at station S since they were dissipated due to breaking before arriving at station S. Computed wave profiles at station S show abrupt rise in water level since wave run-up is not simulated in the model. For $\alpha = 0.3$, dispersed waves were noticed at station S while wave dispersion were less significant for $\alpha = 3$. As further increase in α tended to make the computation unstable, the optimum value of α was determined to be 3.

IV. TRANSFORMATION OF TSUNAMI NEAR OKUSHIRI ISLAND

Noguchi et al. (1995) performed a physical model test which investigated the transformation of the Southwest Hokkaido earthquake tsunami around Cape Aonae using a 1/1100 non-distorted model in a 30m x 35m wave basin. The tsunami was generated with a pneumatic wave generator which suctioned the air and lifted the water surface in a chamber prior to the experiment, and by abruptly releasing air through valves attached to the chamber, the water mass in the chamber is released, which created the tsunami in the basin. Since the wall surrounding the basin was highly-reflective, the basin was soon disturbed by the reflected waves from the walls. It is noted that the first wave observed in the basin was not affected by the reflection disturbances. The propagation of the first wave was recorded by video cameras and wave gages situated mainly on the lee side of the Cape Aonae. Photo 1 shows a series of snapshots taken from the top of the basin. It is noticed that the tsunami experienced breaking on the Okushiri Spur and split into several short waves. The computational domain was determined as a 15m x 25m rectangular region as shown in Fig. 7 which contained southern part of the source region which was considered to affect the tsunami transformation around the Cape Aonae. Computation was carried out and compared with experiments for the condition of 4mm wave height incidence since it corresponded the initial water level rise in the source area (Takahashi et al., 1994).

Figure 7 illustrates the computational domain and the arrangement of wave gages in the experiments. Water depth around the island was reproduced from navigation charts published by the Maritime Safety Agency. It is noticed that the Okushiri Spur is extending from the Cape Aonae and that part of the Murotsu Shoal located on the Spur is above the sea level. The grid sizes were 2cm in the 10m x 10m square region shown in Fig. 7 and 10cm elsewhere. The total number of grids was 550 x 650. The boundary around the island was set at the actual shoreline where normal flux was assumed to be zero in the computation. The minimum depth of the computational grid was 1mm which was scaled to be 1.1m in the prototype. The time step was selected as 0.01s so that the computation could be carried out with a sufficient accuracy. The maximum Courant number, $\sqrt{g(h + \eta)} \frac{\Delta t}{\Delta x}$, was below unity. The incident wave profile was determined from the record of wave gage No. 27 which was located in front of the wave generator.

Figure 8 shows the propagation of tsunami simulated by the present Boussinesq model without wave breaking. The symbol t denotes the time elapsed from the initiation of the computation. The surface elevation becomes high at $t=11s$ in front of the Cape Aonae. The first tsunami seemed to have attacked the lowland of the Cape Aonae from the bottom (west) at this moment, although it was not simulated in the model since the inundation was not allowed in the computation. At this moment, the offshore waves which were focused behind the Murotsu shoal began to be split into several short waves. The wave rays were curved behind the Murotsu shoal and reached Hamatsumae located to the east of Aonae at $t=17s$. The waves were then reflected from

124 Hamatsumae forming a cylindrical wave and attacked the Aonae district again from the east at $t=19s$. The second attack occurred 8s after the first wave attack, which was 4.5 minutes in the prototype scale. The actual propagation of the tsunami was also affected by waves coming from the north of the island since the source area was large compared to the island (tsunamis from the north were not modeled in the present study). The initial tsunami profile in the source area may also affect the tsunami transformation. It was confirmed however that the dispersion effects of the tsunami front tend to enhance the tsunami height at Hamatsumae as well as the height of waves reflected from Hamatsumae which attacked Aonae again from the opposite direction.

Figure 9 shows a comparison of temporal wave profiles along the coast. The number denotes the wave gage number shown in Fig. 7. The left side shows measurements and the right side shows numerical computations. Results of the numerical model simulate the dispersion of the wave front at wave gages No. 8, 13 and 18, which generally agree well with experiments. It should be noted however that the wave heights of dispersed wave at the tsunami front (indicated in the figure) are underestimated in the numerical model. The difference may be due to the nonlinear transformation of tsunami in very shallow water since the Boussinesq theory is valid only for weakly nonlinear and weakly dispersive waves.

Figure 10 shows comparisons of maximum surface elevations along the coastline on the lee side of Cape Aonae. The horizontal axis is y coordinate shown in Fig. 7. In the physical model, Cape Aonae is located at $y = 11m$ and Hamatsumae is at $y = 14m$. The upper figure indicates the maximum surface elevation simulated by the Boussinesq equation. In order to compare the numerical results with field measurements, the numerically predicted values are scaled based on the Froude law. The lower figure shows computation based on shallow-water equation without wave breaking. It is apparent from both figures that the numerical results in the range $15 < y < 20$ tend to overestimate the field data, which suggests that the incident wave height used in the model was slightly large. The magnification rate of the inundation height at Hamatsumae to those in the nearby area are better predicted by the Boussinesq equation than by shallow-water equation, indicating that wave dispersion effect was essential in the estimation of tsunami height around Hamatsumae. Inclusion of wave breaking effect tends to decrease the wave height in the area between Cape Aonae and Hamatsumae. It is difficult however to confirm the significance of wave breaking effect in tsunami simulation from the comparison of maximum surface elevations in this area.

V. CONCLUSIONS

A numerical model was presented for tsunami propagation including the effects of dispersion and breaking of wave front. The numerical model was confirmed with the existing laboratory data of dispersive wave trains breaking on a slope. The model was applied to the propagation of Southwest Hokkaido Earthquake tsunami around the southern part of Okushiri Island and compared with physical model tests. It was confirmed that the model could simulate the dispersion and the breaking of the tsunami front and that the dispersion of waves resulted in the increase of tsunami height at Hamatsumae. The enhancement of run-up at Hamatsumae are explained by the following two mechanisms: 1) tsunami focusing behind Murotsu Shoal due to refraction and 2) the dispersion of the shoaled tsunami which creates a series of dispersed waves riding on the base tsunami. The inclusion of wave breaking tended to suppress the dispersion of wave front due to the mixing caused by wave breaking.

Further study is required on the formulation of eddy viscosity for complex bottom topographies.

REFERENCES

- Goto, C. (1984): Numerical study of Japan Sea tsunami in north Akita coast, Proc. 31st Japanese Conf. on Coastal Eng., JSCE, pp. 233-236. (in Japanese)

- Hokkaido Tsunami Survey Group (1993): Tsunami devastates Japanese coastal region, *Eos, Trans. AGU*, Vol. 74, No. 37, pp. 417, 432.
- Kato, K. and Y. Tsuji (1994): Estimation of fault parameters of the 1993 Hokkaido-Nansei-Oki earthquake and tsunami characteristics, *Bull. Earthq. Res. Inst., Univ. Tokyo*, Vol. 69, pp. 39-66. (in Japanese)
- Maa, J.P.-Y.(1990): An efficient horizontal two-dimensional hydrodynamic model, *Coastal Engineering*, Vol.14, pp.1-18.
- Noguchi, K., S. Sato and S. Tanaka (1995): Propagation of Hokkaido-Nansei-Oki earthquake tsunami around Cape Aonae, *Coastal Eng. in Japan*, Vol. 38, No.2 (in submission).
- Sato, S. and M. B. Kabiling (1994): A numerical simulation of beach evolution based on a nonlinear dispersive wave-current model, *Proc. 24th Conf. on Coastal Eng., ASCE*, pp. 2557-2570.
- Shuto, N. (1985): The Nihonkai-Chubu earthquake tsunami on the north Akita coast, *Coastal Eng. in Japan*, Vol. 28, JSCE, pp. 255-264.
- Shuto, N., H. Matsutomi and M. Ubana (1994): Characteristics of the Southwest Hokkaido earthquake tsunami and remaining problems, *Proc. of Coastal Eng.*, Vol. 41, JSCE, pp. 236-240. (in Japanese)
- Takahashi, T., N. Shuto, F. Imamura and H. Matsutomi (1994): The measured and computed Hokkaido Nansei-oki earthquake tsunami of 1993, *Proc. 24th Conf. on Coastal Eng., ASCE*, pp. 886-900.
- Tsuruya, H., S. Nakano and H. Ichinohe (1984): Experimental study on the deformation and run-up of tsunami in shallow water – Case study of the tsunami caused by 1983 Nihonkai Chubu Earthquake –, *Proc. 31st Japanese Conf. on Coastal Eng., JSCE*, pp. 237-241. (in Japanese)
- Watanabe, A., T. Hara and K. Horikawa (1984): Study on wave breaking condition for compound wave trains, *Coastal Eng. in Japan*, Vol. 27, pp. 71-82.
- Watanabe, A. and M. Dibajnia (1988): A numerical model of wave deformation in surf zone, *Proc. 21st Conf. on Coastal Eng.*, pp. 578-587.
- Yamashita, T., T. Takabayashi and Y. Tsuchiya (1994): Numerical simulation of tsunami inundation caused by Southwest Hokkaido Earthquake, *Proc. of Coastal Eng.*, Vol. 41, JSCE, pp. 231-235. (in Japanese)

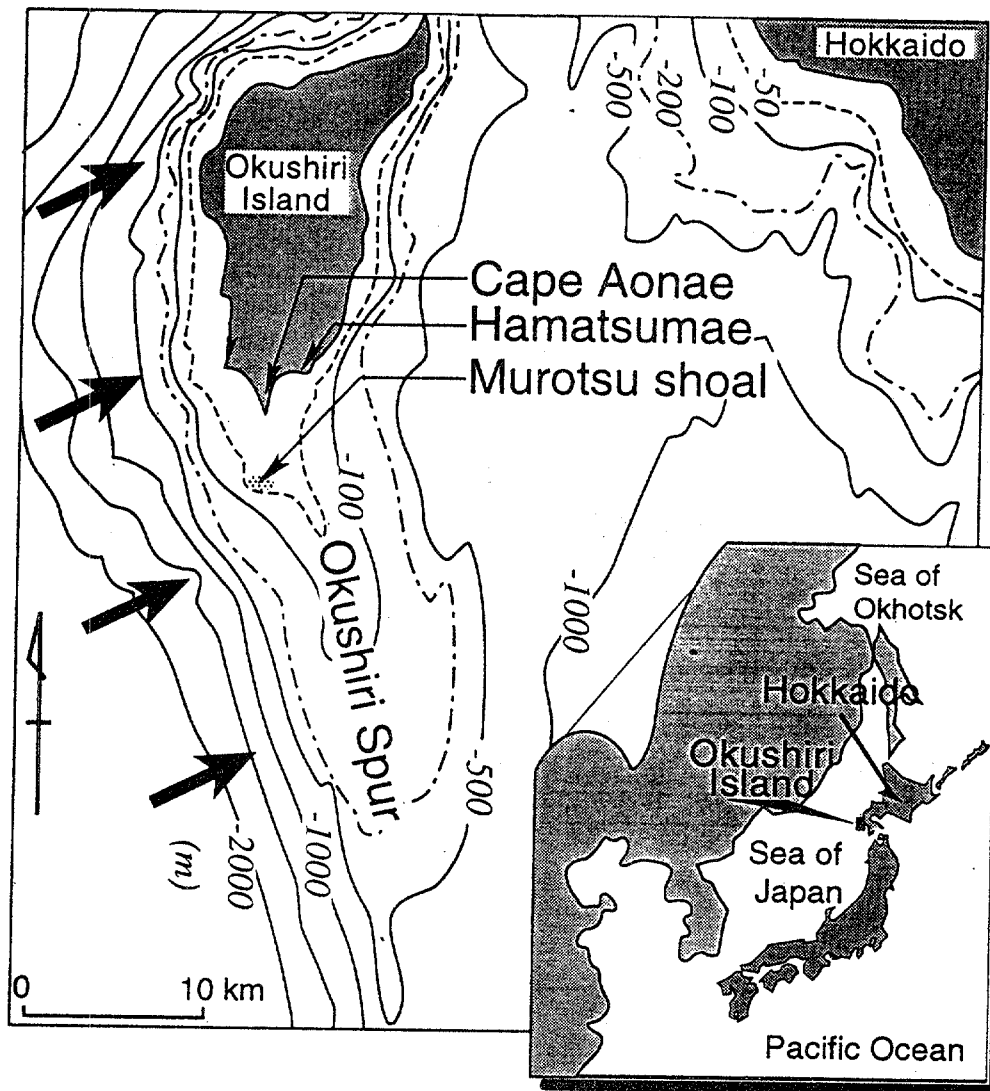


Fig. 1 Sea bottom contours around Okushiri Island. The arrow marks on the left side indicate approximate tsunami attack directions.

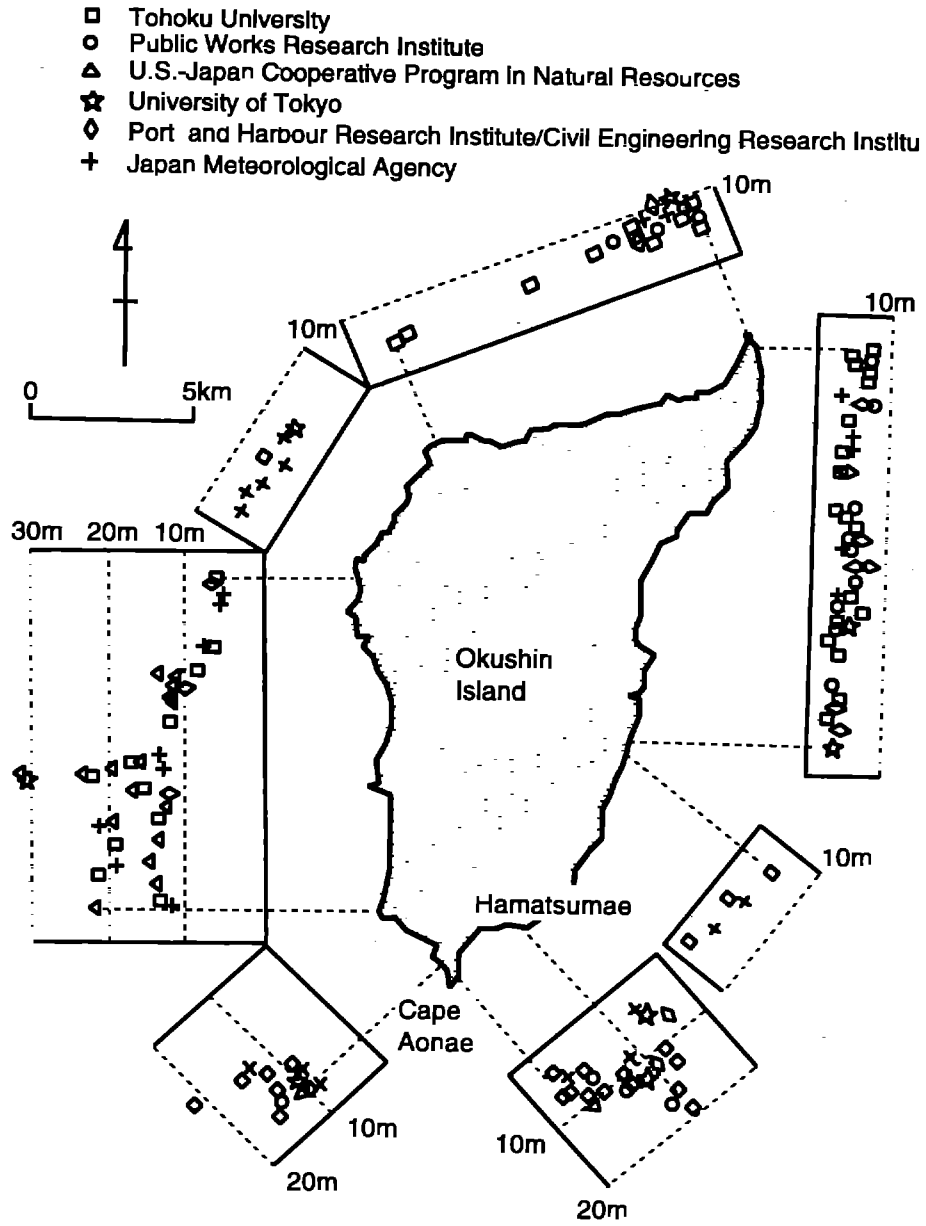


Fig. 2 Distribution of tsunami runup heights measured by the several survey groups (Hokkaido Tsunami Survey Group, 1993).

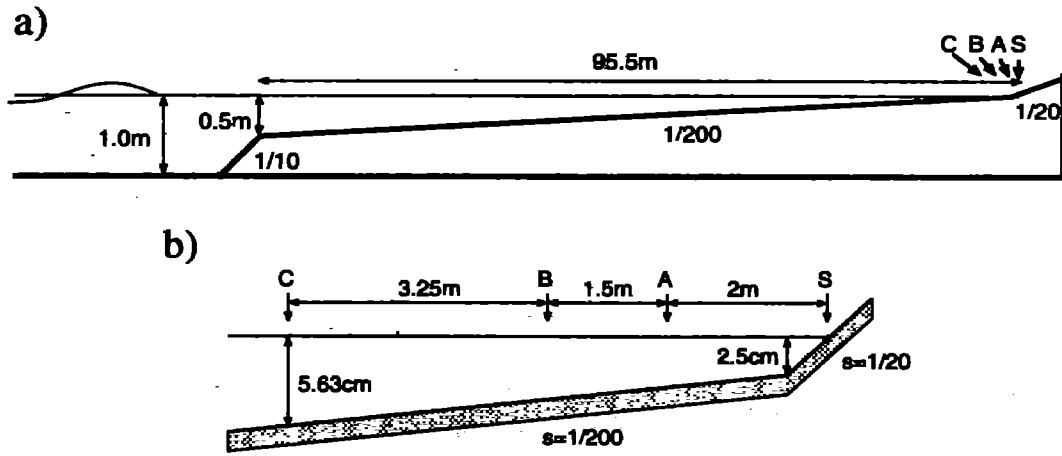


Fig. 3 Experimental set-up of Tsuruya et al. (1983). The tank is 163m long and 1m wide, and a long wave with 40s wave period was generated at 140m from the point C. a) a general view, b) a local view near the shoreline.

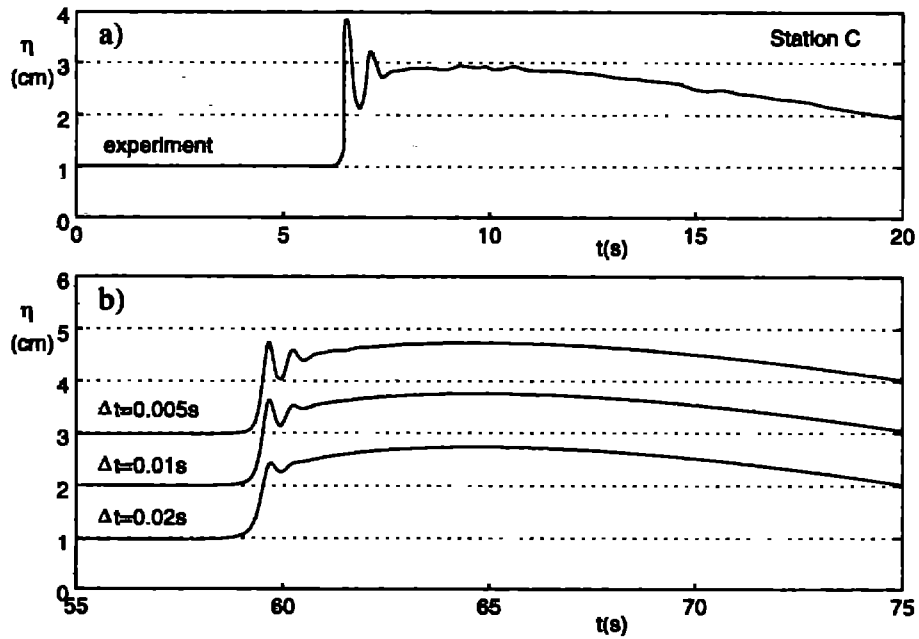


Fig. 4 Comparisons of the wave profiles at Station C (see Fig. 3): a) experimental data from Tsuruya et al. (1983), b) numerical predictions with a variety of time increments.

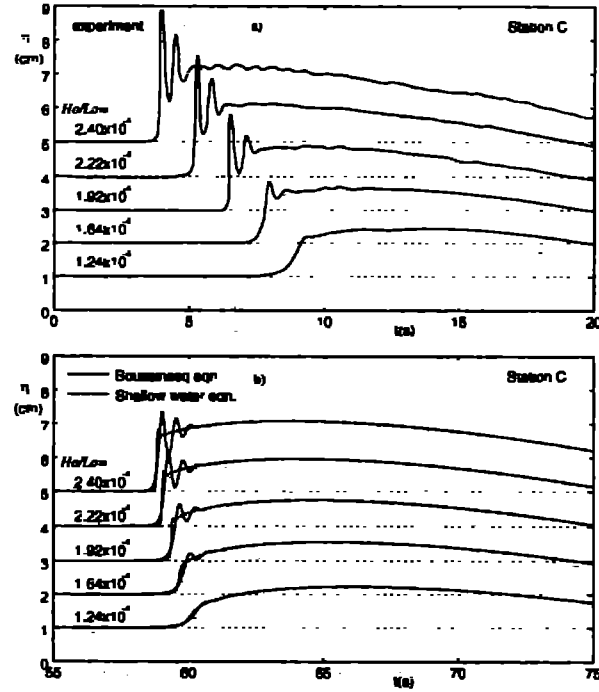


Fig. 5 Comparisons of the wave profiles at Station C for various offshore wave steepness H_o/L_o : a) experimental data from Tsuruya et al. (1983), b) numerical predictions based on the Boussinesq equation ———, and the shallow-water equation - - - - -.

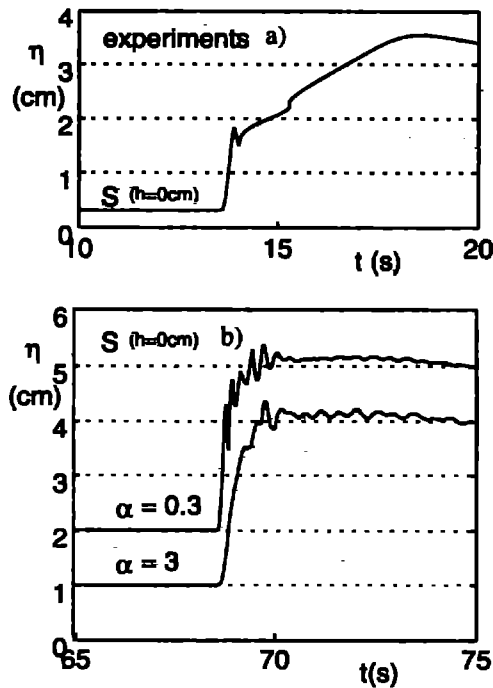


Fig. 6 Wave profiles at initial shoreline: a) experimental data from Tsuruya et al. (1983), b) numerical predictions based on the Boussinesq equation, where α is the eddy viscosity coefficient in Eq. (7).

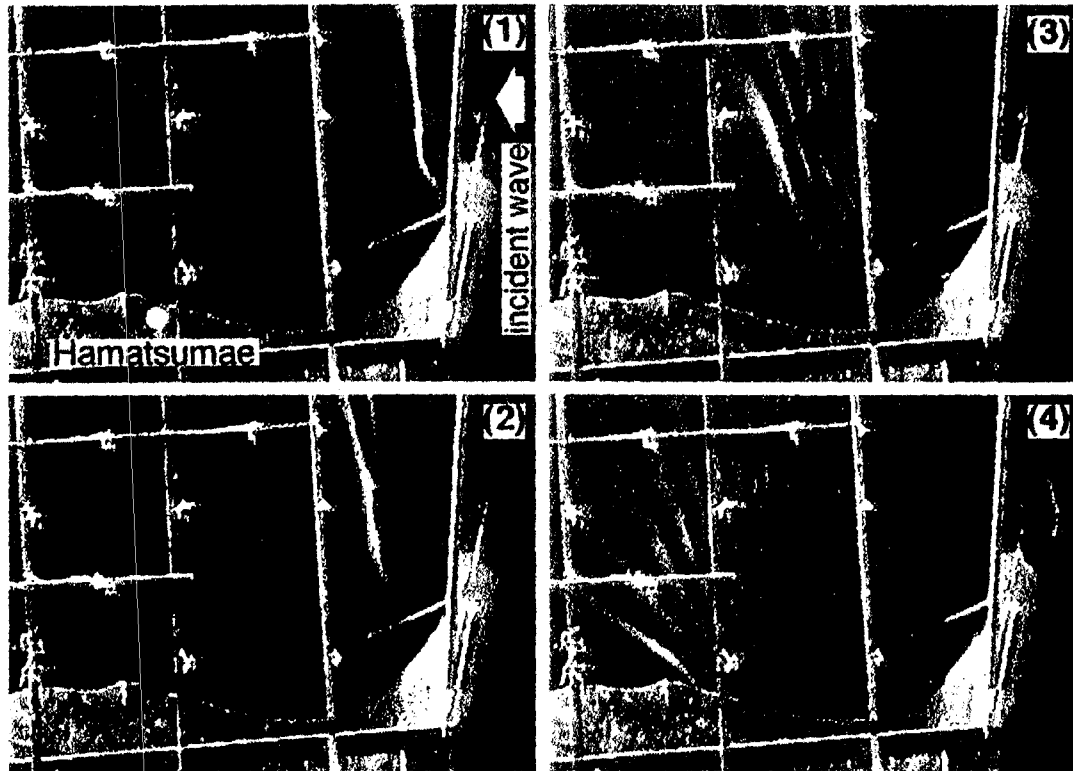


Photo 1 Tsunami propagation in the laboratory experiment. (1) tsunami breaking on the Okushiri Spur, (2) 0.06s after (1), (3) dispersion into several short waves, 2.0s after (1), (4) the first wave hit Hamatsumae, 4.4s after (1).

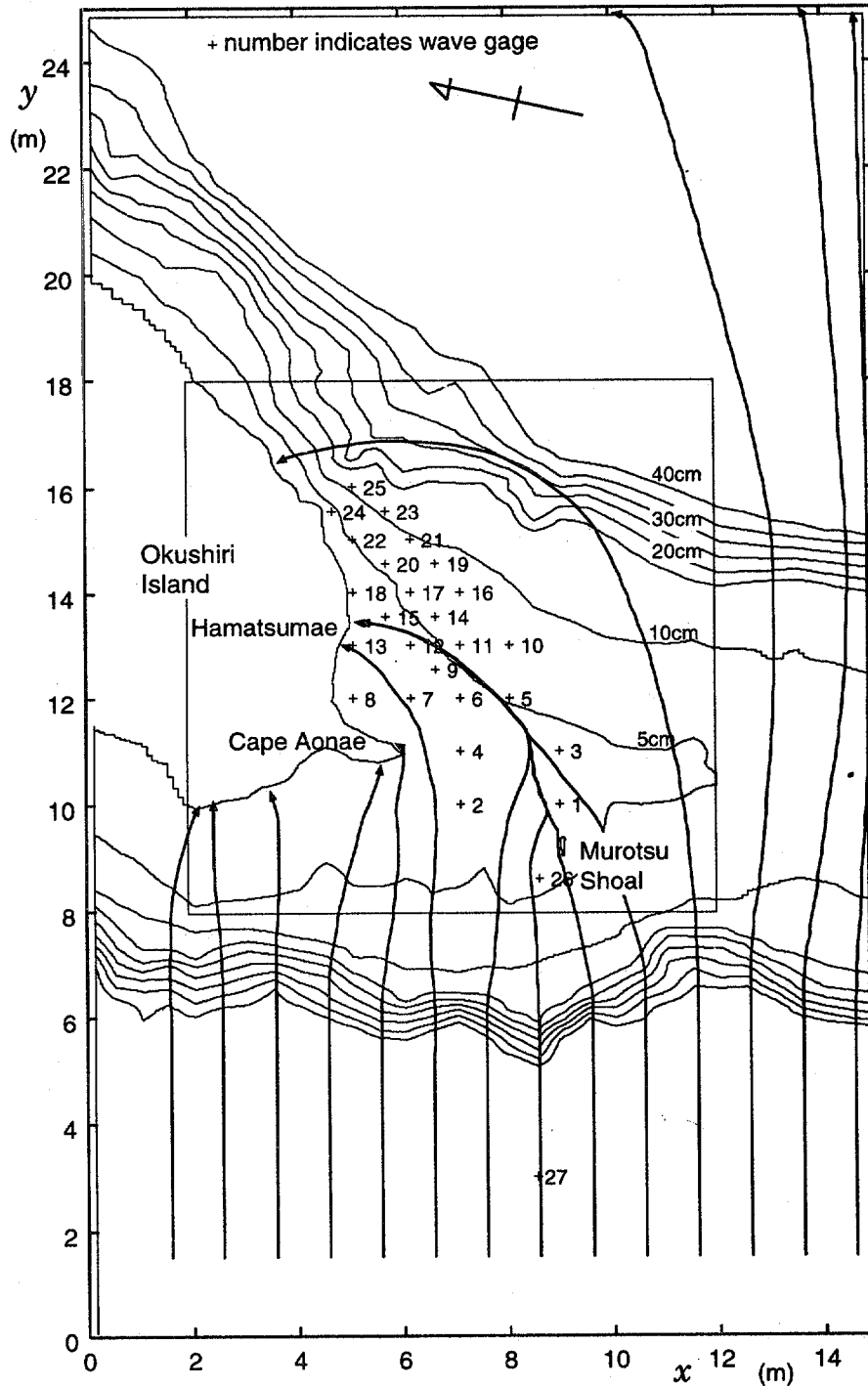


Fig. 7 Computational domain. The symbol + identifies wave gage locations. The line with an arrow indicates the computed ray trajectory of tsunami showing the focusing effect near Hamatsumae, and the caustics behind Murotsu Shoal.

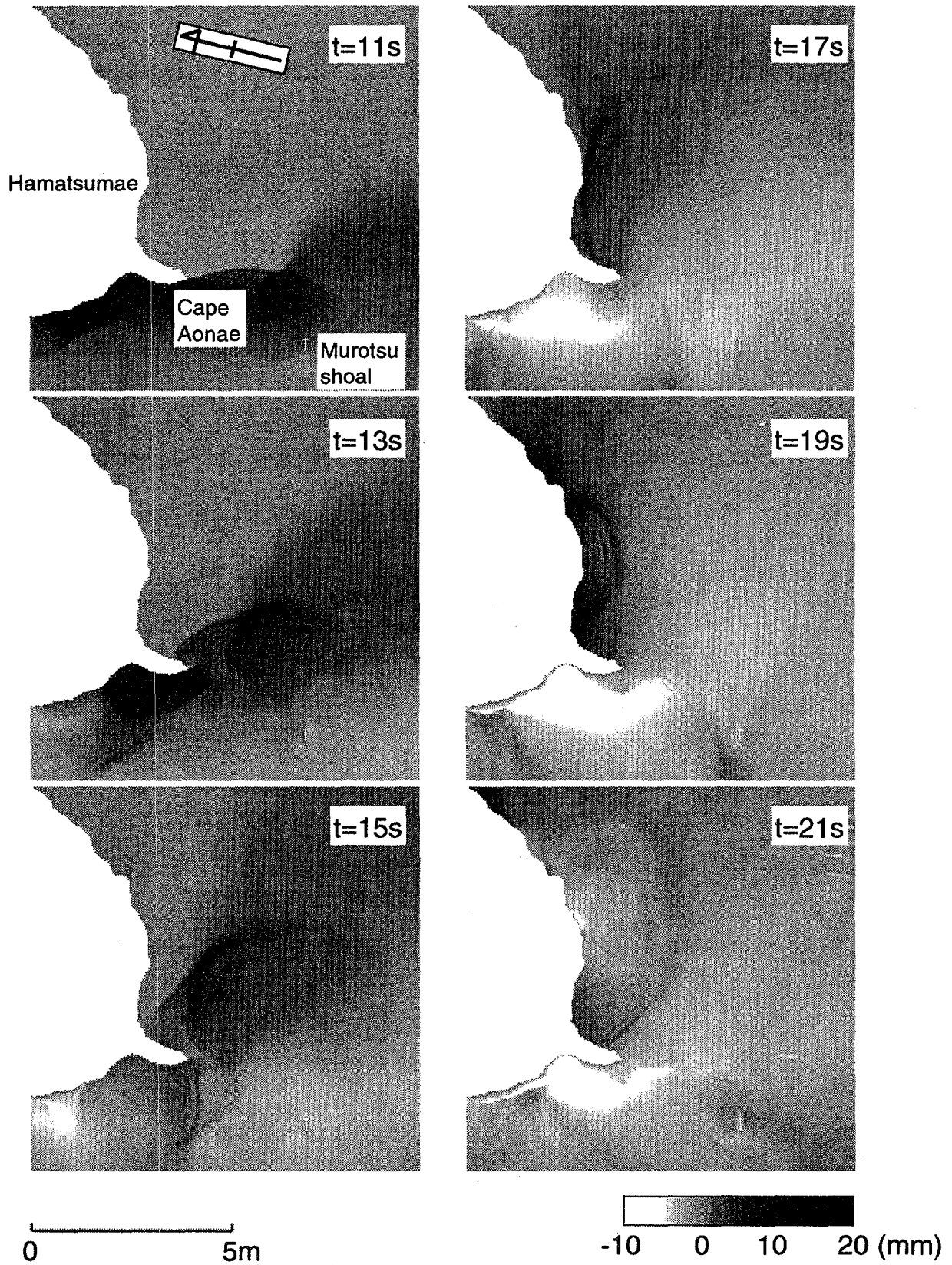


Fig. 8 Propagation of tsunami around the southern part of Okushiri Island. Wave caustics and dispersion effects are shown in the figures at $t = 11s$ and $t = 13s$.

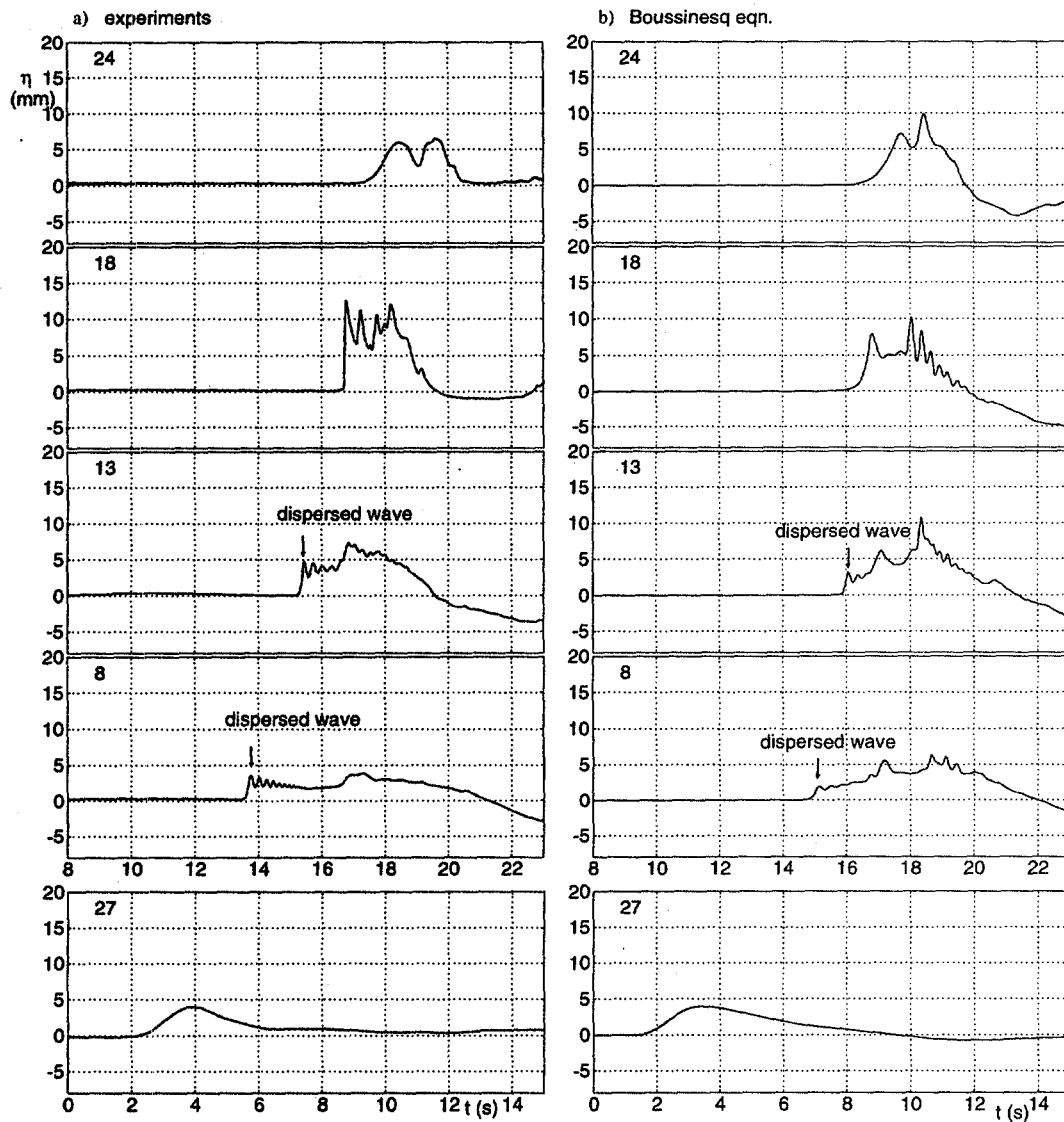


Fig. 9 Comparisons of surface elevations: a) experimental data, b) numerical predictions. The number at the upper left corner indicates the wave gage locations shown in Fig. 7. The numerical model simulates wave dispersion but tends to underestimate the dispersed wave height.

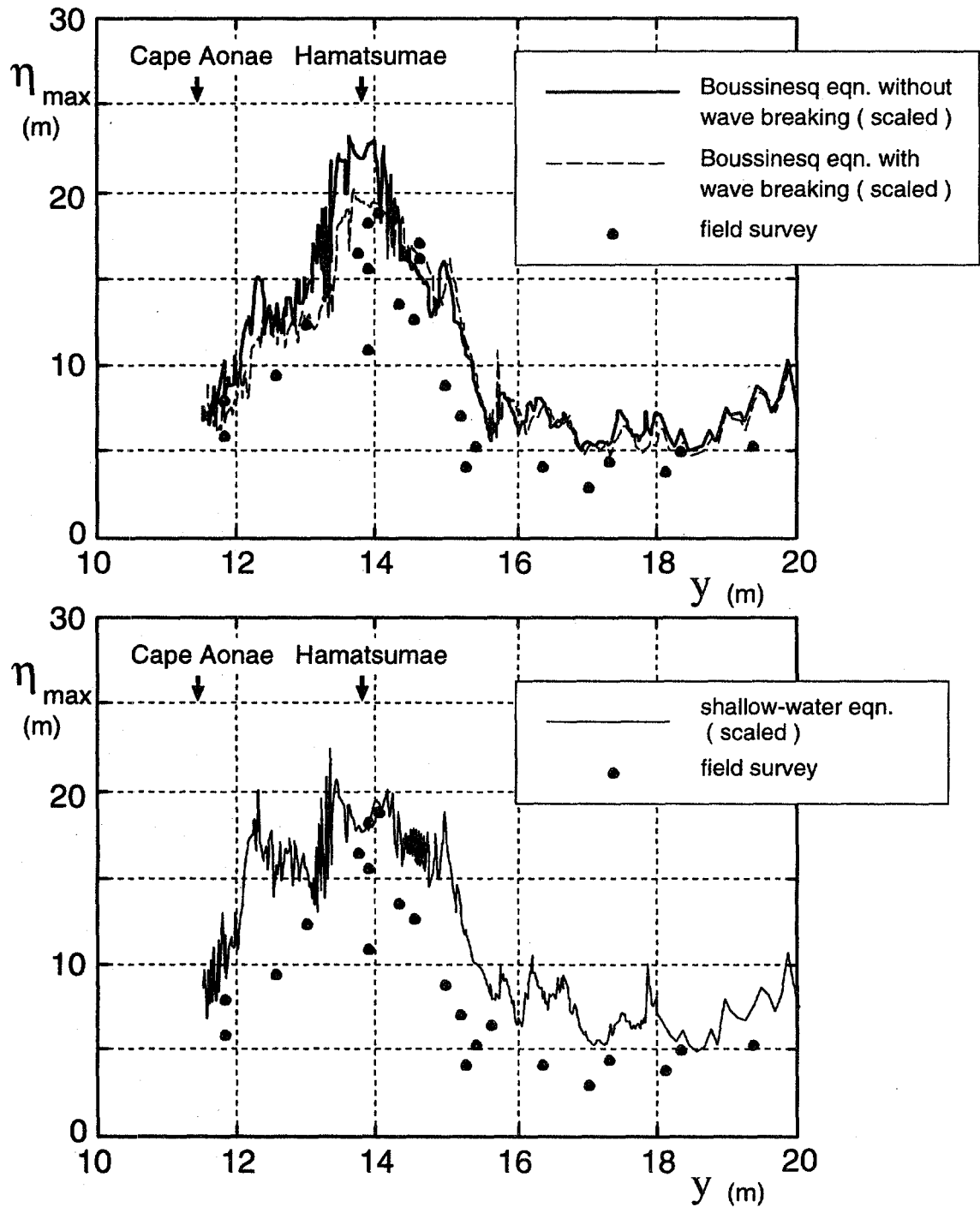


Fig. 10 Distributions of maximum surface elevations along the coastline. The solid line shows computation without wave breaking; the broken line the computation with wave breaking.

DAMAGES OF COASTAL STRUCTURES IN AWAJI AND TOUBAN COASTS DUE TO THE 1995 HYOGOKEN NAMBU EARTHQUAKE

Shigenobu TANAKA and Shinji SATO
Coastal Eng. Div., Public Works Research Institute
1 Asahi, Tsukuba, 305 JAPAN

ABSTRACT

This paper reports damages of coastal structures caused by the 1995 Hyogoken Nambu earthquake. Although no significant tsunami was generated, the strong seismic motion attacked coastal structures on Awaji island, Touban coast and Kobe port, resulting in the collapse of coastal dikes and the failure of water gates in a wide area. Damages in Awaji and Touban coasts are described in detail.

I. INTRODUCTION

The Hyogoken Nambu earthquake occurred at 5:46 a.m. of January 17, 1995, Japan Standard Time. The magnitude of the earthquake was 7.2 on the JMA scale. Since the epicenter was very close to the highly-populated city of Kobe, more than 6,000 lives were lost by the earthquake. Catastrophic damages were caused on houses, high-storied buildings, port facilities, railways and highway bridges.

The epicenter of the earthquake was in the middle of the Akashi straits (see Fig. 1). The earthquake was caused by the sliding motion of several active faults extending from the north of Awaji island to the northern part of Kobe. Damages were especially large in a narrow band along the fault line, in which the seismic intensity reached 7 in JMA scale. Since only a fraction of the fault line was under the sea and the sea depth along the fault line was shallower than 100m, no significant tsunami was observed. However, since the ground motion was tremendously large and resulted in large displacements in a wide area of coastlines, it caused significant damages on various coastal structures. This report describes damages of coastal dikes occurred on Awaji and Touban coasts and those of water gates in port of Kobe.

II. OUTLINE OF THE EARTHQUAKE MOTION

Figure 1 illustrates the distribution of maximum horizontal accelerations compiled by the National Research Institute for Earth Science and Disaster Prevention, Science and Technology Agency. The area of large acceleration is located in an area from the southwest Kobe to the northeast. The maximum horizontal acceleration exceeded 800 gal (cm/s^2) in the north-south component, which was recorded at the Kobe Maritime Meteorological Observatory. On Touban coast, the maximum acceleration was 300 gal at the west end and 600 gal at the east end. Vertical acceleration was also large in this earthquake. The maximum vertical acceleration of 556 gal was recorded on Port Island, an artificial island located on the south of the central Kobe.

Figure 2 shows the distribution of vertical displacements of ground surveyed by Geographical Survey Institute after the earthquake. Relative upheaval is noticed on the west side of the fault and settlement is noticed on the east side. The vertical gap at the fault line is about 30cm, which is located at Suma coast in this figure. Figure 3 shows the distribution of horizontal displacements. On the north of the fault line, the ground was moved relatively to the northeast with displacement of 30cm. On Awaji island, the land on the southern side of the fault was moved to the southwest with displacements larger than 100cm.

III. DAMAGES OF COASTAL DIKES

(1) Awaji coast

Figure 4 shows a location map of the coasts in the northern part of Awaji island at which significant damages to coastal structures are observed. Since the horizontal ground displacement was extremely large on Awaji island, most of the failures of coastal dikes occurred where land slip or land slide were also observed nearby. Wide gaps of 30 to 50 cm were found at the joint section of dikes.

(2) Touban coast

Figure 5 shows a location map of the sites along Touban coast on which significant damages to coastal structures are observed. Compared to the coasts in northern Awaji island, seismic motion on Touban coast was relatively weak (see Fig. 1). The damage pattern of coastal dikes was mostly the settlement of parapet and lateral spreading of the body to the land side of the dike (see Fig. 6). The maximum settlement reached 55cm at the right bank of Akashi river. On most of the sites where significant settlements were observed, the settlement of filled materials was also observed, leading to the presence of a vacancy beneath the parapet. The presence of the vacancy and the lateral spreading to the land side suggests that the filled materials were liquified and settled by the strong seismic motion. It is noticed from Fig. 5 that the failure sites are mostly located near the river mouths, where the structures were based on rather soft foundation, the thickness of mud layer is more than 15m. The failure of dikes along Touban coast strongly depends on the soil characteristics of the foundation.

III. DAMAGES OF WATER GATES

Water gate is a composite structure usually made of steel and concrete. On southern coasts of Hyogo prefecture, many water gates were installed to protect land from storm surges. Even if the damages of the water gates look trivial, they sometimes fail to be operated since the mechanical portions are fragile against strong seismic motion. Electricity shutdown may sometimes be a crucial problem in maintaining the operation.

Fortunately in the 1995 Hyogoken Nambu earthquake, no tsunamis were generated and no storm surges attacked water gates damaged by the quake. However, it should be reminded that the functionality of water gate may sometimes be ceased after it experienced strong seismic motion.

IV. CONCLUDING REMARKS

The damages of coastal structures caused by the 1995 Hyogoken Nambu earthquake were apparently small compared with the tremendous damages occurred in the urbanized area of Kobe city. However, many coastal structures were collapsed by the historically strong seismic motions. Coastal dikes on northern Awaji island were found to be collapsed owing to large ground displacements, resulting in a wide gap of 30 to 50cm at the joint section. On Touban coasts, where seismic motion was relatively weak, the settlement of coastal dikes mostly occurred where they were based on thick mud layers near river mouths. Many water gates also suffered significant damages. These damages suggest a concern about the functionality of coastal dikes and tsunami gates in case they are attacked by both strong seismic motion and tsunamis.

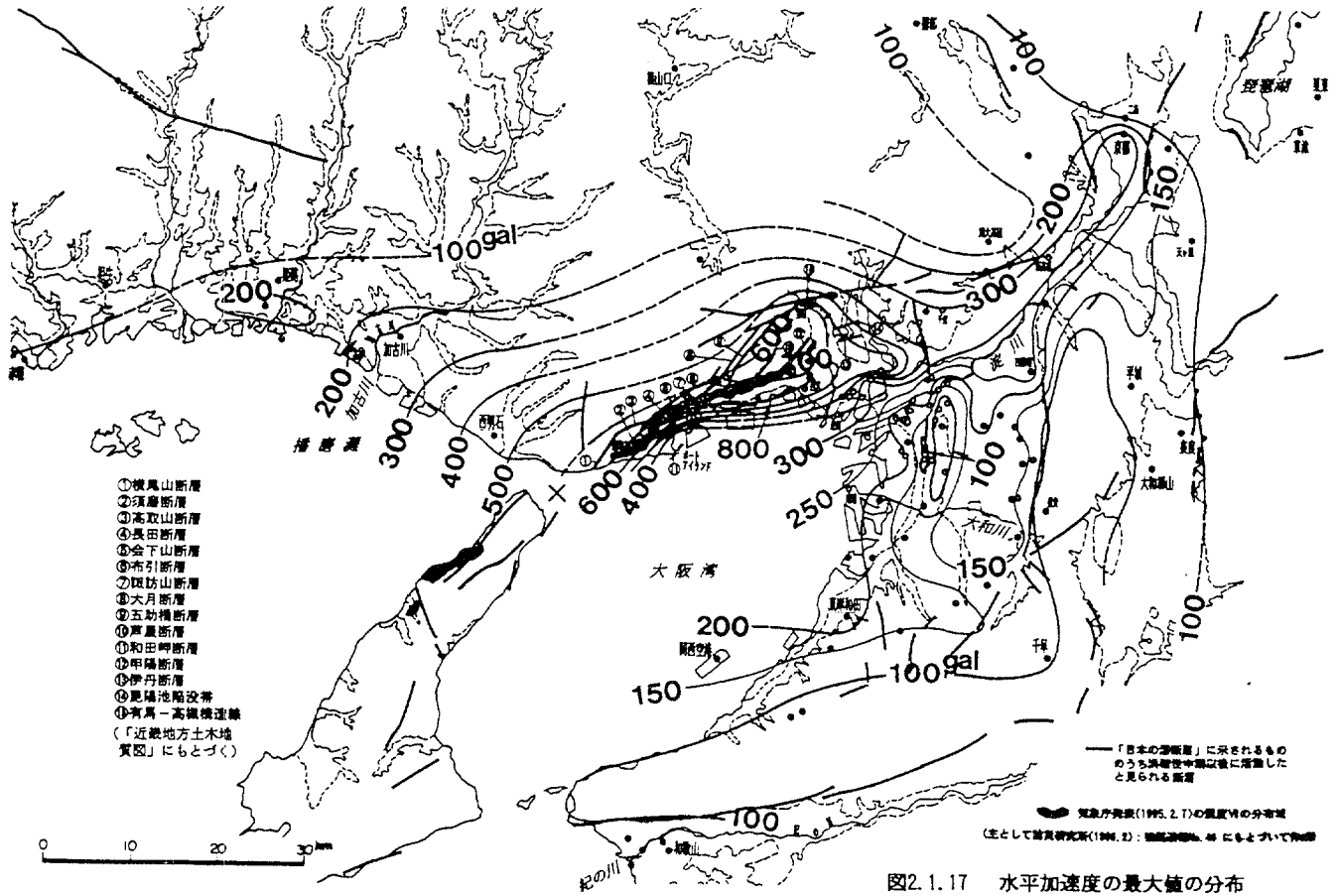


Fig. 1 Distribution of maximum horizontal accelerations

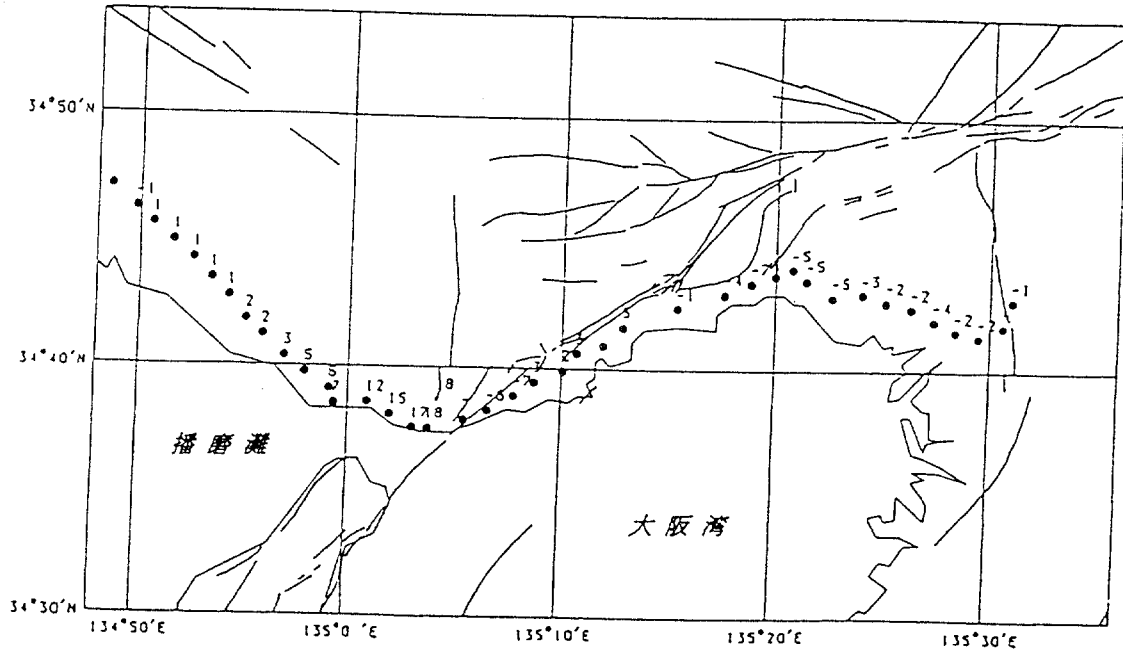


Fig. 2 Distribution of vertical displacements of ground

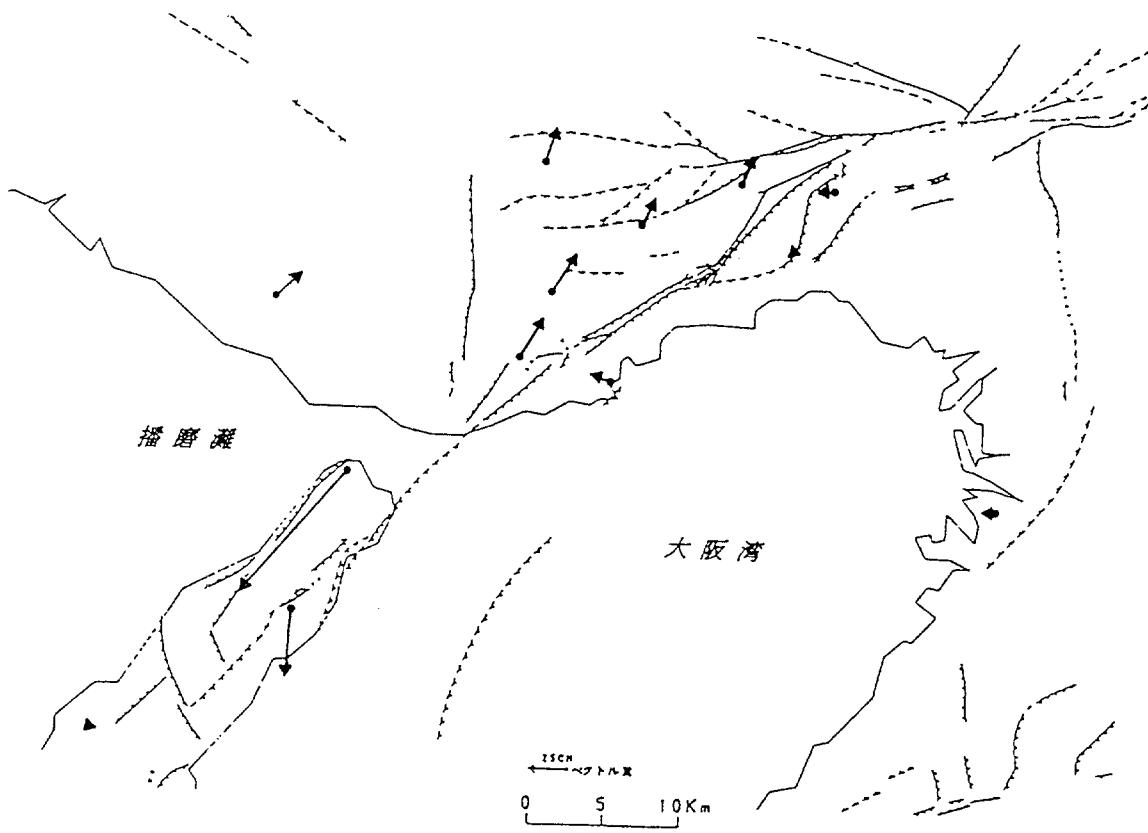


Fig. 3 Distribution of horizontal displacements of ground

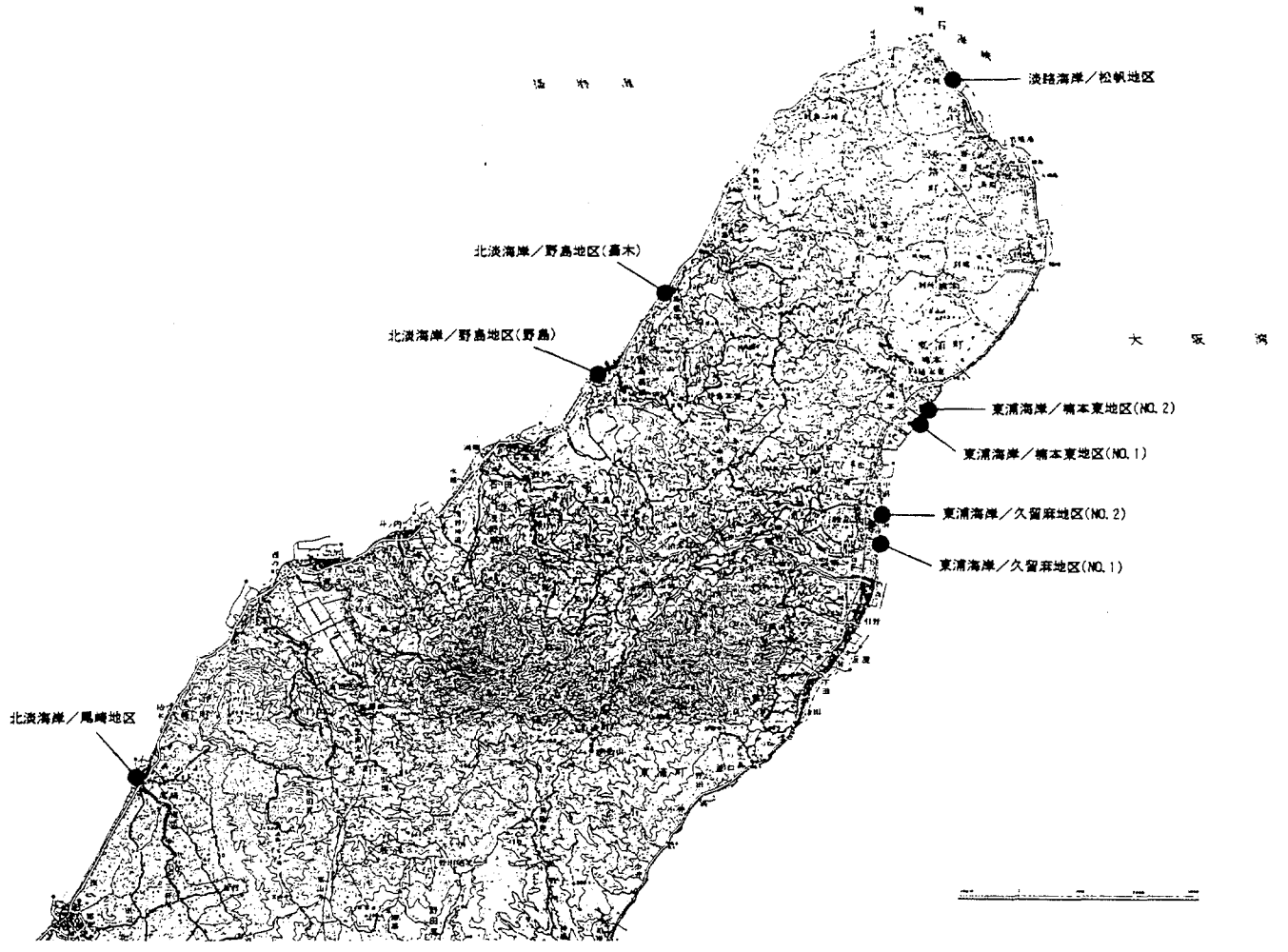


Fig. 4 Location map of northern Awaji island

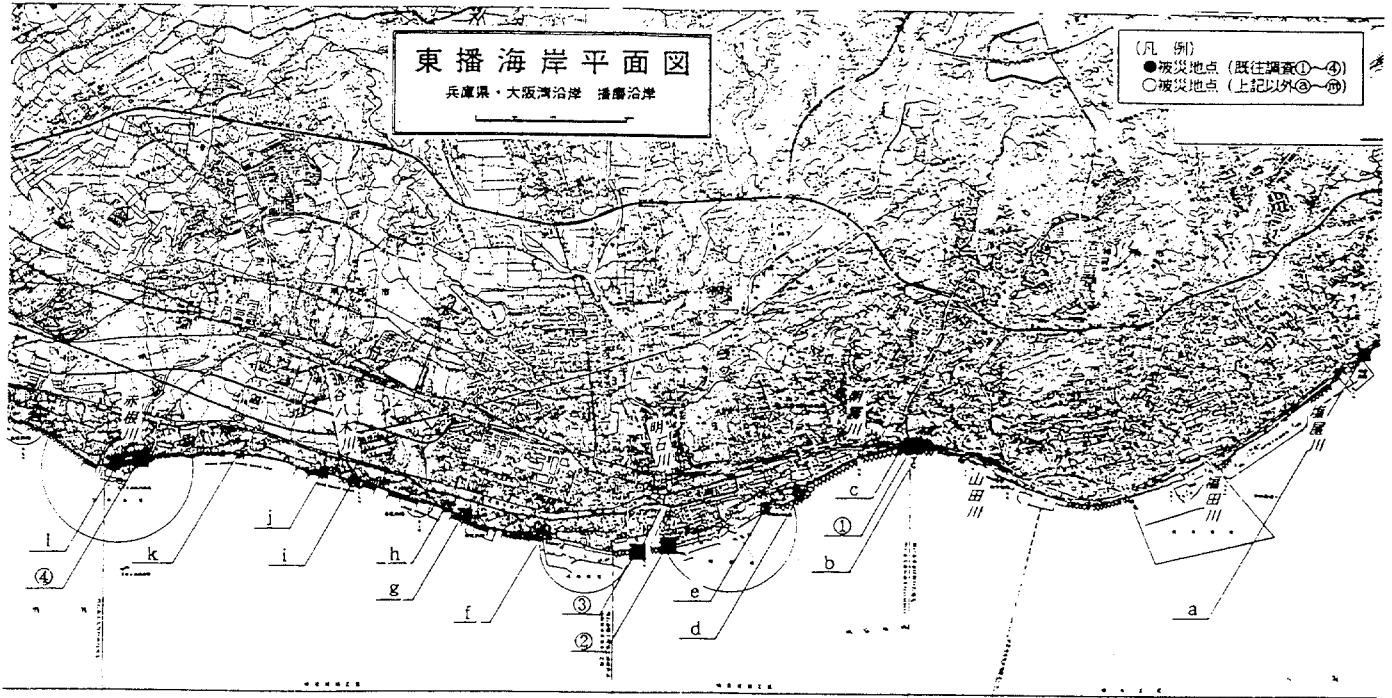


Fig. 5 Location map of Touban coast

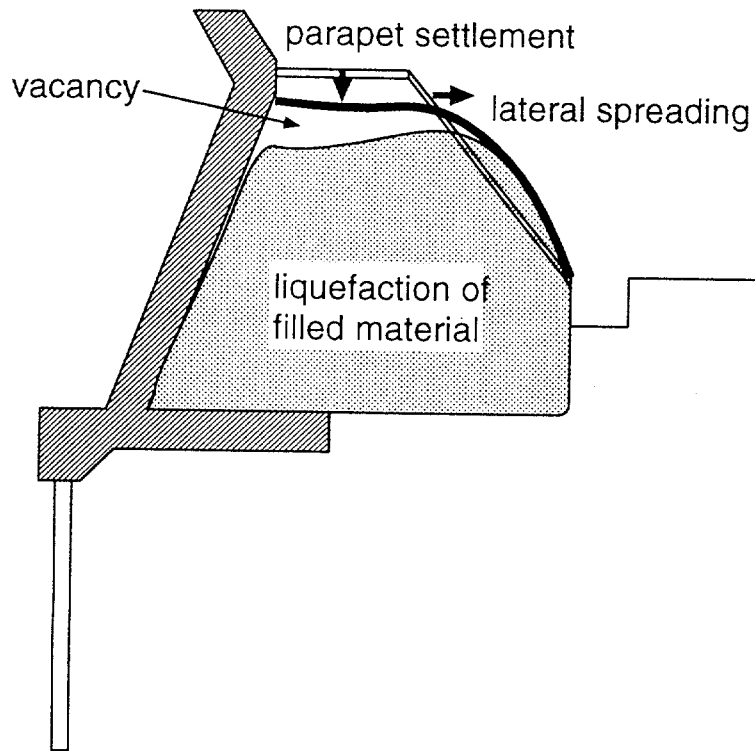


Fig. 6 Typical damages of coastal dike

TWO GREAT TSUNAMIS/UJNR WORKSHOP

PARTICIPANTS

Last Name	First Name	Address or Institution	City, State, Zip, Country
Akiyama	Jun	Ueda 4-1-3	Morioka, Iwate 020 Japan
Blackford	Michael	Pacific Tsunami Warning Center	Ewa Beach, HI, USA
Blay	Chuck	P.O. Box 1078	Waimea, Kauai, HI 96796
Cox	Doak	1929 Kakela Dr.	Honolulu, HI 96822
Curtis	George	Natural Sciences	University of Hawaii at Hilo
Curtis	Jean	Natural Sciences	University of Hawaii at Hilo
Fryer	Gerard	2525 Correa Rd	Honolulu, HI 96822
Fujima	Koji	1-10-20 Hshirimizu Yokosuka	Kanagawa-ken, 239 Japan
Fuka	Louis	P.O. Box 5120	Hilo, HI 96720 USA
Furumoto	Augustine	349 Kekupua St.	Honolulu, HI 96825
Iwasaki	Sin-Iti	3-1 Tennodai	Tsukuba, Ibaraki, Japan
Jones	Anthony	Oceanus Consultants Vancouver	British Columbia, Canada
Kajiura	Kinjiro	2-2-2 Hayabuchi, Tsuzuki-ku	Yokohama 224 Japan
Keith	Elizabeth	2626 Hillside Avenue	Honolulu, HI 96822
Kuhn	Gerry	2439 Sacada Circle,	Carlsbad, CA 92009 USA
Kuniaki	Abe	Hamauracho 1-8, Niigata City	Niigata Prefecture 951 Japan
Lander	Corinne	3763 Spring Valley Road	Boulder, CO 80304
Lander	James	Campus Box 449 CIRES, Univ. of CO	Boulder, CO 80309 USA
Lee	Howard	1132 Bishop St. #1505	Honolulu, HI 96813
Mader	Charles	1049 Kamehame Dr.	Honolulu, HI 96825-2860
Mader	Emma Jean	1049 Kamehame Dr.	Honolulu, HI 96825-2860
Magoon	Orville	1132 Bishop St. # 1505	Honolulu, HI 96813
Matsutomi	Hideo	Tegata Gakuen-Cho 1-1	Akita Japan
McCreery	Charles	Pacific Region, Int. Tsunami Info. Center	Honolulu, HI
Nakajima	Takashi	Palomar College	San Marcos, CA, USA
Nakamura	Kouji	1-1 Nagamine	Tsukuba, Ibaraki-ken 305 Japan
Ogyu	Ichiro	NHK Japan Broadcasting Corporation	Morioka, Ueda 4-1-3 Iwate 020 Japan
Okada	Masami	1-1 Nagamine	Tsukuba, Ibaraki-ken 305 Japan
Priest	George	23131 SW Starlight Dr.	Sherwood, OR 97140
Priest	Mrs.	23131 SW Starlight Dr.	Sherwood, OR 97140
Raichlen	Frederic	California Institute of Technology	Pasadena, CA USA
Russell	Virginia	12 Lamb's Conduit Passage	London WC1R 4RH, United Kingdom
Satake	Kenji	Higashi 1-1-3 Geological Survey of Japan	Trukuba, Ibaraki, 305 Japan
Sato	Shinji	Public Works Research Institute	Tsukuba, Ibaraki, Japan
Sekita	Yasuo	1-3-4 Otemachi	Chiyoda-ku, Tokoyo 100, Japan
Siemers	Rob	P.O. Box 1078	Waimea, Kauai, HI 96796
Tanaka	Shigenobu	Public Works Research Institute	Tsukuba, Ibaraki, Japan
Walker	Daniel	Hawaii Institute of Geophysics & Planetology	Honolulu
Wigen	Syd	Fulford Box 72 Saltspring Island	B.C. Canada V8K2P2
Yamakawa	Ken	Ueda 4-1-3	Morioka, Iwate 020 Japan

SCIENCE OF
TSUNAMI HAZARDS

PUBLICATION FORMAT INFORMATION

Typing area is 25 by 19 cm.

One-column text.

All text to be single-space.

Indent 5 spaces to start a new paragraph.

Page numbers in lower right hand corner in blue pencil.

**Top half of first page to contain title in CAPTIALS,
followed by authors and author affiliation centered on page.**

**Bottom half of first page to contain abstract with
heading ABSTRACT centered on page.**

Send original camera ready paper and a copy to

**Dr. Charles Mader, Editor
Science of Tsunami Hazards
Mader Consulting Co.
1049 Kamehame Drive
Honolulu, Hawaii 96825-2860, USA**

APPLICATION FOR MEMBERSHIP

THE TSUNAMI SOCIETY

P. O. Box 25218
Honolulu, Hawaii 96825, USA

I desire admission into the Tsunami Society as: (Check appropriate box.)

Student

Member

Institutional Member

Name _____ Signature _____

Address _____ Phone No. _____

Zip Code _____ Country _____

Employed by _____

Address _____

Title of your position _____

FEE: Student \$5.00 Member \$25.00 Institution \$100.00

Fee includes a subscription to the society journal: SCIENCE OF TSUNAMI HAZARDS.

Send dues for one year with application. Membership shall date from 1 January of the year in which the applicant joins. Membership of an applicant applying on or after October 1 will begin with 1 January of the succeeding calendar year and his first dues payment will be applied to that year.

